AD-A063 992 BENDIX CORP TETERBORO N J FLIGHT SYSTEMS DIV F/G 1/3
ADVANCED FLIGHT CONTROL ACTUATION SYSTEM (AFCAS-E/P), FEASIBILI--ETC(U)
JUN 78 R E FEUCHT, R W PRESLEY, P FORMAN N62269-77-C-0171
UNCLASSIFIED FSD-7411-78-05 NADC-77001-60 NL

1 OF 2
ADA
063992

LEVEL II

13

SC

TECHNICAL REPORT
NADC 77001-60

ADVANCED FLIGHT CONTROL ACTUATION SYSTEM (AFCAS - E/P)

Feasibility Investigation of an Electro/Pneumatic Dual Power Driven Concept

Robert E. Feucht
Philip Forman
Richard Krehely
Bendix Corporation
Flight Systems Division
Teterboro, New Jersey

Rex W. Presley
Bendix Research Laboratories
Southfield, Michigan

JUNE 1978

FINAL REPORT FOR PERIOD MARCH 1977 - MAY 1978

APPROVED FOR PUBLIC RELEASE;
DISTRIBUTION UNLIMITED

PREPARED FOR

NAVAL AIR DEVELOPMENT CENTER 6013
WARMINSTER, PENNSYLVANIA 18974

UNCLASSIFIED NADC 77001-60

SECURITY CLASSIFICATION OF THIS PAGE (When Data Entered)

REPORT DOCUMENTATION PAGE

READ INSTRUCTIONS BEFORE COMPLETING FORM

1. REPORT NUMBER: NADC-77001-60	2. GOVT ACCESSION NO.
3. RECIPIENT'S CATALOG NUMBER	
4. TITLE (and Subtitle): Advanced Flight Control Actuation System (AFCAS-E/P). Feasibility Investigation of an Electro/Pneumatic Dual Power Driven Concept.	5. TYPE OF REPORT & PERIOD COVERED: FINAL REPORT, March 1977 — May 1978
	6. PERFORMING ORG. REPORT NUMBER: FSD-7411-78-05
7. AUTHOR(s): Robert E. Feucht, Rex W. Presley, Philip Forman, Richard Krehely	8. CONTRACT OR GRANT NUMBER(s): N62269-77-C-0171
9. PERFORMING ORGANIZATION NAME AND ADDRESS: Bendix Corporation, Flight Systems Division, Teterboro, New Jersey 07608	10. PROGRAM ELEMENT, PROJECT, TASK AREA & WORK UNIT NUMBERS: 622-41N-F41400
11. CONTROLLING OFFICE NAME AND ADDRESS: Naval Air Development Center (6013), Warminster, Pennsylvania 18974	12. REPORT DATE: June 1978
	13. NUMBER OF PAGES: 118
14. MONITORING AGENCY NAME & ADDRESS (if different from Controlling Office): AIR-530311 and AIR-34)D, Naval Air Systems Command, Department of the Navy, Washington, DC 20361	15. SECURITY CLASS. (of this report): Unclassified
	15a. DECLASSIFICATION/DOWNGRADING SCHEDULE

16. DISTRIBUTION STATEMENT (of this Report)

Approved for Public Release; Distribution Unlimited.

17. DISTRIBUTION STATEMENT (of the abstract entered in Block 20, if different from Report)

18. SUPPLEMENTARY NOTES

19. KEY WORDS (Continue on reverse side if necessary and identify by block number)

Aircraft Control Actuator, Dual Motor, Rotary Actuator, Pneumatic Motor, Electric Stepper Motor, Dual-Mode Dynavector, Survivability, Reliability, Safety, Bleed-Air Motor, High-Temperature Environment.

20. ABSTRACT (Continue on reverse side if necessary and identify by block number)

Report of design study on Dual-Mode Dynavector Actuator for use as control-surface actuator on aircraft. Actuator operates on pneumatic power and/or electric power. Operation within specifications continues despite loss of either electric or pneumatic power, providing survivability feature for aircraft.

DD FORM 1 JAN 73 1473 EDITION OF 1 NOV 65 IS OBSOLETE

SECURITY CLASSIFICATION OF THIS PAGE (When Data Entered)

409146

1.0 SUMMARY

1.1 BACKGROUND INFORMATION

This final report presents the results of the BENDIX study and design effort on Contract No. N62269-77-C-0171, issued by NAVAL AIR DEVELOPMENT CENTER, Warminster, Pennsylvania. The Dual Mode Dynavector actuator that was produced by this program operates on 270 VDC electric power and/or 20 PSIG pneumatic power. This actuator consists of an electric stepper motor integrated with an anchored-vane pneumatic motor. The orbit rotor delivers the generated power to the output shaft through a step-down epicyclic gear transmission

The final configuration is equipped with a crank arm to convert the rotary output shaft motion to a linear drive that can control the rudder of a T-2C airplane. (See Figure 1).

Computer studies have demonstrated that actuator systems based on the Dual Mode Dynavector have greater survivability than single mode actuators. Operation within specifications is achieved despite loss of either electric or pneumatic power. No interruption of control occurs during or after such power loss.

The Dual Mode Dynavector has a great size advantage over competing actuators. For example, the Dynavector produces stall torques that are twice those generated by a D.C. Torque Motor that is 4 times larger in volume.

Design parameters for the Dual Mode Dynavector are as follows:

Supply Voltage	270 VDC
Supply Pressure	20 PSIG (1.379×10^5 Pa)
Rated Torque, Single Mode	1500 In-Lbs. (169.5 Nm)
Rated Torque, Dual Mode	3000 In-Lbs. (338.95 Nm)
Rated Speed	30^o/Sec. (.52 rad/s)
No-Load Speed	50^o/Sec. (.87 rad/s)
Stall Torque, Single Mode	2200 In-Lbs. (248.6 Nm)
Stall Torque, Dual Mode	4400 In-Lbs. (497.2 Nm)
Resolution	$\pm$ .048^o ($\pm$ .838 millirad)
Diameter	8.125 In. (206.38 mm)
Length, Housing	5.2 In. (132.08 mm)
Air Flow, Rated Speed and Torque	.01946 lb./sec. (.0088 kg/s)
Electric Powr, Rated Speed and Torque	200 watts
Air Temperature, Pneumatic Supply	
Minimum	0^oF (-17.8^oC)
Maximum	350^oF (177^oC)
Frequency Response, dual mode	Flat Within $\pm$ 3 DB Up to 20 Hz, (signal ampl. = .5^o peak-to-peak)

1.2 EXTREME CONDITIONS

The Dual Mode Dynavector will function effectively under these extreme conditions:

1.2.1 Supply Voltage

The nominal supply voltage is 270 VDC. However, operation can be sustained continuously with the supply voltage in the range of 200 VDC to 280 VDC. Transient variations of .1 second duration or less can swing between 125 VDC and 475 VDC without damaging the Dual Mode Dynavector.

1.2.2 Supply Pressure

The nominal supply pressure is 20 PSIG (1.379×10^5 Pa). However, operation can be sustained continuously with the supply pressure in the range 10 PSIG (6.895×10^4 Pa) to 30 PSIG (2.07×10^5 Pa).

1.2.3 Air Temperature, Pneumatic Supply

The nominal air temperature range of the pneumatic supply is 0^{o}F (-17.8^{o}C) to 350^{o}F (177^{o}C). However, transient excursions of 30 seconds duration or less can vary up to 392^{o}F (200^{o}C) without damaging the Dual Mode Dynavector.

The highest bleed-air temperature on the T2-C aircraft is 415^{o}F (212.8^{o}C). This can be reduced to 350^{o}F (177^{o}C) by flowing through a ten foot section of pnuematic tubing that is fitted with air-cooling fins.

1.3 SURVIVAL WITH THE DUAL MODE DYNAVECTOR

The Dual Mode Dynavector provides the pilot with a fast-response control system actuator with dual power options. Failure of primary electric power does not prevent the engine bleed air system from continuing the actuator function. Failure of the engine bleed air system does not prevent the primary electric power from continuing the actuator function.

Wide variations in delivered electric power or pneumatic power do not prevent the actuator from performing normally in the closed-loop control system. Abnormal power conditions are so easily absorbed by the Dual Mode Dynavector's redundancy that such problems might readily pass unnoticed by the pilot.

Wide variations in the temperature of the engine bleed air do not prevent the actuator from performing normally in a closed-loop control application. Temperature swings from 0°F (-17.8°C) to 350°F (177°C) do not produce detectable changes in performance of the control system.

Aircraft survivability now has an ideal control system actuator .... the Dual Mode Dynavector.

1.4 ADVANCED AIRCRAFT APPLICATIONS

Advanced aircraft, such as STOL/VTOL and other high-performance mission fighters require dual-mode actuators which offer the following....

- compact packaging
- easily-changed form factors
- large angular control surface rotation
- high dynamic performance
- normal operation on poorly regulated power sources
- high reliability
- high survivability

The Dual Mode Dynavector meets these needs. For example, a design now under consideration produces high output torque at an outer member output ring. This leaves a 12 inch diameter hole through the actuator which permits thrust vector exhaust gases to exit through the actuator. Deflector vanes can be mounted to the outer member output ring for thrust control in a STOL or VTOL aircraft. The high-temperature environment in such an application can be safely handled by the Dual-Mode Dynavector without danger of fire or explosion in the actuator system. Environmental temperatures as high as 824°F (440°C) are feasible for the Dual Mode Dynavector and 1832°F (1000°C) temperatures are feasible for the Pneumatic Dynavector.

Another design now being reviewed provides high torques in a small diameter, lightweight unit which would be suitable as a hinge-line control surface actuator.

1.5 OPERATION

The Dual Mode Dynavector consists of a pneumatic motor and an electric motor housed within a single rotary actuator assembly. The pneumatic motor is designed to operate on 20 PSIG pneumatic power and the electric motor is designed to operate on 270 VDC electric power. The pneumatic motor and the electric motor share the same rotor, and when electric power and pneumatic power are applied concurrently, the output torques produced by each add geometrically. Thus, each motor powered singly develops 1500 IN-LBS of torque at 5 RPM output shaft speed. When full electric and pneumatic power is supplied concurrently, the Dual Mode Dynavector develops 3000 IN-LBS of torque at 5 RPM.

Pneumatic Motor

Figs. 1, 2, & 3 show the essential features of the Dual Mode Dynavector. The electro-pneumatic valve (1) is controlled by a bipolar d.c. electrical current which is typically derived from the control system error signal. The d.c. current drives a linear-displacement torque motor (2) which in turn strokes the single-stage spool valve (3). The spool valve provides modulated bi-directional flow of pneumatic power from inlet (4), through the pneumatic motor (5), then out the exhaust port (6). Reversal of flow direction by the spool valve through the motor ports (7), (8) reverses the direction of the pneumatic motor torque. Pneumatic force on the rotor (9) is converted by eccentric reaction into a rotary torque.

Commutation slots on the rotor ends act with the manifold plate (11) and the transfer plate (12) to transfer the air flow to adjacent chambers as the rotor orbits. This in turn rotates the pneumatic force vector so that the orbiting reaction of the rotor continues.

Electric Motor

Electric current flows through three adjacent coils (13), (14) (15). The magnetic flux lines crossing the air gap between the stator (16) and rotor (9) result in a radial force vector which attracts the rotor to the stator. This force is converted by eccentric reaction into a rotary torque.

The next electrical step produced by the electric controller deenergizes coil (15) and energizes coil (17) resulting in a force vector rotation, and the orbiting reaction of the rotor continues.

The pneumatic commutation slots of the rotor are designed to coordinate the force vectors of the pneumatic motor and the electric motor so that they act synergistically.

Gear Transmission

The integral epicyclic gear transmission consists of the ring gear (18), the ground gear (19), and the output gear and shaft (20). The input to the transmission from the rotor (9) is transferred through the roller bearings (21). Reduction ratio from rotating motor force vector speed to output shaft speed is 468.4 to 1.

Position Transducers

RVDT (22) and LVDT (23) are rotary and linear position transducers that are used as feedback elements in closed-loop instrumentation circuits.

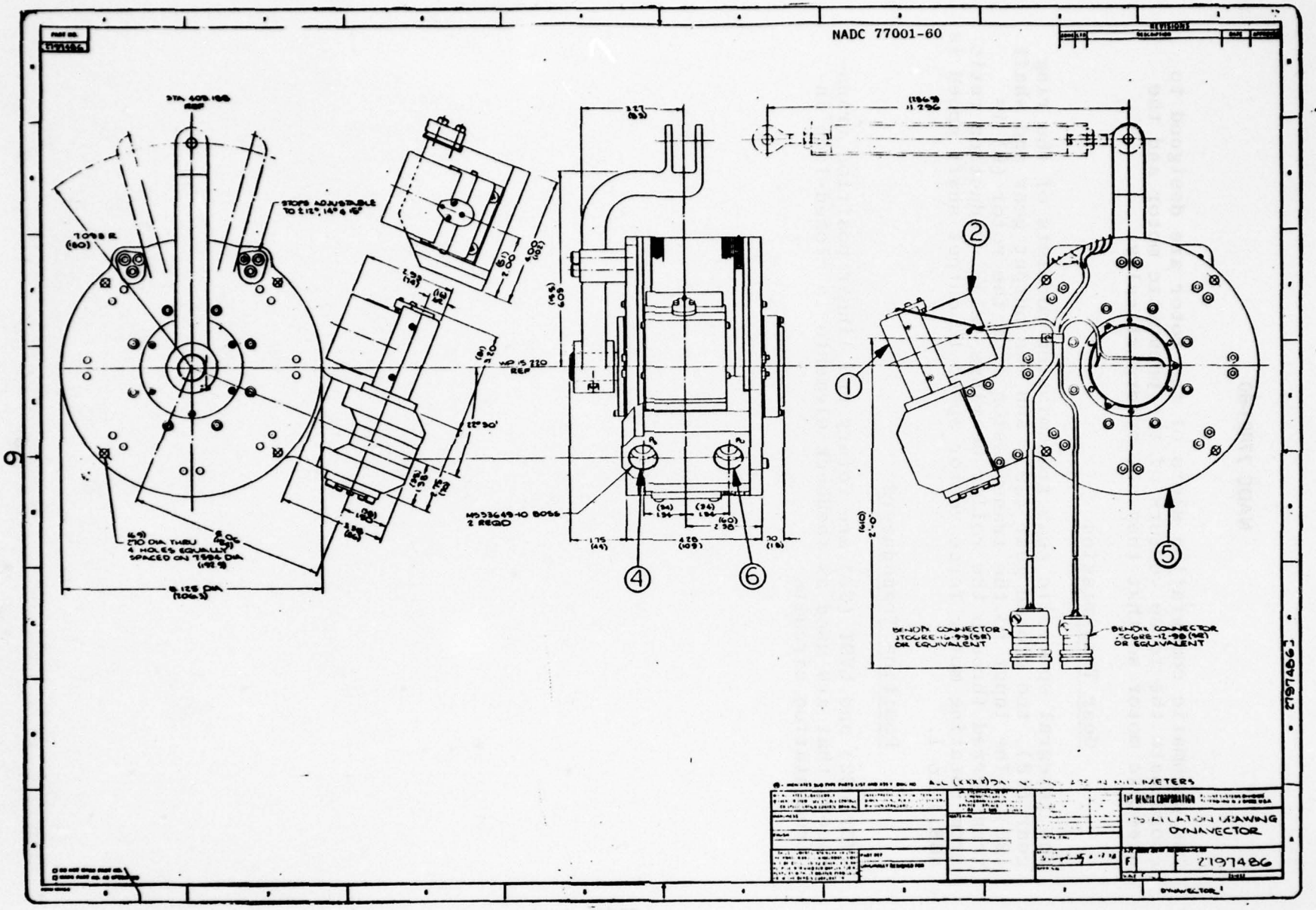
STOPS ADJUSTABLE TO ± 12°, 14° & 16°
MS 15 220 REF
MS 33649-10 BOSS 2 REQD
BENDIX CONNECTOR -TCGRE-11-98(SR) OR EQUIVALENT
BENDIX CONNECTOR -TCGRE-11-98(SR) OR EQUIVALENT
DYNAVECTOR
2197486

FIGURE 1

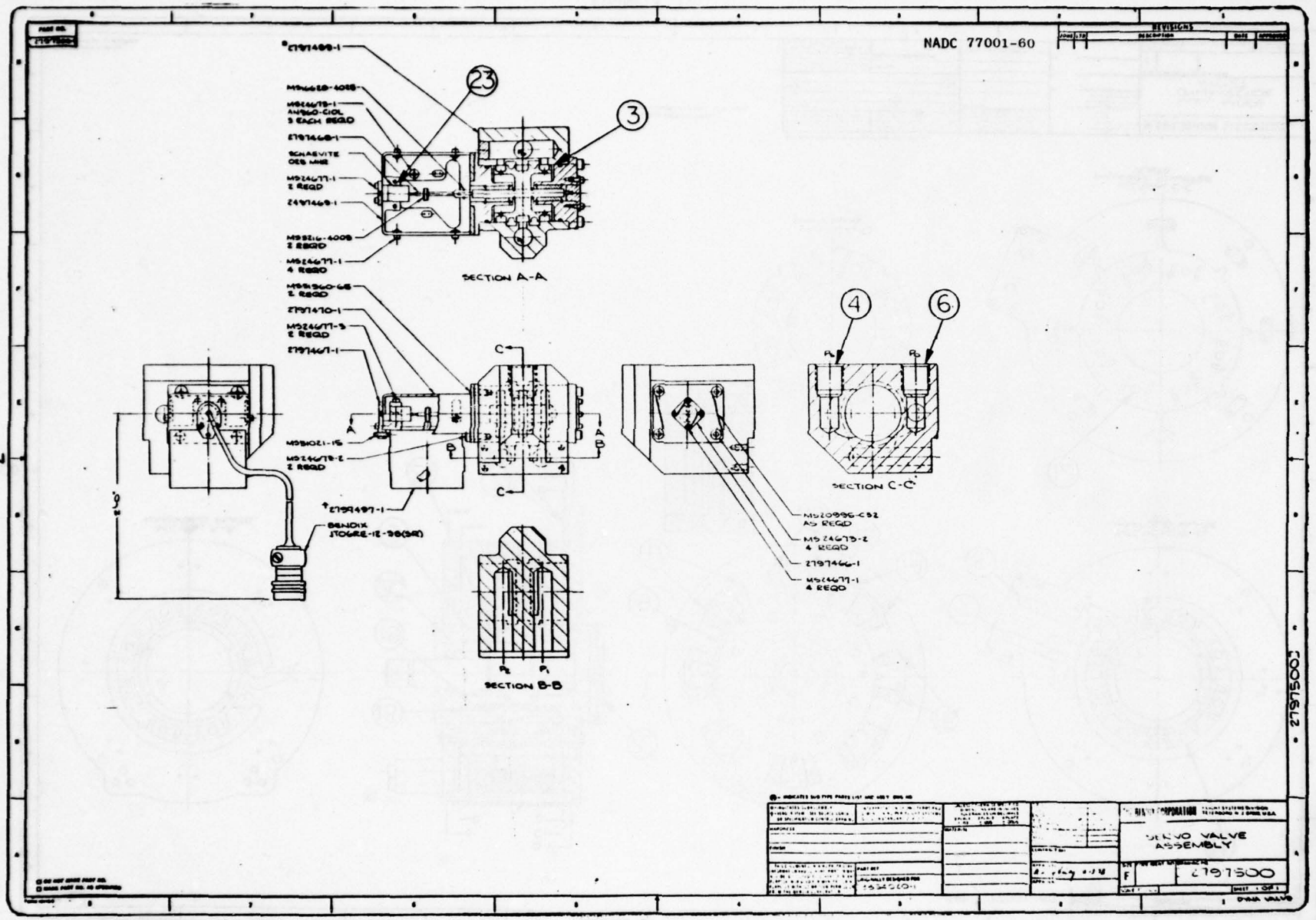
SECTION A-A
SECTION B-B
SECTION C-C
BENDIX
SERVO VALVE ASSEMBLY
2797500

FIGURE 2

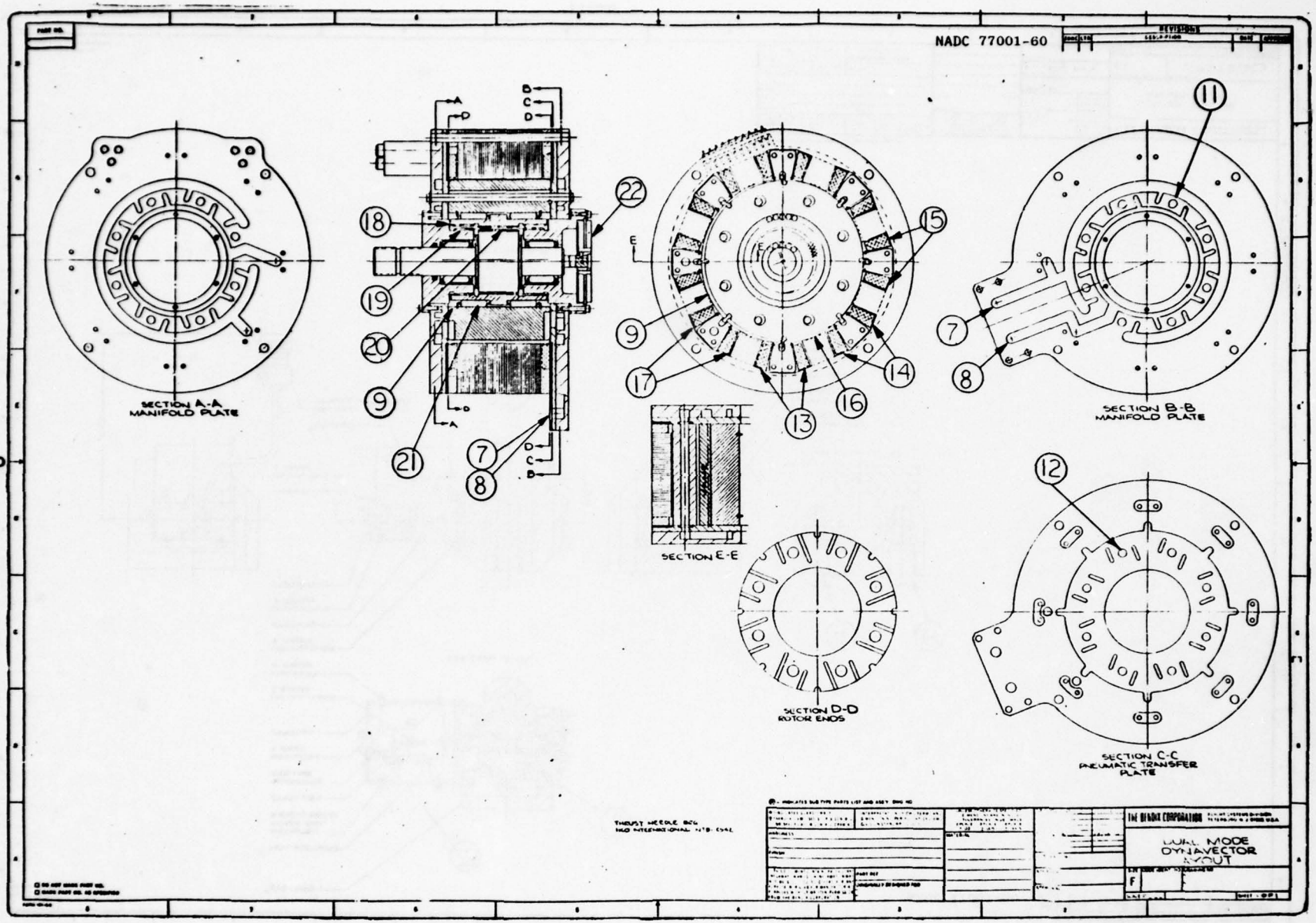
NADC 77001-60
SECTION A-A
MANIFOLD PLATE
SECTION E-E
SECTION D-D
ROTOR ENDS
SECTION B-B
MANIFOLD PLATE
SECTION C-C
PNEUMATIC TRANSFER
PLATE
THE BENDIX CORPORATION
DUAL MODE
DYNAVECTOR
LAYOUT

FIGURE 3

TABLE OF CONTENTS

TABLE OF CONTENTS (CONT.)

LIST OF ILLUSTRATIONS

LIST OF ILLUSTRATIONS (CONT)

LIST OF TABLES

2.0 DISCUSSION

2.1 TRANSMISSION DESIGN

Ratio

Several factors must be considered in selecting the reduction ratio of the epicyclic gears. The ratio for a pneumatic Dynavector is usually selected to provide a maximum orbiting speed of about 3000 rpm. Electric Dynavectors generally use a higher ratio. The gear diameter should be as large as the space permits to reduce the gear tooth stresses. For a given gear diameter and diametral pitch only a few ratios can be obtained.

A computer study of gear tooth motion has indicated that 32 diametral pitch and 20° pressure should be used to minimize gear tooth interference. A tooth difference of 3 between the ring gear and pinion can be used to provide 3/64 inch eccentricity.

The eccentricity acts as a lever arm for converting the pole forces to torque. If the eccentricity is very small, very little torque will be developed. Also the epicyclic gearing will not work if the eccentricity is too small. On the other hand, increasing the eccentricity increases the air gap in the magnetic circuit. Electrical power loss becomes excessive when the gap is excessively large due to fringing and increased flux leakage. The number of ampere turns required for a given flux level increases as the gap increases.

Previous experience has indicated that an eccentricity of 3/64 inch is the best choice for electrical performance of a motor this size, and for a good gear design.

The transmission form is shown in Figure 4. The reduction ratio is given by

$$R = \frac{N_2 N_4}{N_1 N_3 - N_2 N_4}$$

where N_1 = Number of teeth in ground gear

N_2 = Number of teeth in ring gear-ground gear mesh

N_3 = Number of teeth in ring gear-output gear mesh

N_4 = Number of teeth in output gear

The ratios obtainable are listed in Table 1.

A ratio of 468.4:1 was selected. This ratio should provide the specified torque and speed in both modes of operation. The orbiting speed at the rated speed is

$$30 \frac{\text{deg}}{\text{sec}} \times \frac{1 \text{ rpm}}{6 \text{ deg/sec}} \times 468 = 2340 \text{ rpm}$$

TABLE 1 - GEAR RATIOS

Diametral Pitch = 32
3 Teeth Difference

N1	65	65	64	63	62	61	60	59
N2	68	68	67	66	65	64	63	62
N3	65	64	64	63	62	61	60	59
N4	62	61	61	60	59	58	57	56
RATIO	468.4	345.7	454.1	440.0	426.0	412.4	399.0	385.8

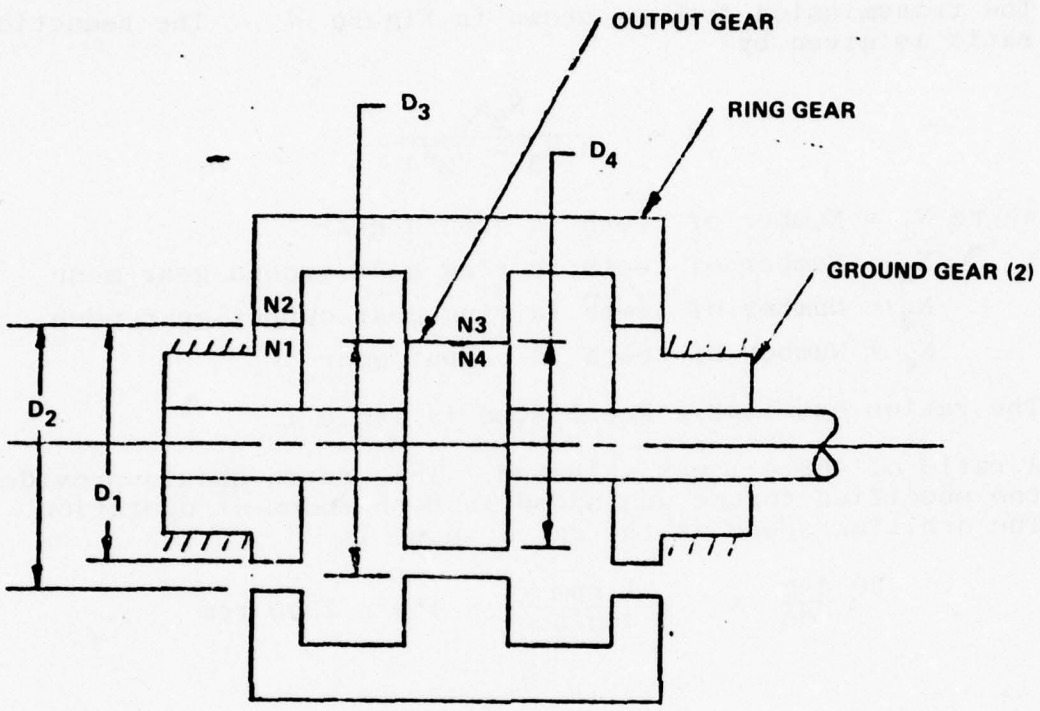

FIGURE 4 TRANSMISSION CONFIGURATION

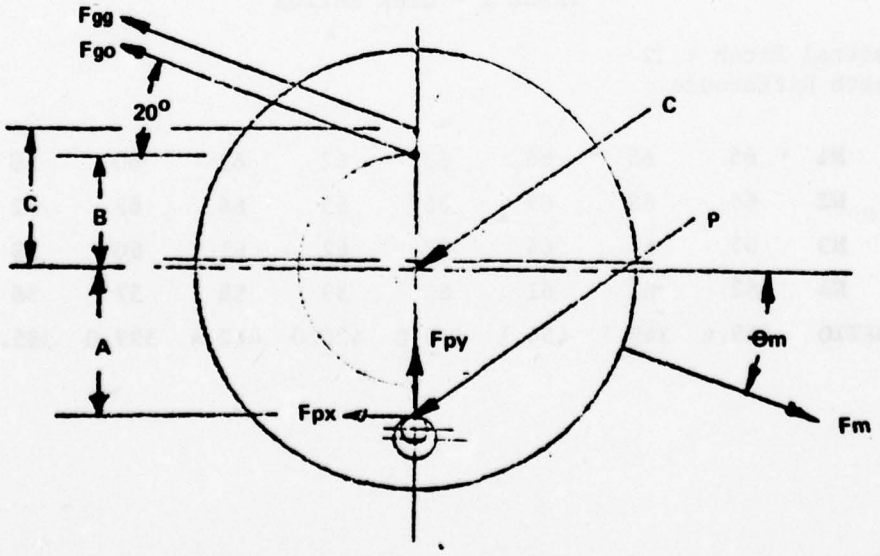

FIGURE 5 ROTOR FREE BODY DIAGRAM

2.2 STRESS ANALYSIS

The forces and moments acting on the rotor are shown in Figure 5. The equations for summing forces and moments are

$$\Sigma F_x: \quad F_{mx} - F_{gox} - F_{ggx} - F_{px} = 0 \qquad (1)$$

$$\Sigma F_y: \quad F_{my} - F_{goy} - F_{ggy} - F_{py} = 0 \qquad (2)$$

$$\Sigma M_c: \quad AF_{px} - BF_{gox} - CF_{ggx} = 0 \qquad (3)$$

$$\Sigma M_p: \quad AF_{mx} - (A+B)F_{gox} - (A+C)F_{ggx} = 0 \qquad (4)$$

The symbols used in this section are defined as follows.

F_x	=	Net horizontal force acting on the rotor	lbs
F_y	=	Net vertical force acting on the rotor	lbs
M_c	=	Moment about point C, the center of the rotor	in. lbs
M_p	=	Moment about point P, where the rotor contacts the pin, as shown in Fig	in. lbs
F_{ggx}	=	Horizontal component of force acting on the rotor at the ground gear mesh point	lbs
F_{ggy}	=	Vertical component of force acting on the rotor at the ground gear mesh point	lbs
F_{gox}	=	Horizontal component of force acting on the rotor at the output gear mesh point	lbs
F_{goy}	=	Vertical component of force acting on the rotor at the output gear mesh point	lbs
F_{mx}	=	Horizontal component of electro-magnetic or pressure force acting on the rotor	lbs
F_{my}	=	Vertical component of electro-magnetic or pressure force acting on the rotor	lbs

F_{px}	= Horizontal component of pin force on the rotor	lbs
F_{py}	= Vertical component of pin force on the rotor	lbs
A	= Distance from center of rotor to contact point of pin with rotor	in.
B	= Distance from center of rotor to output gear mesh point	in.
C	= Distance from center of rotor to ground gear mesh point	in.
T	= Torque	in.lbs
F_{go}	= Output gear force	lbs
n_t	= Torque efficiency	
R	= Gear ratio	
e	= Eccentricity	in.
θ_m	= Vector angle of force F_m	deg

F_m is the force which causes the motor to have an output torque. F_{gg} and F_{go} are the reaction forces of the ground gear and the output gear on the rotor. F_p is the reaction force of the pin on the rotor. In this analysis all of the load is considered to be taken by one pin.

The output gear force for the maximum stall torque of T_o = 4400 in-lbs. is

$$F_{go} = \frac{T_o}{B_{go} \cos 20^o} = \frac{4400}{.970 \cos 20^o} = 4827 \text{ lbs.}$$

$$F_{gox} = F_{go} \cos 20^o = 4536 \text{ lbs.}$$

$$F_{goy} = F_{gox} \tan 20^o = 1651 \text{ lbs.}$$

The torque is given by

$$T_o = n_t \, Re \, F_{mx}$$

where n_t = efficiency
R = gear ratio
e = eccentricity

$$F_{mx} = \frac{T_o}{n_t Re}$$

$$F_{mx} = \frac{4400}{.48 \times 470 \times .047} = 415 \text{ lbs.}$$

$$F_{my} = F_{mx} \tan \Theta_m$$

From equation (4),

$$F_{ggx} = \frac{A}{A+C} F_{mx} - \frac{A+B}{A+C} F_{gox}$$

$$F_{ggx} = \frac{1.812}{2.8745} \times 415 - \frac{2.8276}{2.8745} \times 4536$$

$$F_{ggx} = -4200 \text{ lbs.}$$

$$F_{ggy} = -F_{ggx} \tan 20^o = 1529 \text{ lbs.}$$

From equation (3),

$$F_{px} = \frac{B}{A} F_{gox} + \frac{C}{A} F_{ggx}$$

$$F_{px} = \frac{1.0156}{1.812} \times 4536 - \frac{1.0625}{1.812} \times 4200$$

$$F_{px} = 80 \text{ lbs.}$$

From equation (2),

$$F_{py} = F_{mx} \tan \Theta_m - F_{goy} - F_{ggy}$$
$$F_{py} = 415 \tan \Theta_m - 1651 - 1529$$
$$F_{py} = 415 \tan \Theta_m - 3180$$

F_{py} is negative for θ_m less than 83 degrees. When the sign is negative there is no vertical force component on the reaction pin. The vertical force acts instead on the gearing.

Reaction Pin Stress

Since θ_m should never exceed 83 degrees, the pin force is

$$F_p = F_{px} = -80 \text{ lbs.}$$

The reaction pin stress is given by

$$S_s = \frac{F_p}{A_p}$$ where A_p = pin cross-section area.

The stress in shear is

$$S_s = \frac{80}{0.0276} = 2{,}899 \text{ psi.}$$

Yield strength of the reaction pin steel in shear is 65,000 psi.

Steady-State Gear Mesh Stress

The maximum steady-state gear mesh bending stress S_b is found from the Lewis Formula,

$$S_b = \frac{4\ T_o}{Ybcd^2}$$

where T_o = maximum stall torque, 4400 in-lbs.

$$S_b = \frac{(4)\ (4400)}{(0.37)(1.13)(0.16)(1.94)^2}$$

$$S_b = 70{,}000 \text{ psi}$$

Y = Lewis form factor, 0.37

b = Face width, 1.13 in.

c = Percent teeth driving the load, 16%

d = Pitch diameter, 1.94 in.

Yield strength of the gear steel is 330,000 psi.

I_o, Inertia from Rotor to Output Gear

The moment of inertia of the actuator mechanism referenced to the output gear is expressed by:

$$I_o = \left[\frac{Wmp}{g} (e)^2 + \frac{I_{BB}}{(R_r)^2} \right] \cdot (RATIO)^2$$

The first term in the bracketed expression represents the kinetic reaction due to the eccentric orbiting motion of the rotor The second term represents the kinetic reaction due to the rotational motion of the gear mechanism. In this equation,

Wmp = weight of rotor, lbs.

g = 386 inches/sec.^{2}

R_r = transmission ratio of ring rotation to ground, 22

e = eccentricity, 3/64 inch

RATIO = overall actuator ratio, 468:1

I_{BB} = inertia of ring gear, in-lb. sec.^{2}

$$I_o = \left[\frac{Wmp}{g} (e)^2 + \frac{I_{BB}}{(R_r)^2} \right] \cdot (RATIO)^2$$

$$I_o = \left[\frac{7.7}{386} \left(\frac{3}{64}\right)^2 + \frac{.0045}{(22)^2} \right] \cdot (468)^2$$

$$I_o = \left[.0000438 + .0000093 \right] \cdot (468)^2$$

$$I_o = 11.63 \text{ in.-lb.-sec.}^2$$

Dynamic Gear Mesh Stress

Maximum gear mesh bending stress occurs when the crank arm impacts a limit stop while slewing at maximum speed. The crank arm, gearing and resisting members absorb the kinetic energy of the Dynavector while stopping through .005 radian of arc of the output shaft. Thus θ_{om} = .005 rad as shown below.

Assume a simple harmonic motion of the output shaft upon stopping.

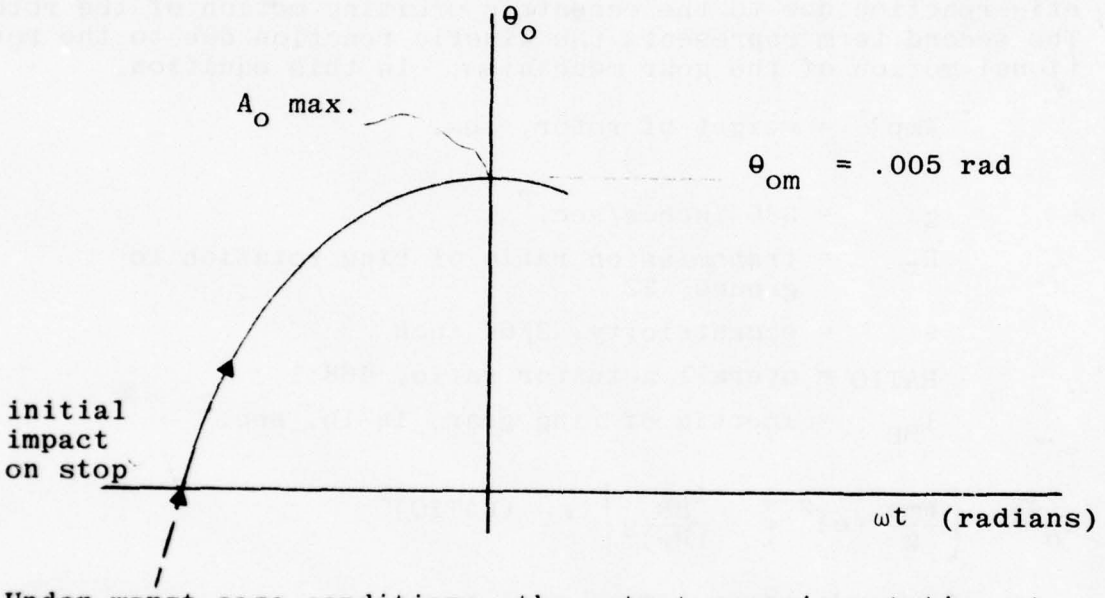

Under worst-case conditions, the output gear is rotating at
V_o max. = 10 RPM
= 1 rad/sec.

For simple harmonic motion

$$\theta_o = \theta_{om} \sin \omega t \qquad (5)$$

$$V_o = \frac{d\,\theta_o}{dt} = \theta_{om}\ \omega \cos \omega t$$

Maximum velocity occurs when cos ωt = 1; this occurs at t =0 and,

$$V_{o\ max.} = \theta_{om}\ \omega \qquad (6)$$

Acceleration, $$A_o = \frac{d^2\theta_o}{dt^2} = - \theta_{om} \omega^2 \sin \omega t$$

Maximum acceleration occurs when $\sin \omega t = 1$; this occurs at $\omega t = \pi/2$ and,

$$A_o \text{ max} = - \theta_{om} \omega^2 \qquad (7)$$

from (6), $V_{o \text{ max.}} = \theta_{om} \omega$,

at 10 RPM, $V_{o \text{ max.}} = 1$ rad/sec.,

1 rad/sec = .005 radian x ω

$\omega = 200$ sec.$^{-1}$

from (7)

$$A_o \text{ max.} = - \left[.005 \text{ radian } (200 \text{ rad/sec.})^2\right]$$

$$A_{o \text{ max.}} = - \left[200 \text{ rad/sec.}^2\right]$$

The worst-case loading on the gear mesh upon stopping is equal to the maximum steady-state torque plus the maximum dynamic torque at the output shaft.

$$T_o' = T_{o \text{ max.}} + I_o \; A_{o \text{ max.}}$$

$$T_o' = 4400 + 12 \; (200)$$

$$T_o' = 6800 \text{ in-lbs.}$$

where T_o' = (stall + energy torque), max.

T_o = stall torque, in-lbs.

A_o = max. output deceleration, rad/sec^2

I_o = inertia of Dyna-vector ref. to output gear, in-lb-sec^2

The worst-case dynamic gear mesh stress based on the Lewis Formula is

$$S_b' = \frac{4\ T_o'}{ybcd^2}$$

$$S_b' = \frac{(4)(6800)}{(0.37)(1.13)(0.16)(1.94)^2}$$

$$S_b' = 108{,}000 \text{ psi}$$

Yield strength of the gear maraging steel is 330,000 psi.

Dynamic Crank Arm Stress

The crank arm impacts the limit stop at a point 4 inches from the output shaft centerline. The bending force

$$P_{max} = \frac{6800 \text{ in-lbs.}}{4 \text{ inches}} = 1700 \text{ lbs.}$$

The maximum deflection of the crank arm is

$$\Delta = \frac{1}{3} \times \frac{P_{max}\ L^3}{EI} \quad (8)$$ where L = 4 inches

$$\Delta = \frac{1}{3} \times \frac{1700\ (4)^3}{3 \times 10^7 \times .06}$$

$$\Delta = .02 \text{ inch}$$

moment of inertia,
$I = .0833\ bh^3$
$I = .0833(7.5)(1)^3$
$I = .06\ in^4$

The maximum stress in the crank arm is

$$S_b = \frac{Mc}{I}$$

$$S_b = \frac{6800 \times .5}{.06}$$

$$S_b = 57{,}000 \text{ psi}$$

Yield strength of the crank-arm steel is 110,000 psi.

θ_{om} Calculation

From equation (8) above, the maximum deflection of the crank arm upon stopping is Δ = .02 inch.

$$\theta_{om} = \frac{\Delta}{\text{circumf.}} \times 2\pi \text{ rad}$$

$$\theta_{om} = \frac{.02 \text{ inch}}{2\pi \text{ (4 inches)}} \times 2\pi \text{ rad} = .005 \text{ rad}$$

θ_{om} = .005 radian.

Ring Gear Stress and Deflection

The ring gear shear stress and deflection are given by

$$J = \frac{\pi}{32}(d_i^4 - d_o^4)$$

$$S_s = \frac{Td_i}{2J}$$

$$\phi = \frac{TL}{JG} \times \frac{180}{\pi}$$

where d_i = inside diam., in.
d_o = outside diam., in.
G = modulus of elasticity in shear, psi
J = polar moment of inertia, in.^4
L = length, in.

$$J = \frac{\pi}{32}(2.5^4 - 2.15^4) = 1.74 \text{ in.}^4$$

$$S_s = \frac{4400 \times 2.15}{2 \times 1.74} = 2718 \text{ psi}$$

$$\phi = \frac{4400 \times 2.625}{1.74 \times 10.5 \times 10^6} \times \frac{180}{\pi} = .036 \text{ deg.}$$

Bearings

The actuator has two roller bearings supporting the output shaft with a load of 2420 lbs. These bearings rotate at the low speed of the output shaft. Torrington bearing HJ-142216 was selected for this application. The dynamic load rating for this bearing is 4860 lbs.

Two roller bearings separate the ring gear and rotor. These bearings support a maximum load of 2860 lbs. each and rotate at the output shaft speed. The bearing selected for this application, Torrington WJ-40416, has a 9110 lb. dynamic load rating.

The bearings selected have a safety factor of 2 or 3 and should have a long life at the low speeds of this application.

2.3 ELECTRIC MODE

The computer program described in Appendix B was used to compute torque-speed curves for the electric mode. The correlation of this computer program with test data for the Bendix Model EH-441-U1 motor is shown in Figure 6.

Stator Design

A stator length of 2.6 inches was selected for the Dual Mode Actuator. It is theoretically possible to develop the required torque with a shorter stator. However, more electrical power would be required. Conversely, if the stator is too long, the inductance of the coils will be unacceptably high and the speed of the electric motor will be reduced. The 2.6 inch length appears to be the best compromise between inductance and power input.

Stator Voltage Waveform

The motor excitation voltage waveform used for this design is shown in Figure 7. A high-voltage pulse is used for fast current buildup. To develop maximum torque with the least possible current, the high-voltage pulse should be of duration to just cause magnetic saturation at low speed. A computer simulation indicates that this time is about 7 milliseconds. The voltage is then reduced to the value that just maintains saturation, then reduced linearly with time to a value of about

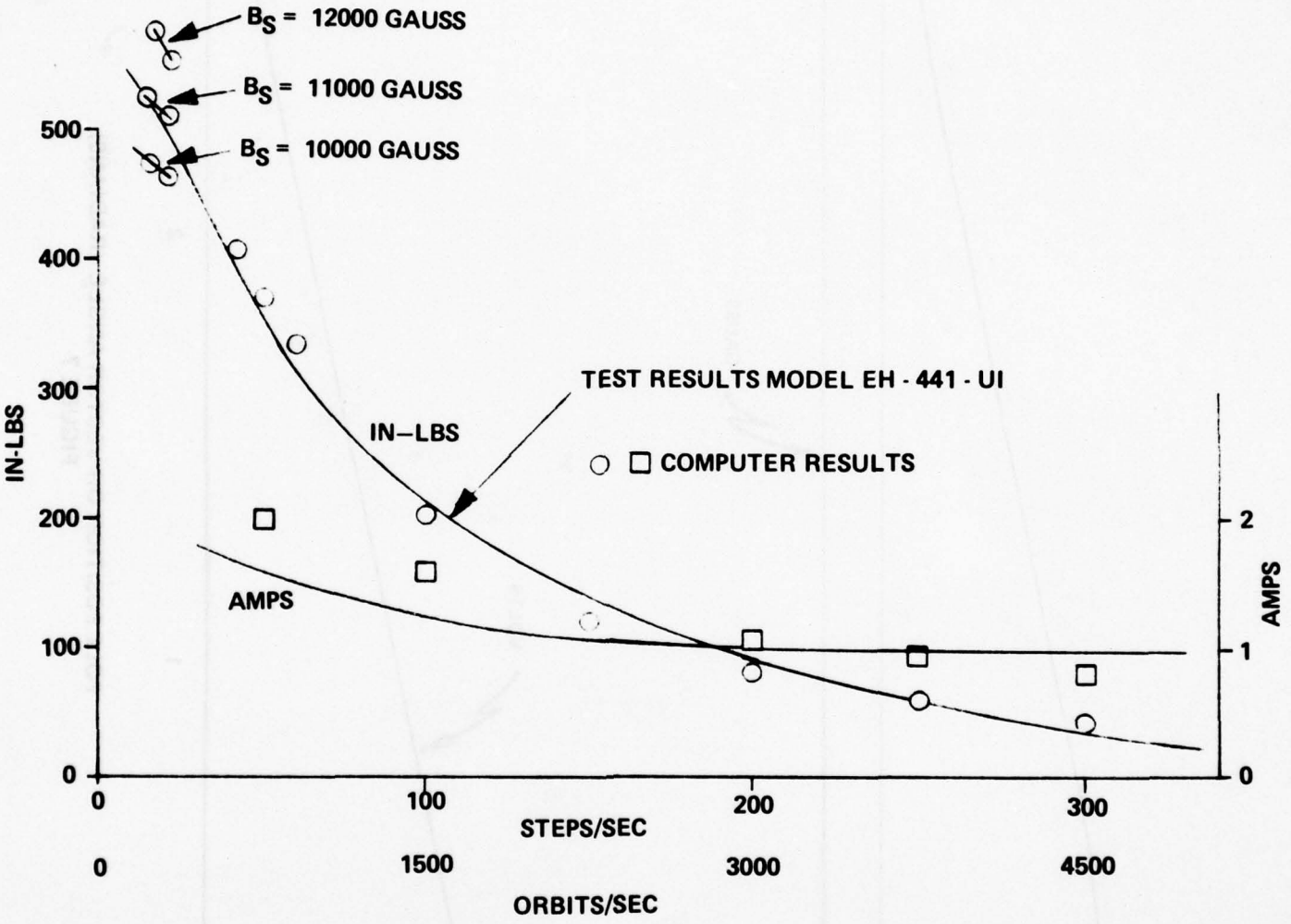

FIGURE 6 CORRELATION OF COMPUTER MODEL WITH TEST DATA

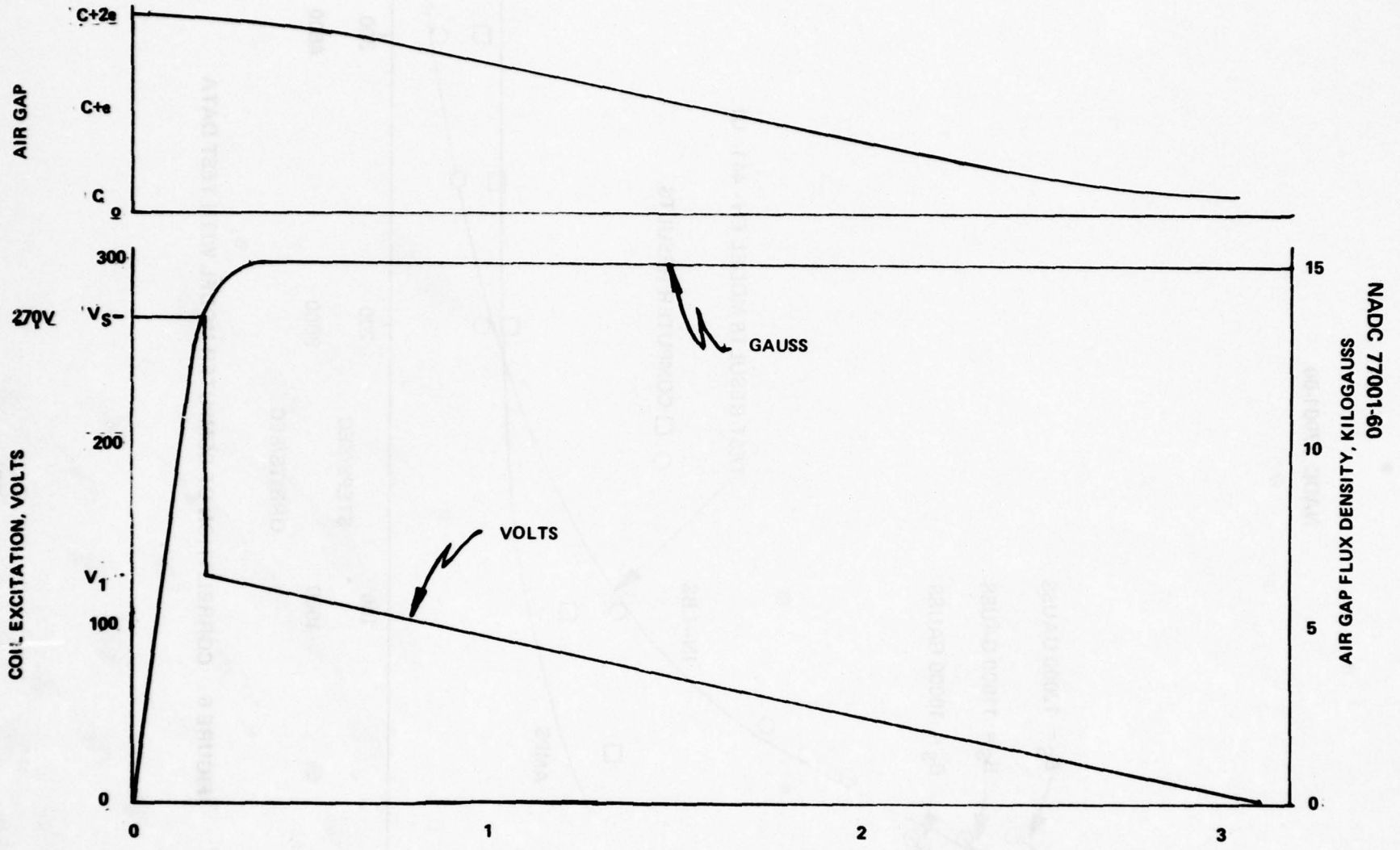
C+2e
C+e
C
AIR GAP
300
270V
V_S
200
V_1
100
0
COIL EXCITATION, VOLTS
GAUSS
VOLTS
15
10
5
0
AIR GAP FLUX DENSITY, KILOGAUSS
NADC 77001-60
0
1
2
3
POLE POSITION OR VECTOR ANGLE (RADIANS)

FIGURE 7

5 volts at 180 degrees (3.14 radians) vector rotation. This voltage waveform maintains a constant flux density for maximum efficiency.

Torque and current at 30 deg/sec vs gear ratio are shown in Figure 8 for 48% and 64% torque efficiency. An efficiency of 64% was obtained with previous Electric Dynavectors, and 48% is the expected efficiency for the pneumatic mode. Torque increases and current decreases as the ratio increases. The highest ratio considered was 470, because higher ratios could reduce performance in the pneumatic mode.

A reduction ratio of 470:1 gives an orbiting speed of 4008 rpm at an output rate of 55 deg/sec. Previous experience has shown that the pressure loading on the rotor will result in reduced bearing life if the maximum orbiting speed is much in excess of 4000 rpm. The loading is different in the electrical mode and higher speeds could be used for electrical operation only.

Figure 9 shows the effect of the number of turns per coil. Both the torque and current decrease as the number of turns is increased. However, the current decreases more than the torque. Therefore, increasing the number of turns should improve efficiency.

A ratio of 468:1 and 450 turns per coil were selected. The torque-speed curve with these parameters, and 48% efficiency, is shown in Figure 10.

The space available for the coil wires is 0.188 sq in. The wire size selected, AWG 25, has the following characteristics:

dia = 0.0179 inch

circular mils = 320

turns per square inch = 2475

The space needed is

450 turns/2475 = 0.182 sq. in.

Therefore, the area available is adequate.

At the specified maximum torque, 2200 in lbs., the current is 14 amps.

Amps per coil = 14/8 = 1.75 amps/coil

320/1.75 = 183 circular mils/amp

At the rated torque, 1500 in lbs., the current is 10 amps, or 1.25 amps per coil.

320/1.25 = 256 circular mils/amp

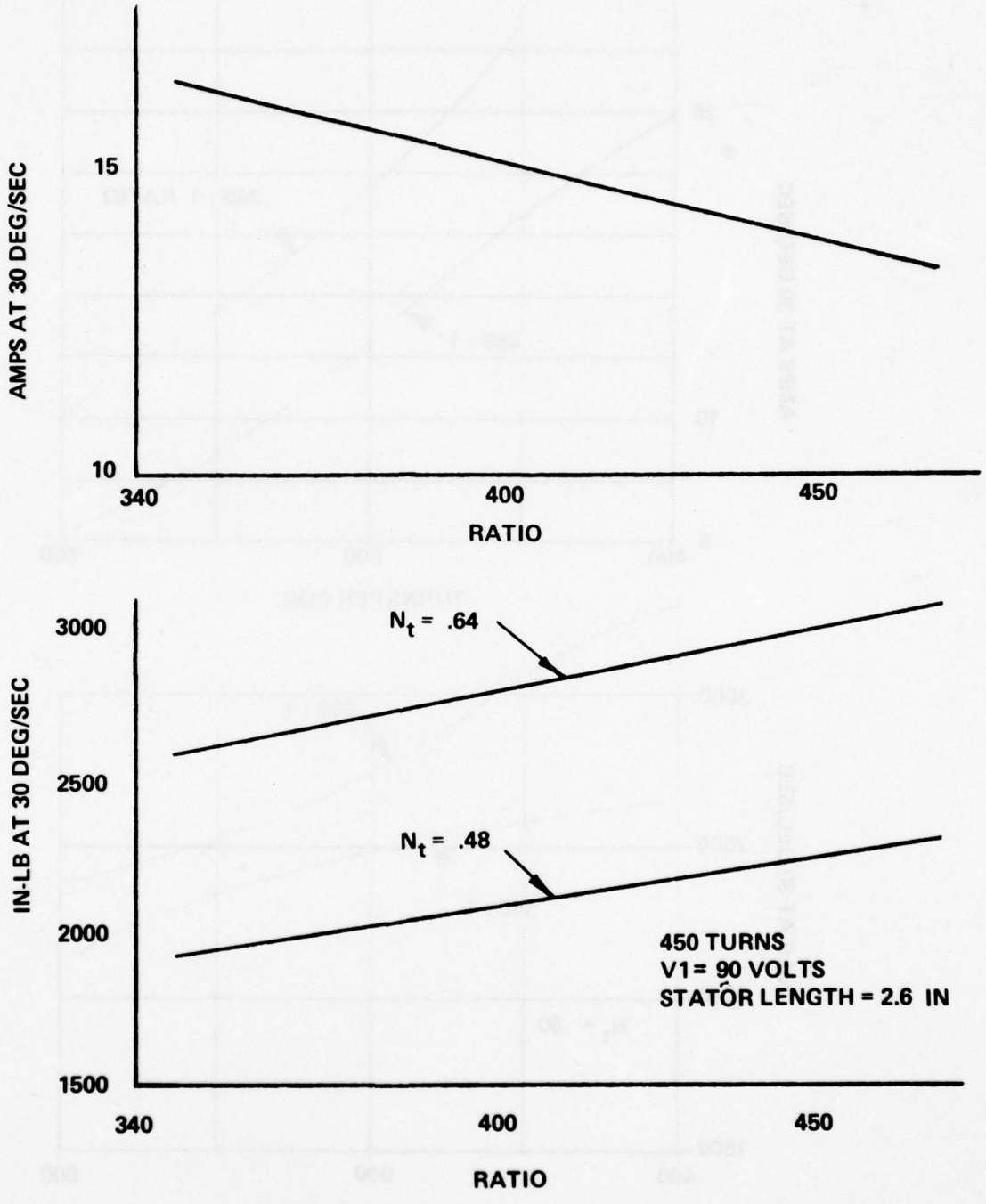

FIGURE 8 TORQUE AND CURRENT VS RATIO

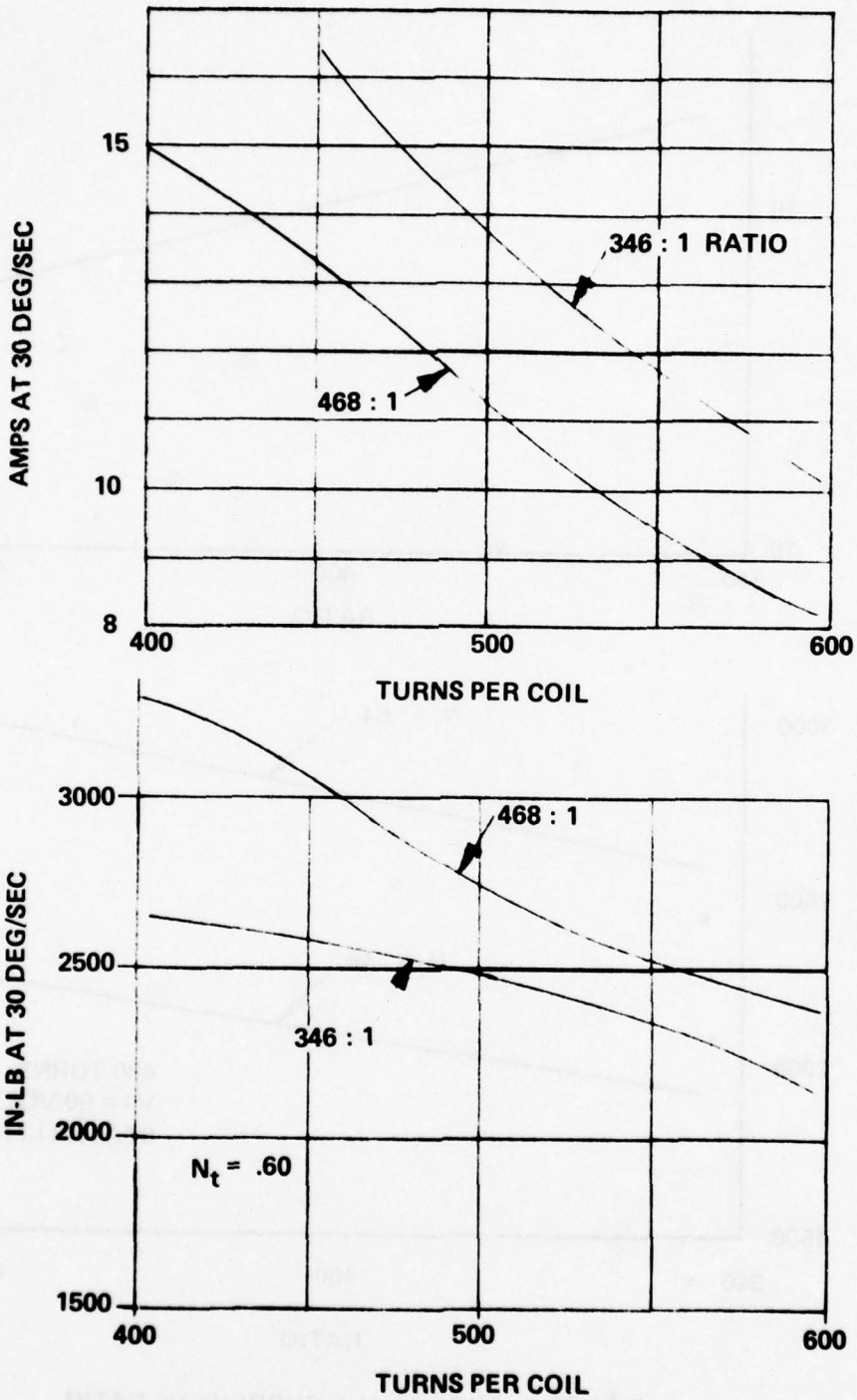

FIGURE 9 TORQUE AND CURRENT VS NUMBER OF TURNS

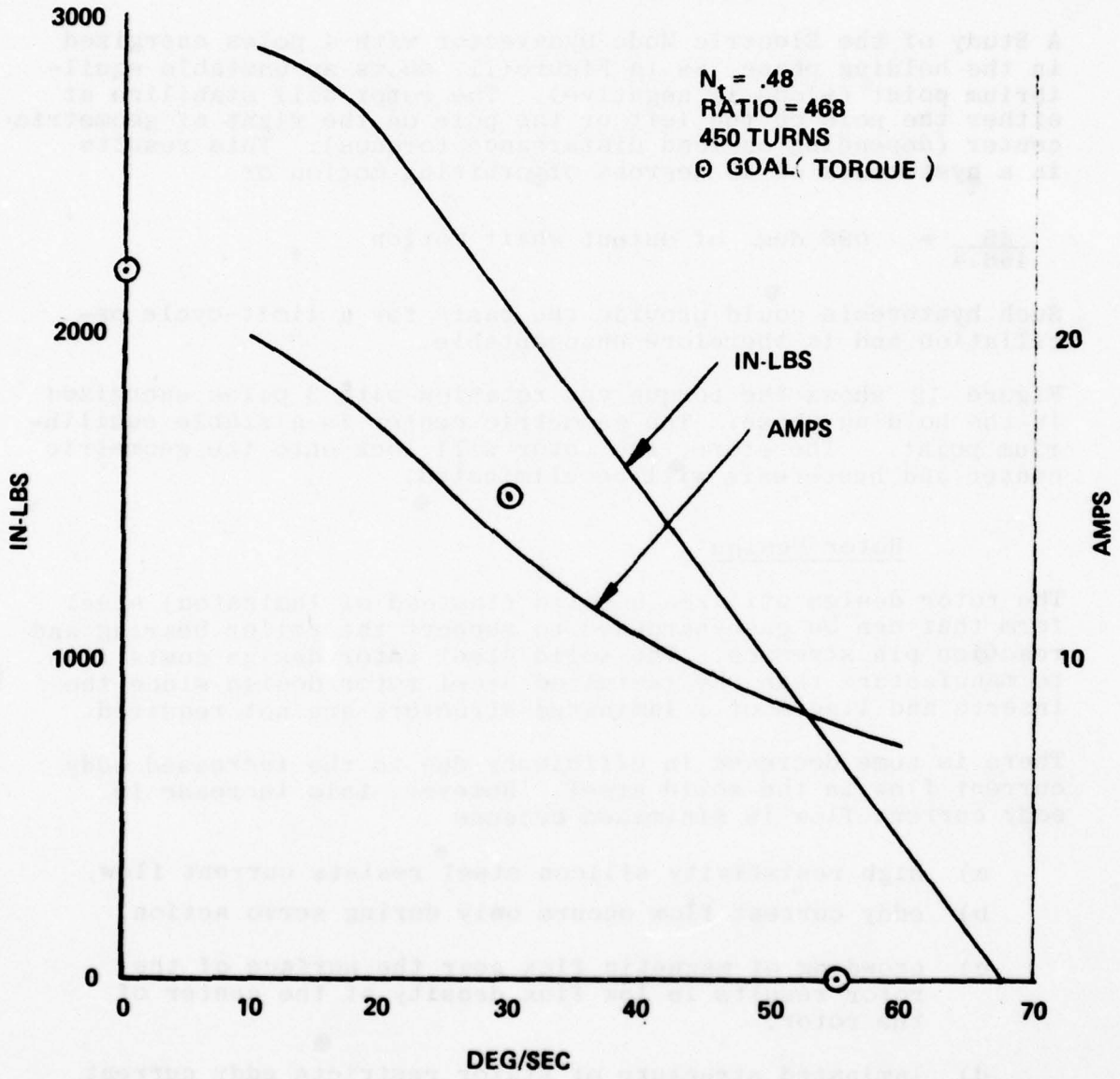

FIGURE 10 ELECTRIC MODE TORQUE – SPEED CURVE

Previous Electric Dynavectors have operated continuously with 200 circular mils/amp. Therefore, heating of the Dual Mode Actuator should not be a problem.

A Study of the Electric Mode Dynavector with 4 poles energized in the holding phase, as in Figure 11, shows an unstable equilibrium point (slope is negative). The rotor will stabilize at either the pole on the left or the pole on the right of geometric center (depending on load disturbance torques). This results in a hysteresis of 45 degrees of orbiting motion or

$$\frac{45}{468.4} = .096 \text{ deg. of output shaft motion}$$

Such hysteresis could provide the basis for a limit-cycle oscillation and is therefore unacceptable.

Figure 12 shows the torque vs. rotation with 3 poles energized in the holding phase. The geometric center is a stable equilibrium point. Therefore, the rotor will lock onto the geometric center and hysteresis will be eliminated.

Rotor Design

The rotor design utilizes a solid (instead of laminated) steel form that can be case-hardened to support the roller bearing and reaction pin stresses. The solid steel rotor design costs less to manufacture than the laminated steel rotor design since the inserts and liners of a laminated structure are not required.

There is some decrease in efficiency due to the increased eddy current flow in the solid steel. However, this increase in eddy current flow is minimized because

a) high resistivity silicon steel resists current flow,

b) eddy current flow occurs only during servo action,

c) crowding of magnetic flux near the surface of the rotor results in low flux density at the center of the rotor,

d) laminated structure of stator restricts eddy current flow.

Rotor Power Loss

The flux density cycles from 0 to 15,000 gauss with amplitude of 7,500 gauss. The core loss of M-19 silicon iron 0.025 inch thick at this amplitude and at 60 Hertz is 0.4 watts per pound. This loss is approximately 1/3 eddy current loss and 2/3 hysteresis loss. Eddy current power loss is proportional to frequency squared; hysteresis power loss is proportional to frequency. The rotor frequency at rated speed is 39.2 Hertz. The power loss for a laminated rotor is

$$Pr = D\ L\ w \left[\frac{1}{3}\left(\frac{n}{N}\right)^2 + \frac{2}{3}\left(\frac{n}{N}\right)\right]$$

where Pr = power loss, watts

D = servo action duty cycle

L = power loss per pound at 60 Hertz, watts

w = weight of rotor, lbs

n = rotor frequency, Hertz

N = 60 Hertz

$$Pr = 0.15 \times 0.4 \times 8.29 \left[\frac{1}{3}\left(\frac{39.2}{60}\right)^2 + \frac{2}{3}\left(\frac{39.2}{60}\right)\right]$$

$$Pr = .29 \text{ watts}$$

The eddy current loss for a solid rotor theoretically varies as the square of the thickness. However, the rotor is not an ideal flux generator, and the losses will be less than for an ideal generator. The rotors of previous Dynavectors have demonstrated an efficiency as an eddy current generator of 20%. Thus, the eddy current power loss for a solid rotor is

$$P_e = \left(\frac{\text{mean rotor thick}}{\text{lamination thick}}\right)^2 E\ D\ L\ w\left[\frac{1}{3}\left(\frac{n}{N}\right)^2\right]$$

where E = eddy current efficiency, 20%

$$P_e = \left(\frac{.875}{.025}\right)^2 \times 0.20 \times 0.15 \times 0.4 \times 8.29\left[\frac{1}{3}\left(\frac{39.2}{60}\right)^2\right]$$

$$P_e = 17.3 \text{ watts}$$

The hysteresis power loss for the solid rotor will be the same as for a laminated rotor, about 0.225 watt.

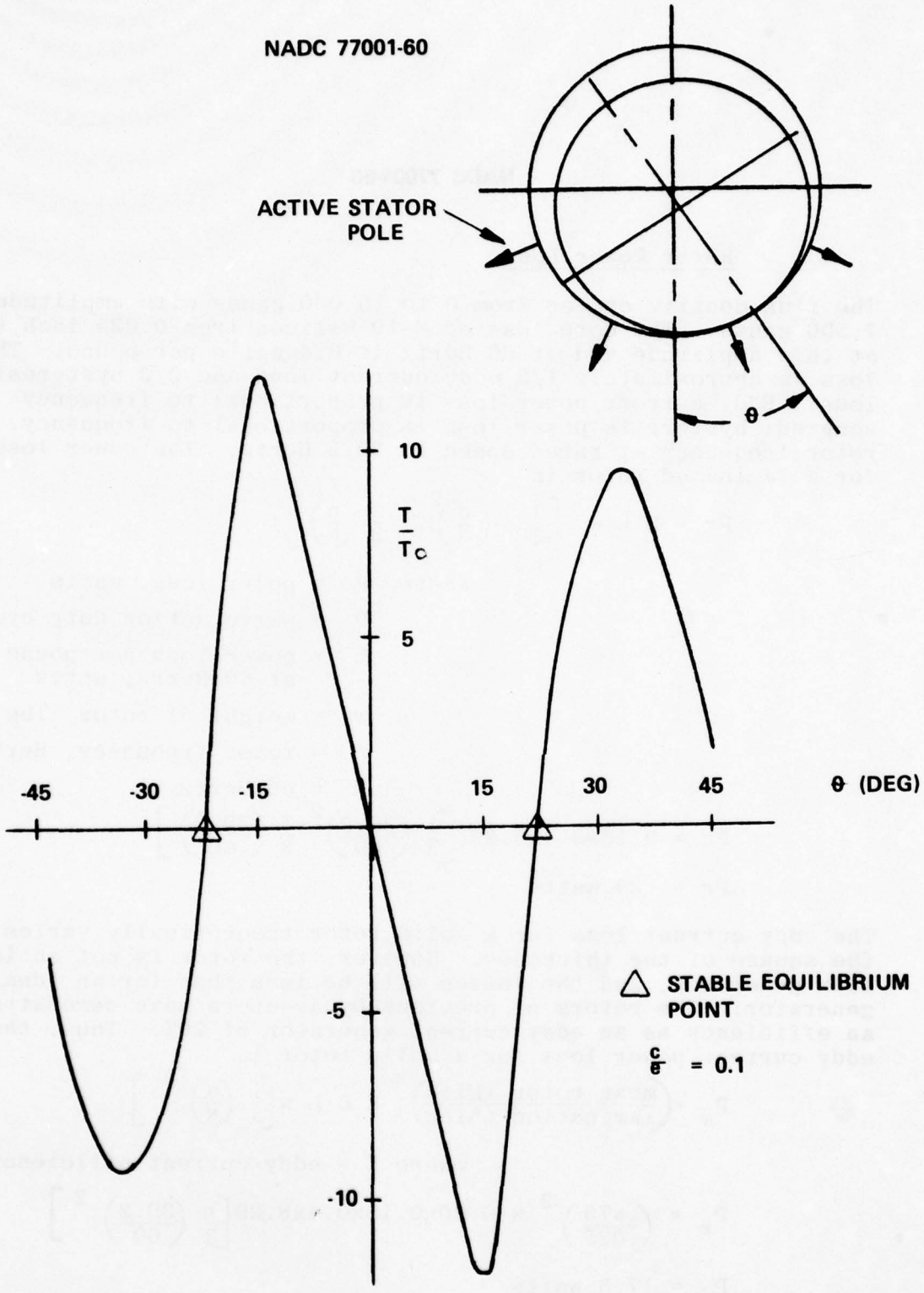

FIGURE 11 TORQUE VS ROTATION – 4 POLES EXCITED

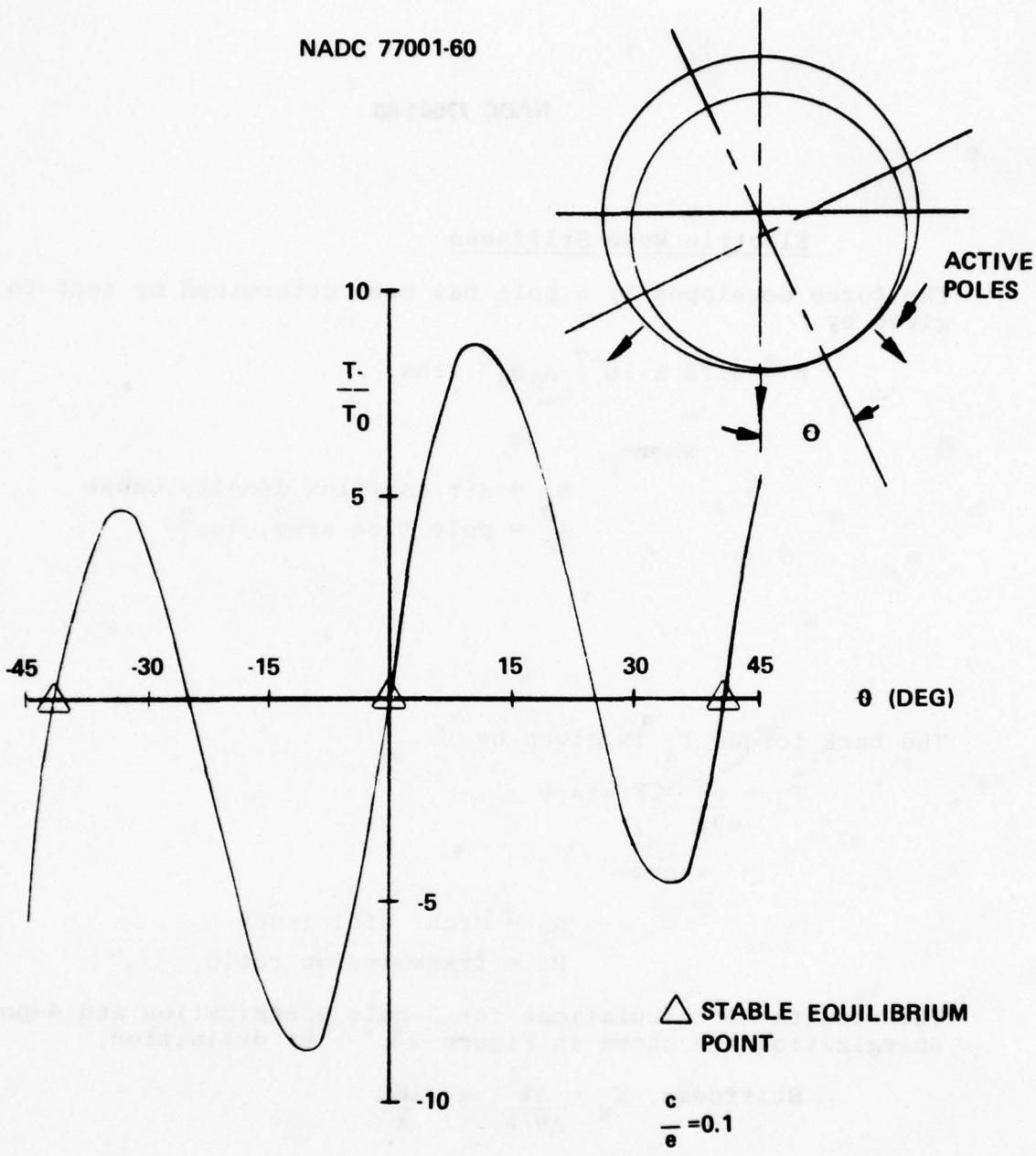

FIGURE 12 TORQUE VS ROTATION – 3 POLES EXCITED

Electric Mode Stiffness

The force developed by a pole has been determined by test to be given by

$$F = 3.75 \times 10^{-7} A_p B_a^2 \text{ lbs.}$$

where

B_a = air gap/flux density, Gauss
A_p = pole face area, in.^{2}

The back torque T_s is given by

$$T_s = \frac{eR}{n_t} \Sigma F \sin \theta$$

where

n_t = mech. efficiency
R = transmission ratio

The results of calculations for 3-pole energization and 4-pole energization are shown in Figure 13. By definition,

$$\text{Stiffness, } K_s = \frac{\Delta T}{\Delta \theta / R} \times \frac{180}{\pi}$$

where

ΔT = back torque, in.-lbs.
$\Delta \theta$ = orbit displacement, deg.
R = transmission ratio

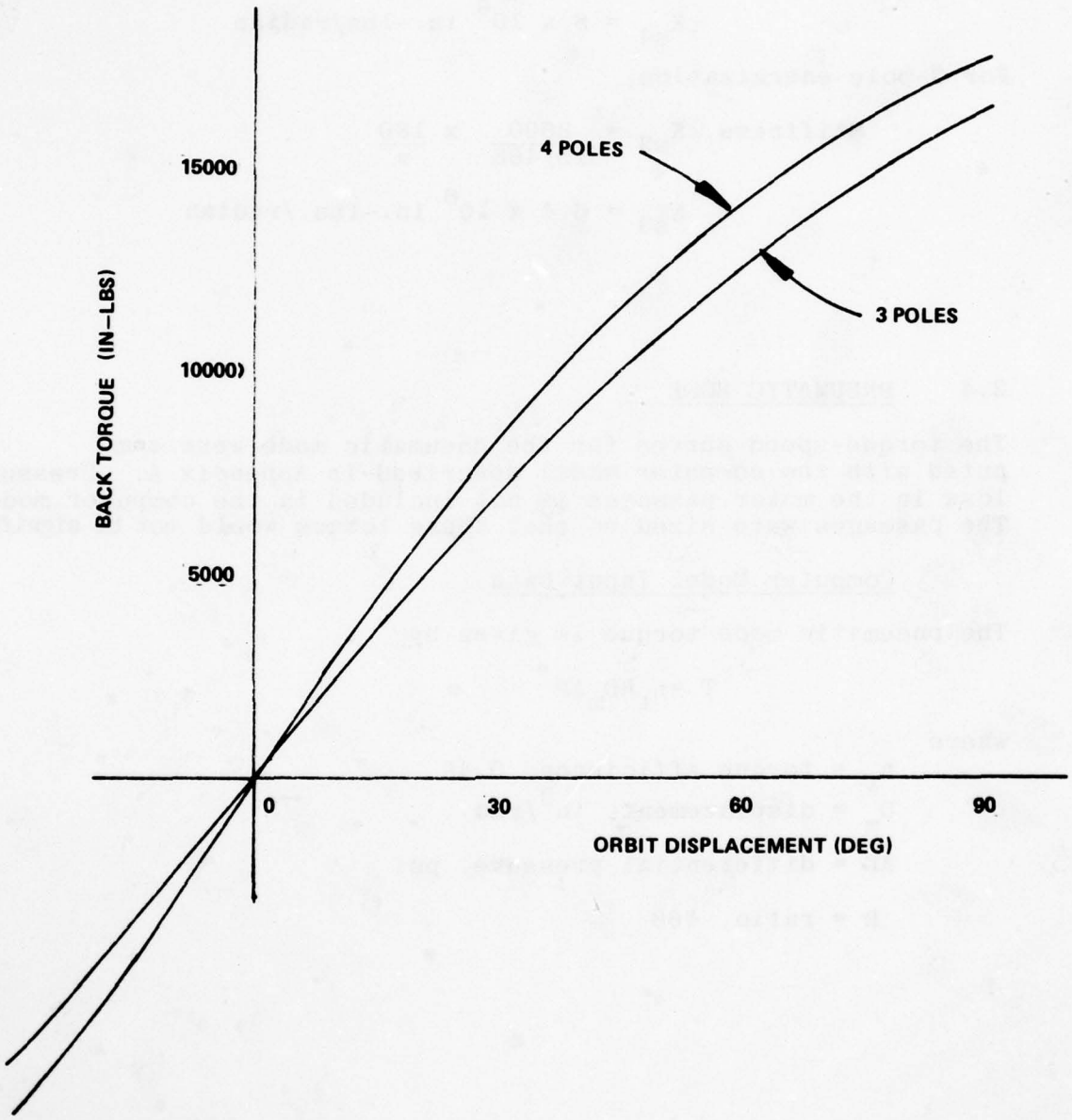

BACK TORQUE VS ORBIT DISPLACEMENT FOR 4–POLE ENERGIZATION AND 3–POLE ENERGIZATION
FIGURE 13

For 4-pole energization,

$$\text{Stiffness, } K_{s4} = \frac{4529}{15/468} \times \frac{180}{\pi}$$

$$K_{s4} = 8 \times 10^6 \text{ in.-lbs/radian}$$

For 3-pole energization,

$$\text{Stiffness, } K_{s3} = \frac{3600}{15/468} \times \frac{180}{\pi}$$

$$K_{s3} = 6.4 \times 10^6 \text{ in.-lbs./radian}$$

2.4 PNEUMATIC MODE

The torque-speed curves for the pneumatic mode were computed with the computer model described in Appendix A. Pressure loss in the motor passages is not included in the computer model. The passages were sized so that these losses would not be significant.

Computer Model Input Data

The pneumatic mode torque is given by

$$T = \eta_t R D_m \Delta P$$

where

η_t = torque efficiency, 0.48

D_m = displacement, in^3/rad

ΔP = differential pressure, psi

R = ratio, 468

The displacement is

$$D_m = D_v eb$$

where

b = rotor face width, in

D_v = vane chamber diameter

e = eccentricity

Inserting numerical values

$$D_m = 4.953 \times 0.0468 \times 3.1888 = 0.740 \text{ in}^3/\text{rad}$$

The differential pressure at the rated torque is

$$\Delta P = \frac{T}{\eta_t R D_m} = \frac{1500}{0.48 \times 470 \times 0.74} = 9 \text{ psi}$$

The principal case drain leakage path is from the commutator slot ends to the rotor inside diameter. Thus, the case drain leakage area equals the commutator slot width times the end clearance times the sum of the number of commutator feed slots and one-half the number of commutator slots.

$$A_{cd} = 0.125 \times 0.0015 \times 24 = 0.0045 \text{ in.}^2$$

There are two commutator slots for each chamber. The total commutator flow area for the motor inlet flow is equal to two times the maximum area for one chamber. Thus, the effective commutator area is

$$A_c = 4 \times \text{slot length} \times \text{eccentricity}$$

$$= 4 \times 0.438 \times 0.0468 = 0.082 \text{ in.}^2$$

There are two cross port leakage paths. The first is from the high pressure commutator slots to the low pressure slots. The flow area equals the slot length times the end clearance times the number of slots at upstream pressure. Thus

$$A_{cpl} = 0.875 \times 0.0015 \times 16 = 0.021 \text{ in.}^2$$

The second cross port leakage path is across the ends of the vanes. This leakage area is

$$A_{cp2} = 2 \times \text{vane height} \times \text{end clearance}$$

$$= 2 \times 0.391 \times 0.0015 - 0.0012 \text{ in.}^2$$

The total cross port leakage area is then

$$A_{cp} = A_{cp1} + A_{cp2} = 0.021 + 0.0012 = 0.0222 \text{ in.}^2$$

Computer Results

The pneumatic mode torque-speed curves for several valve areas at 0 deg. F are shown in Figure 14. A valve area of 0.072 sq. in. provides the specified torque and speed. The effect of gas temperature is shown in Figure 15. At 140°F there is about a 12% increase in speed.

The effect of reducing the end clearance to 0.001 inch is shown in Figure 16. With the reduced clearance, the valve area can be reduced to 0.060 sq. in.

The motor torque will be a little lower than shown in these curves due to pressure drop in the motor passages. This pressure drop is shown in the next section to be about 2 psi.

Figures 17 and 18 show the effect of reduced supply pressure. These curves can be used to estimate the effect of line pressure drop. A 2 psi line pressure drop is approximately equivalent to lowering the supply pressure 2 psi.

Figure 19 shows the effect of of varying the commutator flow area. It appears that reducing the commutator flow area 50%, to 0.082 sq. in., will result in more torque at 30 deg/sec., due to the decreased leakage area. This would also reduce the total flow, and thus would reduce the pressure drop in the passages.

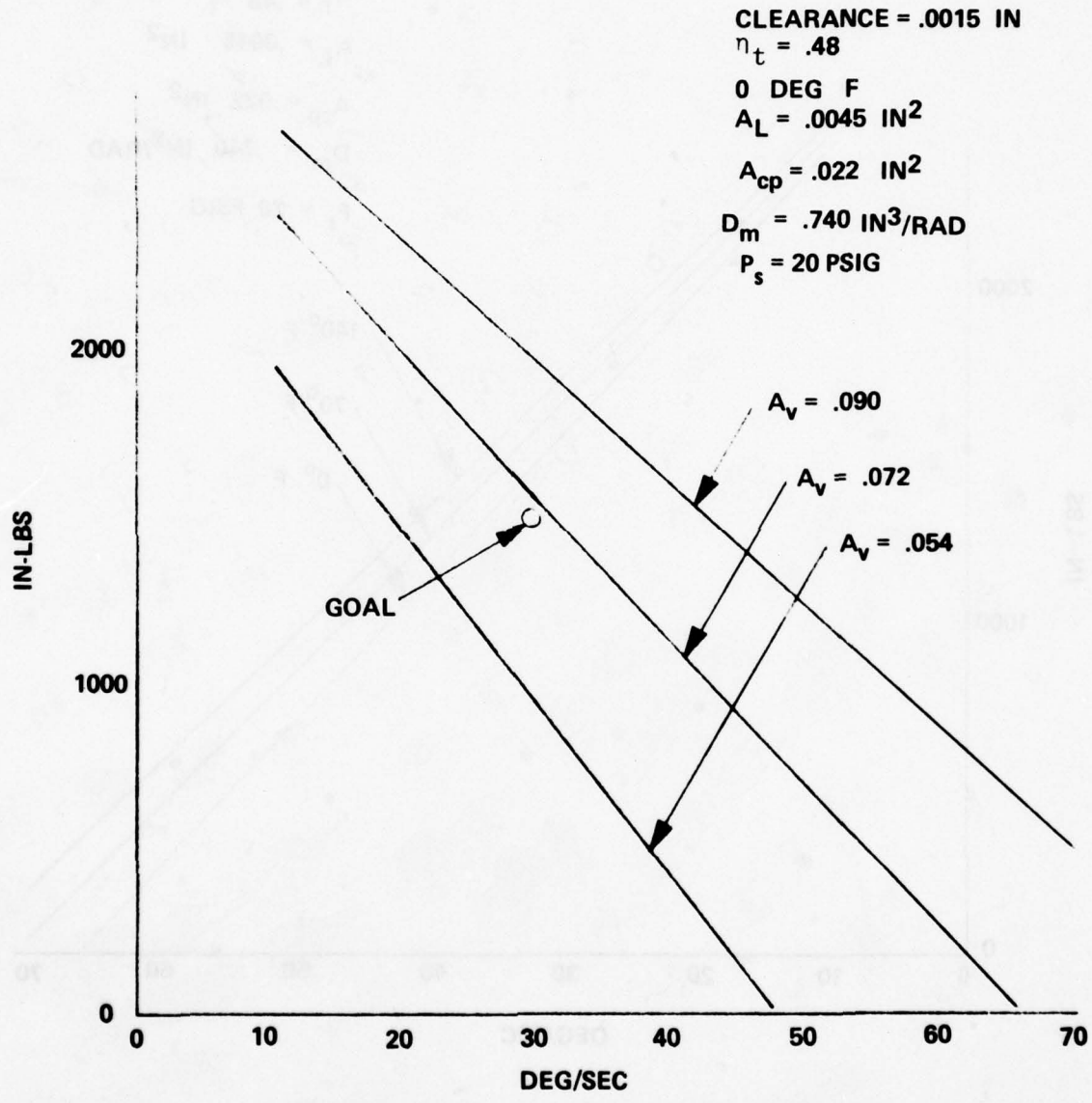

FIGURE 14 PNEUMATIC MODE TORQUE – SPEED CURVES

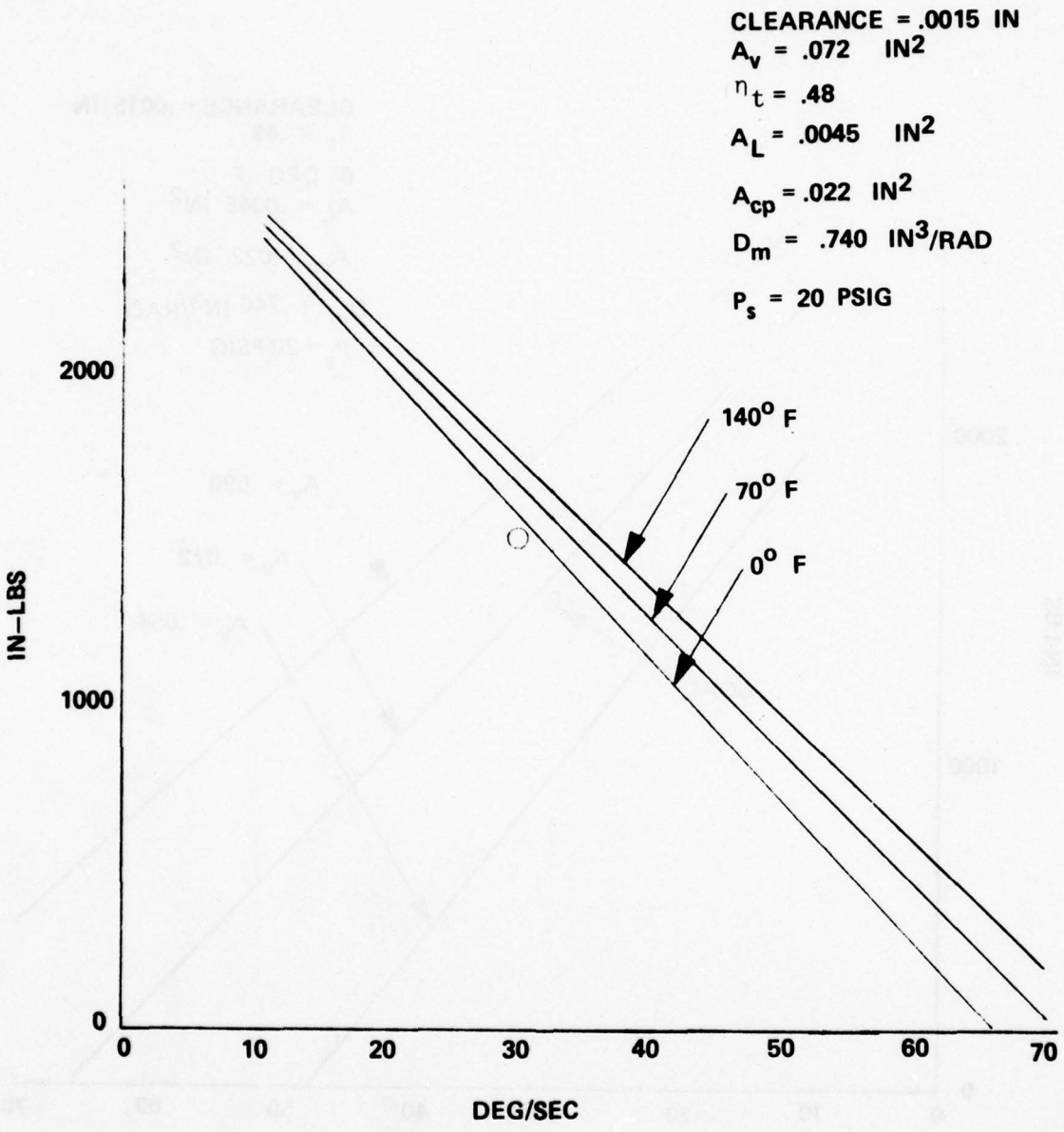

FIGURE 15 EFFECT OF GAS TEMPERATURE

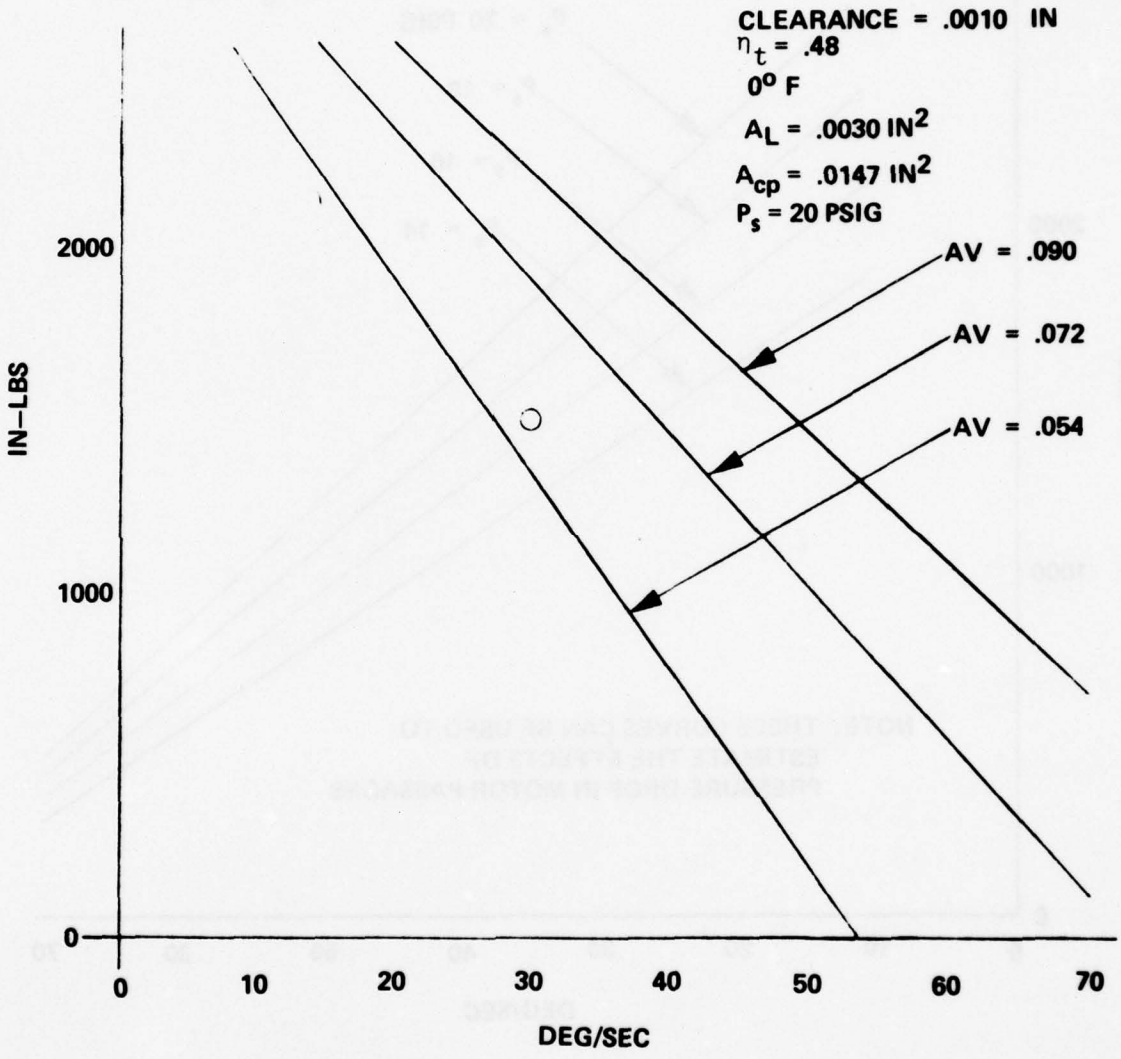

FIGURE 16 EFFECT OF REDUCED END CLEARANCE

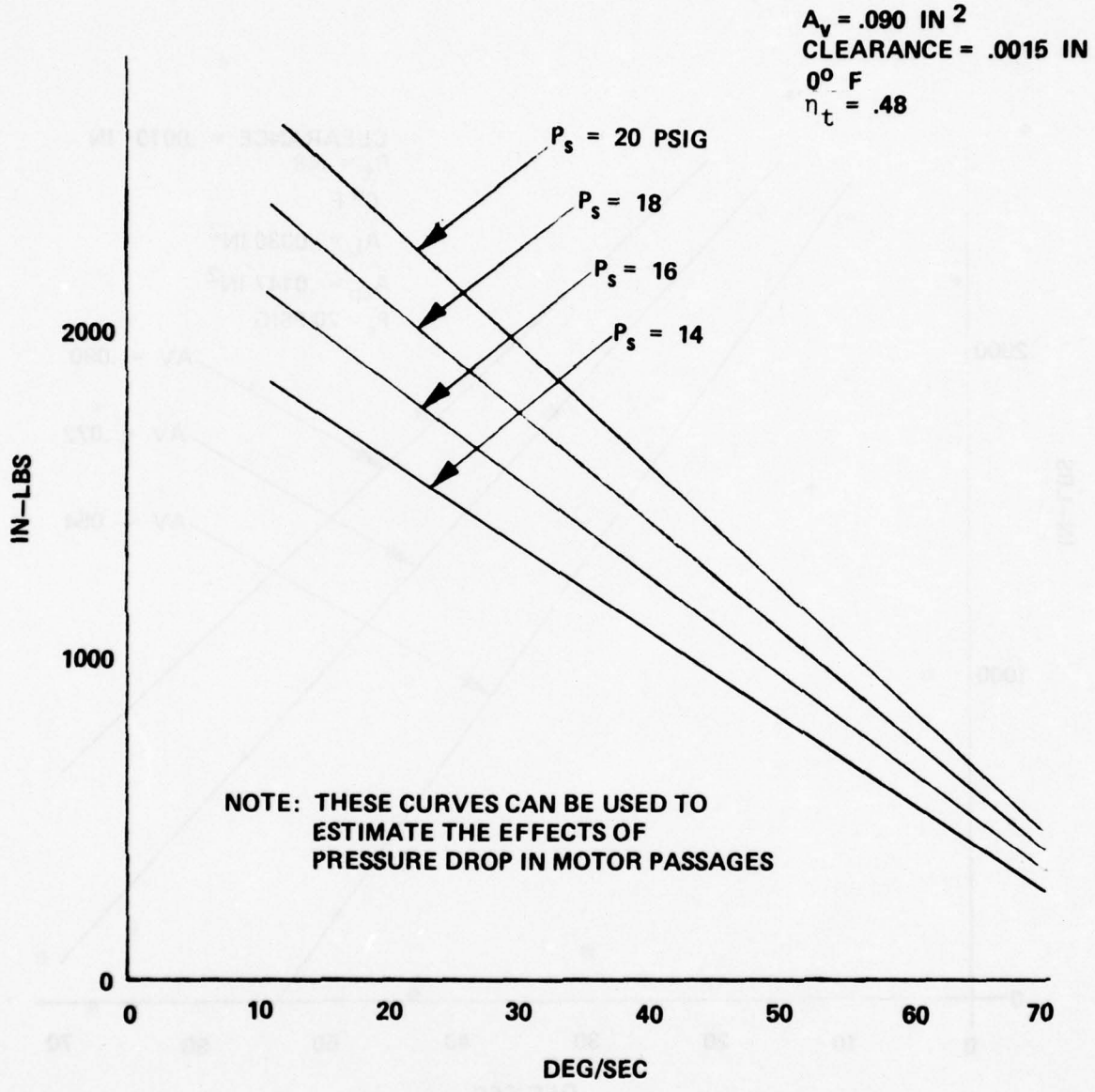

FIGURE 17 EFFECT OF REDUCED SUPPLY PRESSURE

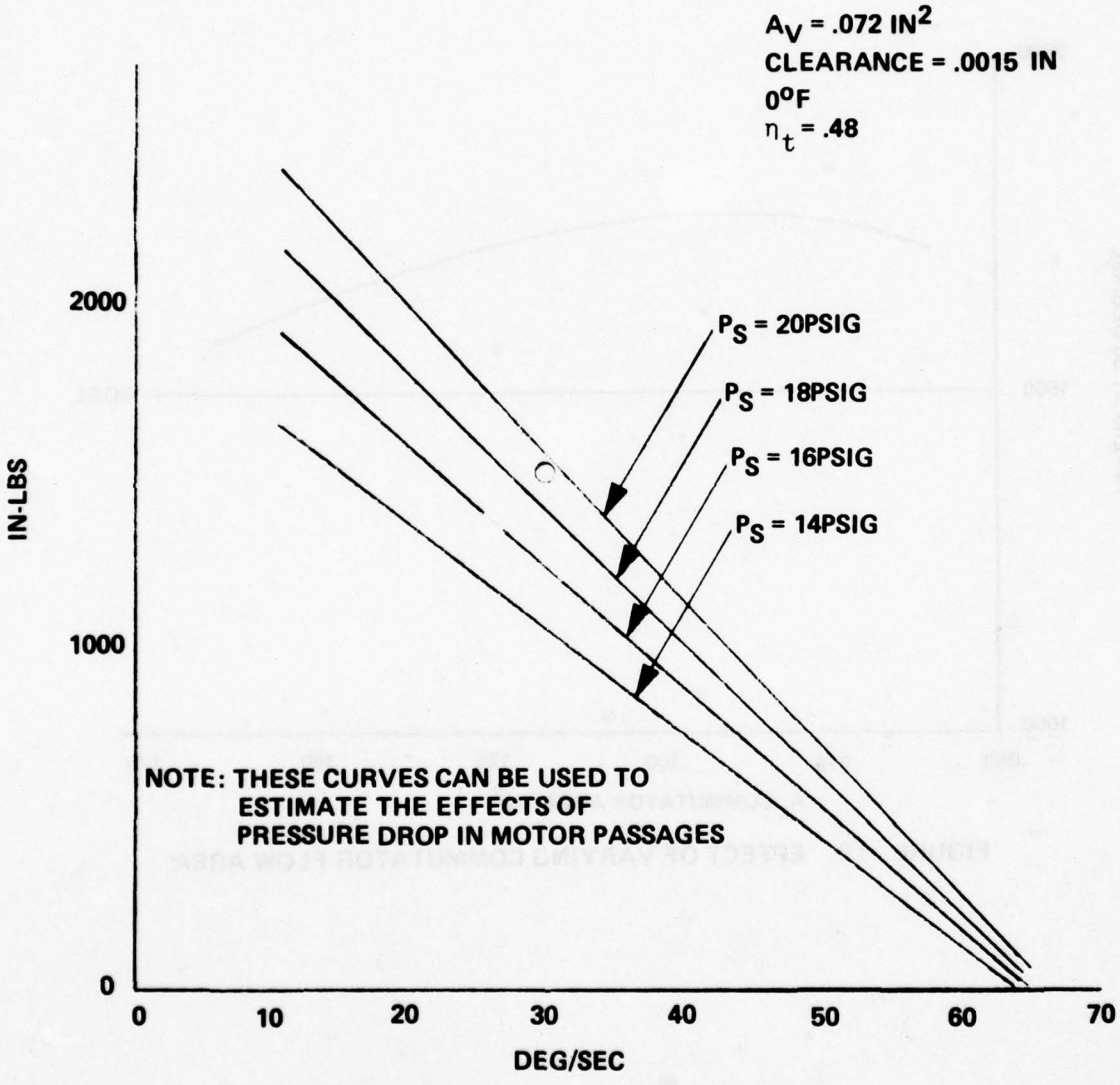

FIGURE 18 EFFECT OF REDUCED SUPPLY PRESSURE

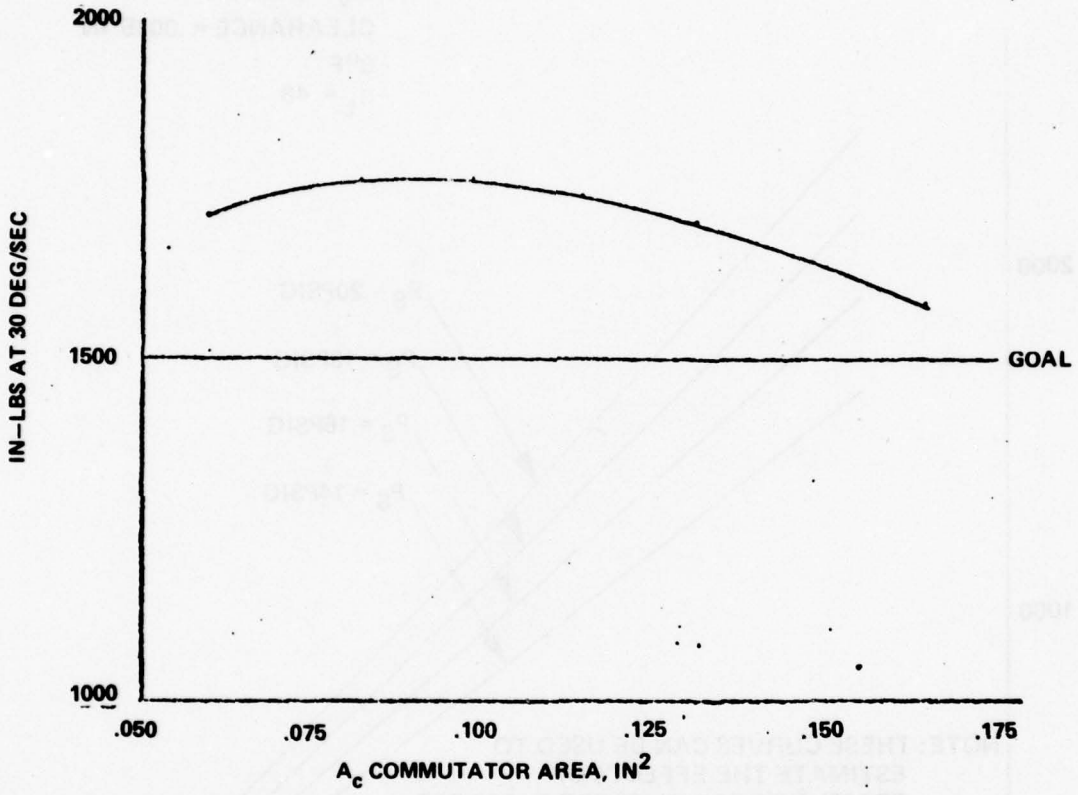

FIGURE 19 EFFECT OF VARYING COMMUTATOR FLOW AREA

2.4.1 Pressure Drop in Passages

The computer model for the torque-speed curves does not include pressure drop in the motor passages. Due to the low supply pressure, the motor passages must be sufficiently large to cause little pressure drop.

The pressure drop in a passage is given by

$$\Delta P = f \frac{L}{d} \quad \frac{1}{2g\rho} \left(\frac{W}{A}\right)^2$$

where

A = flow area, sq in

d = diameter, in

f = friction factor

g = acceleration of gravity, 386 in/sec^2

L = passage length, in

The air density is given by

$$\rho = \frac{P}{RT} \quad \frac{lb}{in^3}$$

where

P = pressure, psi

R = gas constant, 640 $in/^oR$

T = air temperature, ^oR

The procedure is to assume a value for f, calculate the flow and Reynolds number N_R, and then find the correct value of f from curves of f vs N_R.

From the computer results, at rated speed and torque:

Air flow = 0.01946 lb/sec

PV1 = 32.67 psi, ρ = 0.0000963 lb/in^3

PM1 = 31.03 psi, ρ = 0.0000915 lb/in^3

PM2 = 19.69 psi, ρ = 0.0000580 lb/in^3

PV2 = 17.75 psi, ρ = 0.0000523 lb/in^3

The calculated pressure drops are

PASSAGE	DIAMETER in	LENGTH in	ΔP psi	VOLUME cu-in
Inlet	0.312	1.000	0.07	0.0764
Discharge	0.312	1.000	0.13	0.0764
Bypass-inlet	0.250	3.812	0.21	0.2383
Bypass-discharge	0.250	3.812	0.40	0.2383
Commutator manifold	0.312	4.950	0.10	0.4822
inlet	0.312	11.000	0.19	1.0700
Sum			1.10	2.1816

There is an additional pressure drop due to direction change of the flow. This pressure drop is given by

$$\Delta P = 0.4\rho \frac{V^2}{2g} n = \frac{0.2}{\pi^2 \rho g} \frac{W^2}{\frac{4}{d}} n$$

n = number of 90 degree bends

There are approximately ten 90 degree bends. Therefore, the pressure loss is

$$\Delta P = \frac{0.2}{\pi^2 (0.52 \times 10^{-4})(386)} \frac{(0.01946)^2}{(0.312)^4} \times 10 = 0.40 \text{ psi}$$

Total pressure drop = 1.10 + 0.40 = 1.5 psi

Percent of motor differential pressure

$$= \frac{1.5}{12.98} \times 100 = 11.6\%$$

The volume under compression is one-half the motor clearance volume plus one-half the passage volume. Thus

One-half passage volume	= 1.09 sq. in.
One-half motor clearance volume	= 1.17 sq. in.
Volume under compression	= 2.26 sq. in.

2.4.2 Servovalve

A single state electro-pneumatic servovalve was developed for this program.

Figure 20 shows the assembly drawing for this valve. The frequency response is 25 Hz at 90 deg. phase shift. Rated torque motor power is 2 watts.

The torque motor provides a ± 0.015 in. stroke. The spool diameter of 1.75 inches generates a maximum flow area,

$$A_v = \pi Dx = \pi(1.75)(.015) = 0.0825 \text{ in.}^2$$

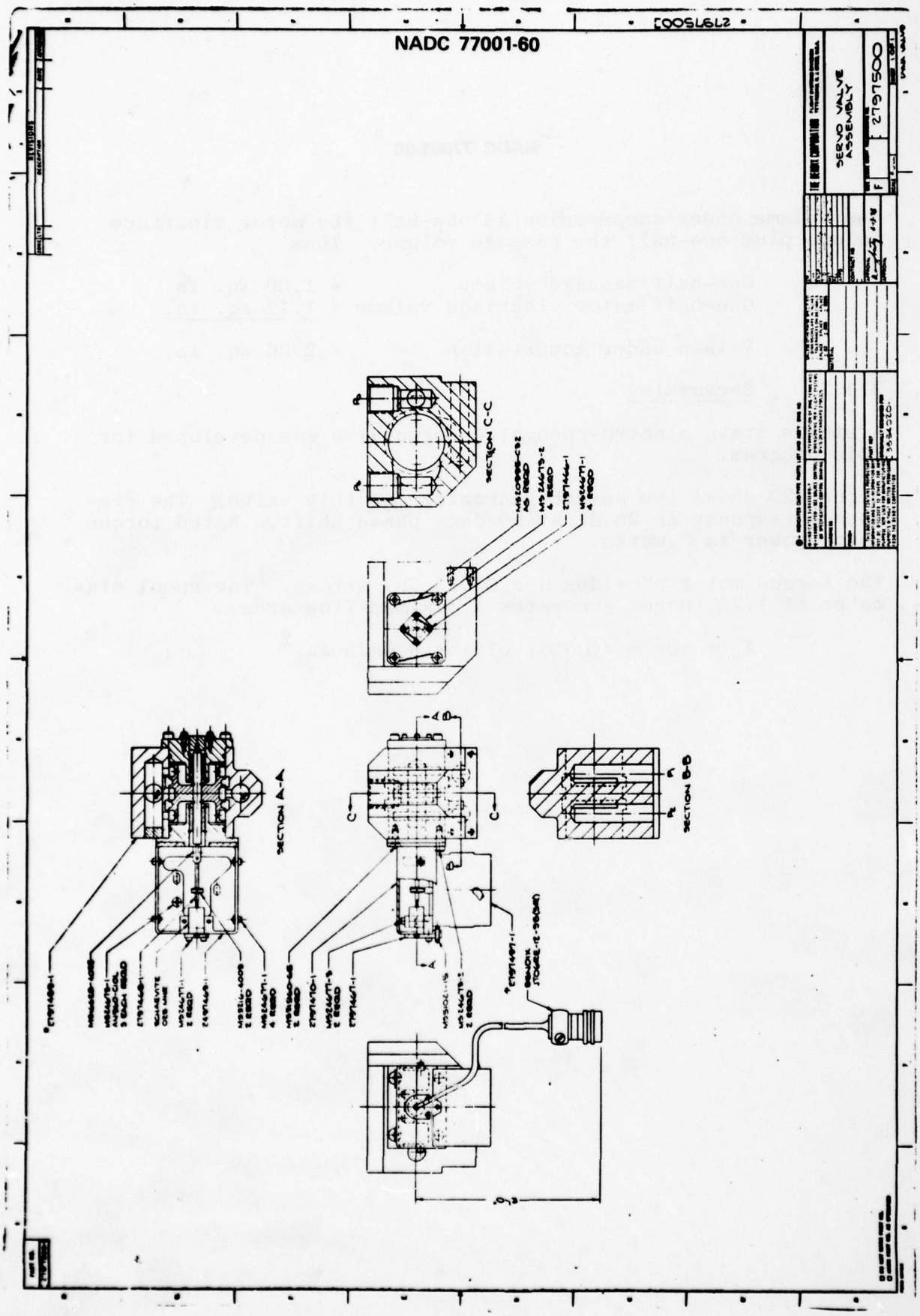
SERVO VALVE ASSEMBLY
27997500
SECTION A-A
SECTION B-B
SECTION C-C

FIGURE 20

If the flow of $70^{o}F$ air is sonic-limited by the valve,

$$W = \frac{.53\ AcP_1}{\sqrt{T_R}}$$

where

W = flow, lb./sec.
A = flow area, $in.^2$
C = discharge coeff.
P_1 = upstream pressure, psia
T_R = temperature of air, ^{o}R

$$W = \frac{.53 \times .0825 \times .75 \times 35}{\sqrt{460 + 70}}$$

W = .05 lb./sec., $70^{o}F$ air

W = .053 lb./sec., $0^{o}F$ air

W = .047 lb./sec., $140^{o}F$ air

Thus, the valve control range adequately covers the computer-rated air flow requirement of W = .01946 lb/sec., $70^{o}F$ air.

One noteworthy feature of this valve design is that the spool is connected to a drive rod which is guided by ball bushings. This suspension method effectively eliminates many of the problems that are associated with stiction and friction in pneumatic spool valves.

An LVDT transducer, Schaevity 025 MHR, provides position feedback information for the torque motor-spool position loop. This inner servo loop acts to linearize and smooth the control action of the servo valve assembly.

3.0 RESPONSE

3.1 PNEUMATIC MODE

The block diagram for pneumatic mode response is shown in Figure 21.

The open loop actuator transfer function, assuming the load spring rate to be negligible, is

$$\frac{\theta_r}{T_c} = \frac{1}{\partial T/\partial n} \quad \frac{1}{S\left(1 + \frac{2\zeta}{\omega_n}S + \frac{1}{\omega_n^2}S^2\right)} \qquad (9)$$

where

$$\omega_n^2 = \frac{1}{\tau J} \quad \frac{\partial T}{\partial n}$$

$$\zeta = \frac{1}{2} \omega_n \frac{J}{\partial T/\partial n}$$

J = Combined inertia of motor and load, in lb sec^2

$\frac{\partial T}{\partial n}$ = Slope of torque-speed curve

The compressiblility time constant is given by

$$\tau = \frac{V\frac{\partial T}{\partial n}}{kP_o(RD_m)^2}$$

D_m = Actuator displacement, in ^{3}/rad

k = Specific heat ratio, 1.4 for air

P_o = Nominal pressure, psia

R = Transmission ratio

V = Volume under compression, in^3

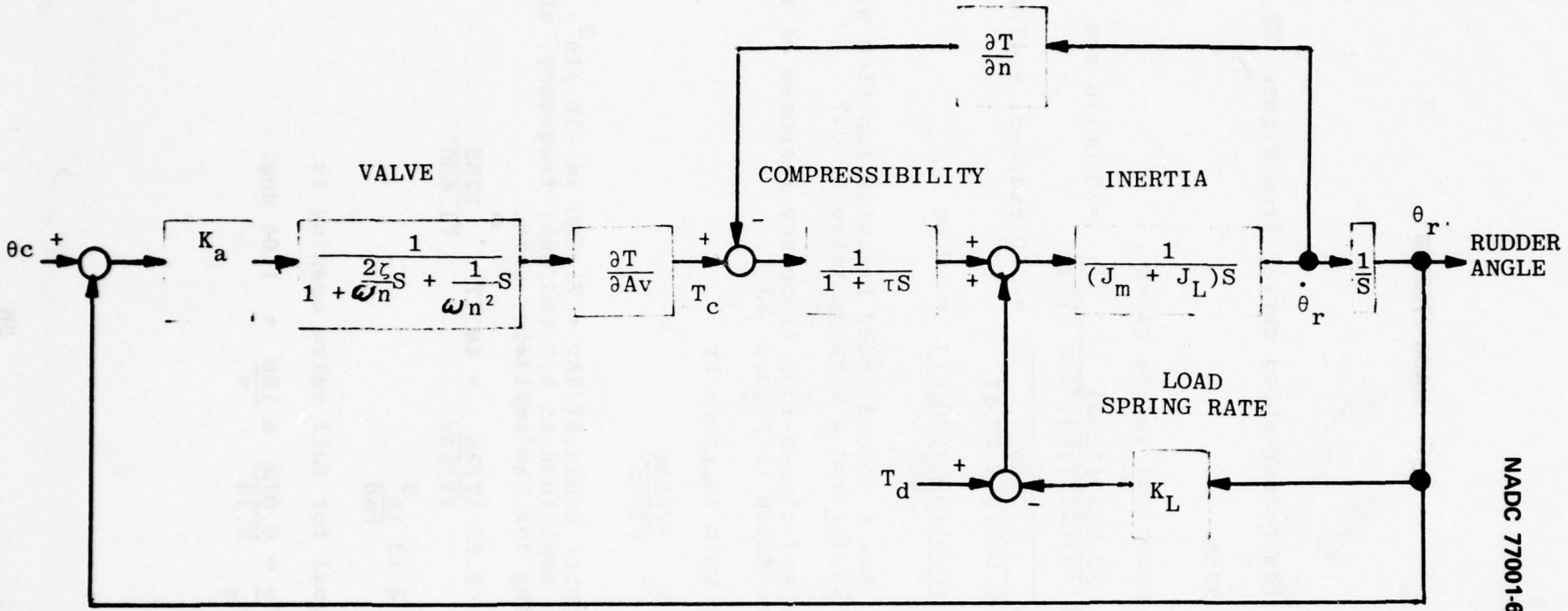

FIGURE 21 PNEUMATIC MODE BLOCK DIAGRAM

The slope of the torque-speed curve, from Figure 22, is

$$\frac{\partial T}{\partial n} = 3255$$

Substituting numerical values gives

$$\tau = \frac{(2.262)(3255)}{(1.4)(24.7)(0.74 \times 470)^2} = 0.00176 \text{ sec.}$$

$$\omega_n = \sqrt{\frac{3255}{0.00176 \times 20.47}} \approx 300 \text{ rad/sec.} = 47.75 \text{ Hz.}$$

$$\zeta = \frac{(0.5)(300)(20.47)}{3255} \approx 0.94$$

The servovalve has a second order transfer function with a natural frequency of 25 Hz. and a damping ratio of 0.7.

The open-loop and closed-loop frequency response of the actuator with valve are shown in Figure 23.

The open-loop gain is given by

$$K_o = K_a \frac{\partial T/\partial Av}{\partial T/\partial n}$$

From the computer study, $\partial T/\partial Av = 71{,}600$ in.-lb./in^2. K_o equals the open loop amplitude at 1.0 rad/sec. frequency, which is 46.77. Solving for the amplifier gain,

$$K_a = 46.77 \frac{\partial T/\partial n}{\partial T/\partial Av} = 46.77 \frac{3255}{71{,}600}$$

$$K_a = 2.13 \frac{\text{in}^2}{\text{rad}}$$

The error signal for full valve opening is

$$\varepsilon = \frac{Av}{K_a} = \frac{0.072}{2.13} \times \frac{180}{\pi} = 1.94 \text{ deg.}$$

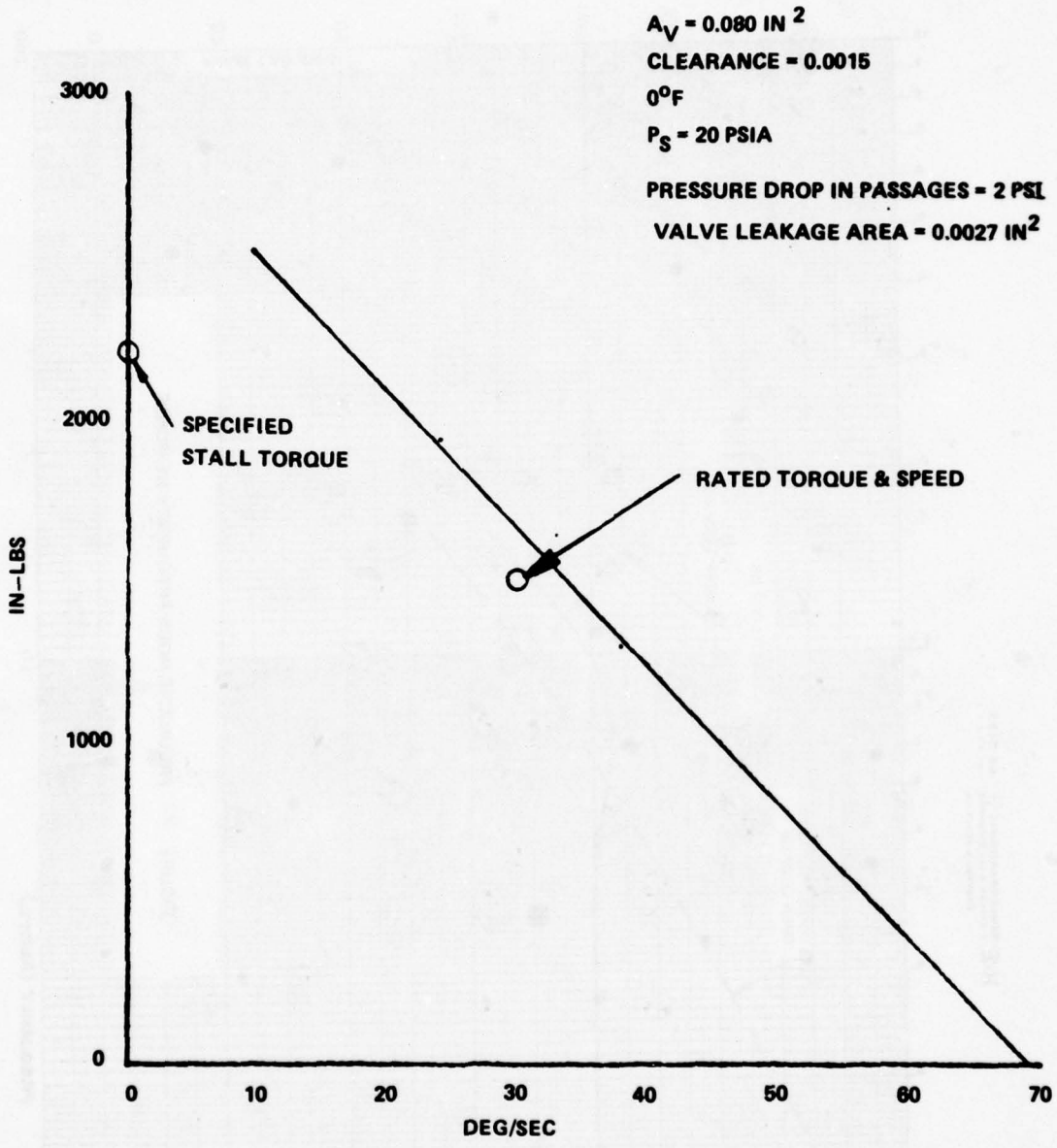

FIGURE 22 PNEUMATIC MODE TORQUE–SPEED CURVE

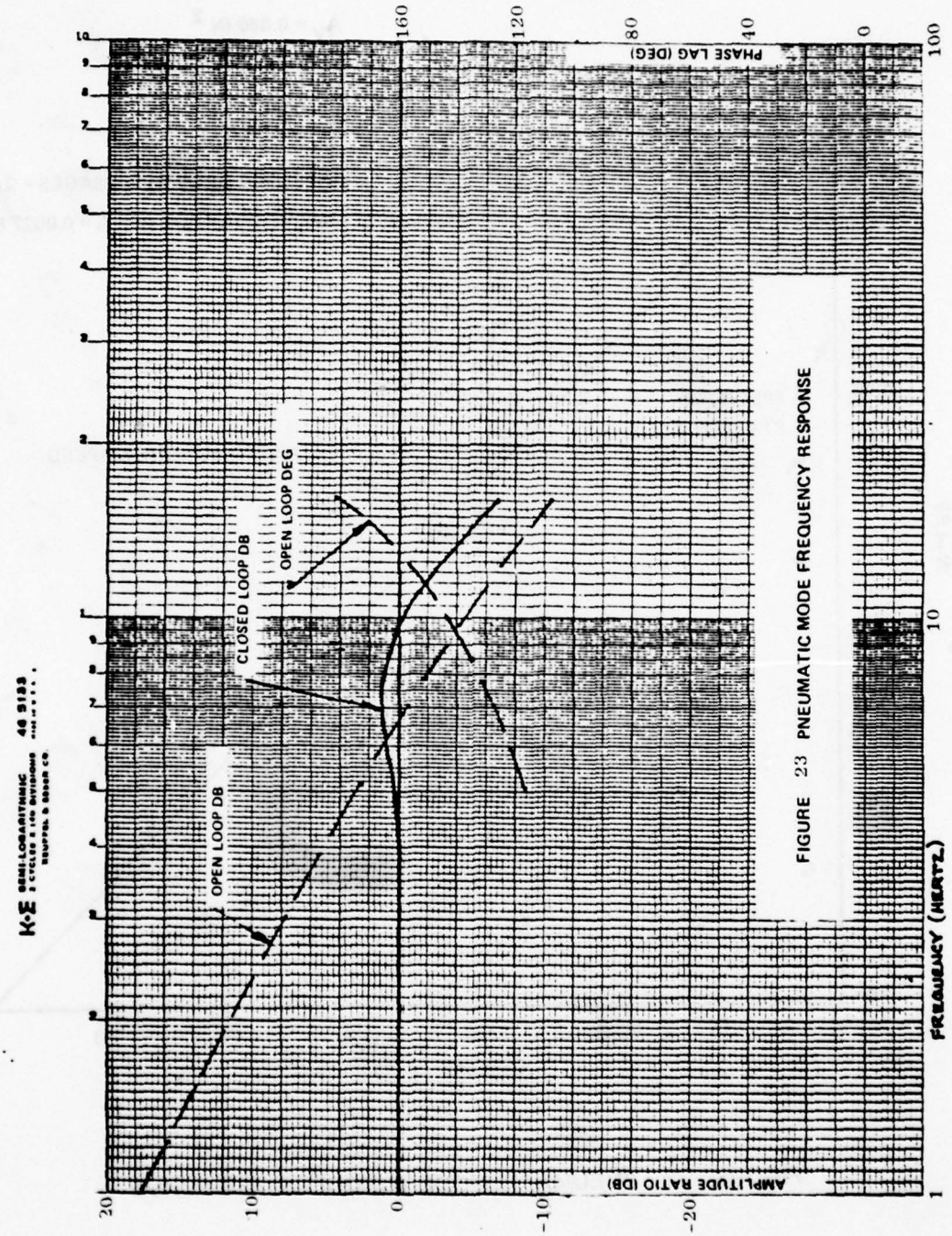

FIGURE 23 PNEUMATIC MODE FREQUENCY RESPONSE

Pneumatic Mode Stiffness

The pneumatic mode stiffness varies with amplitude. The small signal stiffness is

$$K_s = K_a \frac{\partial T}{\partial A} = 2.13 \times 71{,}600$$

$$K_s = 1.525 \times 10^5 \text{ in.-lb./rad}$$

The stiffness at maximum amplitude equals the peak torque divided by the error to saturate.

$$K_s' = \frac{2200}{1.94} = 6.5 \times 10^4 \text{ in.-lb./rad}$$

Electric Mode Stiffness and Synchronization

The electric mode stiffness with 3 poles energized and magnetically saturated is

$$K_{s3} = 6.4 \times 10^6 \text{ in-lb/rad}$$

as shown in Section 2.3. Thus, the electric mode stepping-motor stiffness is 40 to 100 times greater than the pneumatic mode motor stiffness. Consequently the electric motor forces will dominate the rotor movement and the pneumatic commutation plates that are part of the rotor will then automatically synchronize the pneumatic motor force vector to the electric motor force vector.

Pneumatic Mode Torque Saturation

The amplitude at which pneumatic torque saturation will occur is determined from the open loop transfer function (9). Thus

$$\theta = \frac{2Ts}{\partial T/\partial n} \left[\frac{1}{Re^2 + Im^2}\right]^{1/2} \cdot \frac{180}{\pi} \text{ deg}$$

where

$$Re = \frac{-2\zeta}{\omega_n}\omega = \frac{-2 \times .94}{300}\omega^2 = -0.00626\omega^2$$

$$Im = \frac{\omega - \omega^3}{\omega_n^2} = \omega - \frac{\omega^3}{90000}$$

Figure 24 shows the amplitude at which torque saturation occurs vs frequency. For frequency response testing to 20 hertz, the input amplitude should not exceed 0.5 degree peak to peak.

3.2 ELECTRIC MODE RESPONSE

The linear block diagram for response in the electric mode is shown in Figure 25. Figure 26 shows a nonlinear block diagram. The commanded step rate ω_c, which is actually the pulse frequency, is proportional to the error signal ε. Each pulse provides full excitation to the motor coils. The torque developed is proportional to the torque angle θ_t, which is the phase angle between the commanded angle θ_c and the rudder angle θ_r. $\partial T/\partial n$, the slope of the torque-speed curve, accounts for the decrease in torque with increasing speed due to the back emf. The controller makes the effect of inductance negligible.

The actuator open loop transfer function, with the load spring rate assumed negligible, is

$$\frac{\omega r}{\omega_c} = \frac{1}{1 + \frac{25}{\omega_n} S + \frac{1}{\omega_n^2} S^2}$$

where

$$\omega_n^2 = \frac{R}{J} \frac{\partial T}{\partial \theta_t}$$

$$\zeta = \frac{1}{2} \omega_n \frac{1}{R} \frac{\partial T/\partial n}{\partial T/\partial \theta_t}$$

J = Combined inertia of motor and load, in lb sec^2

R = Gear ratio

The actuator stall torque equals the maximum stall torque times the sine of the torque angle.

$$T = T_s \sin \theta_t$$

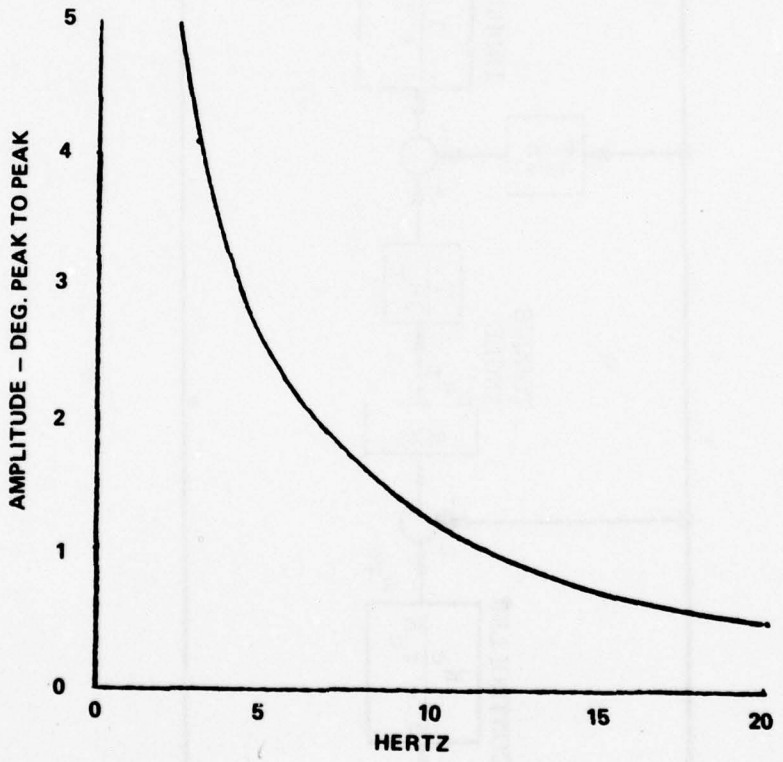

FIGURE 24 AMPLITUDE AT WHICH TORQUE SATURATION OCCURS – PNEUMATIC MODE

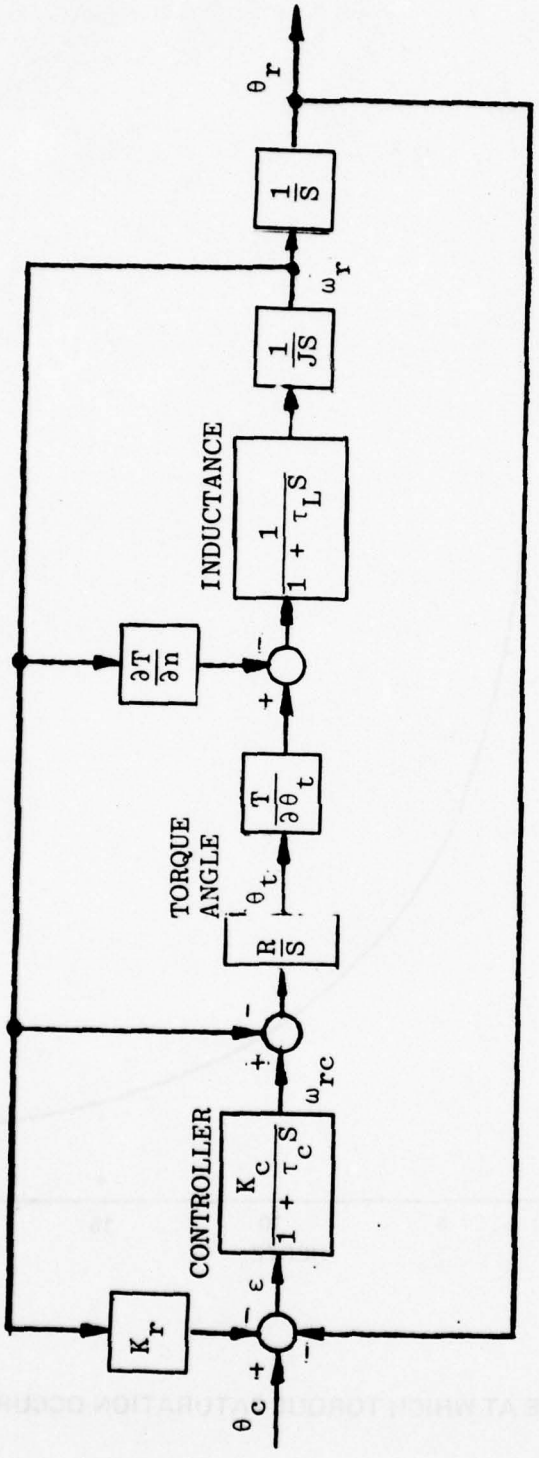

FIGURE 25 LINEAR BLOCK DIAGRAM – ELECTRIC MODE

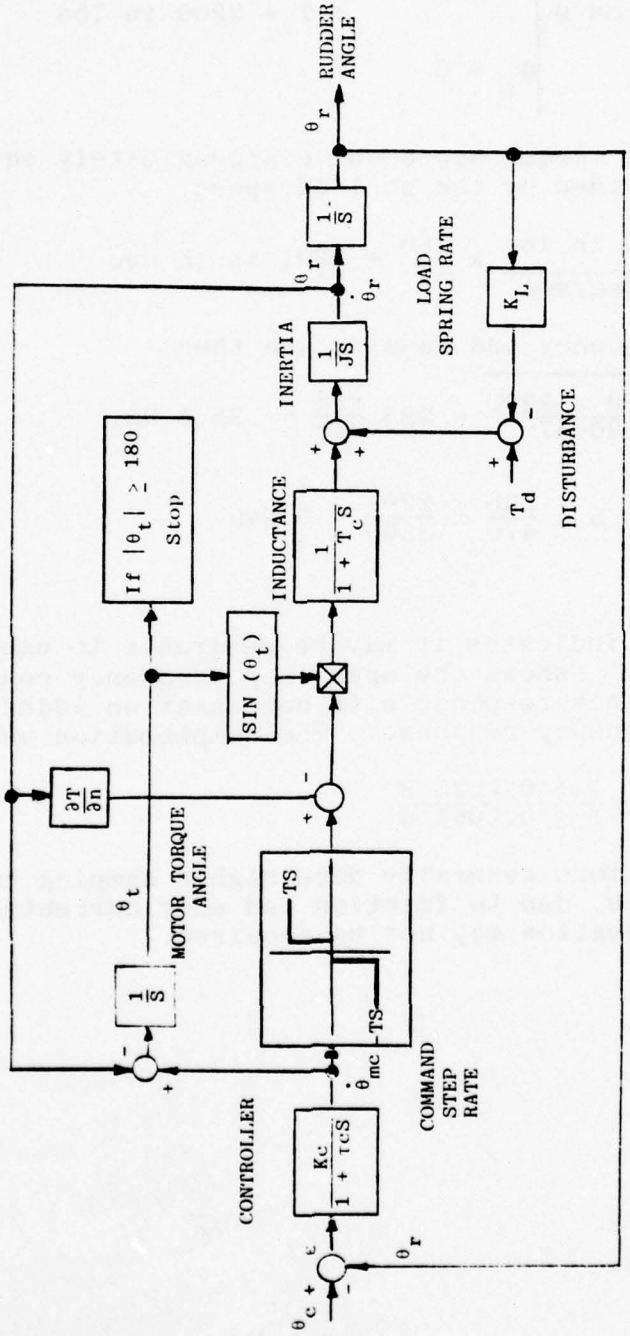

FIGURE 26 NON-LINEAR ELECTRIC MODE BLOCK DIAGRAM

Thus $\frac{\partial T}{\partial \theta_t} = T_s \cos \theta_t \Big|_{\theta_t = 0} = T_s = 2200$ in lbs

The slope of the torque-speed curve approximately equals the stall torque divided by the no load speed.

$$\frac{\partial T}{\partial n} = \frac{2200 \text{ in lbs}}{55 \text{ deg/sec}} \times \frac{180}{\pi} = 2291 \text{ in lb sec}$$

The natural frequency and damping are then

$$\omega_n = \sqrt{\frac{470 \times 2200}{20.47}} = 225 \frac{\text{rad}}{\text{sec}} = 35.8 \text{ Hz.}$$

$$\zeta = 0.5 \times \frac{225}{470} \times \frac{2291}{2200} = 0.249$$

The low damping indicates it may be desirable to use compensation. Figure 27 shows the open loop frequency response, the open loop frequency response with compensation added, and the closed loop frequency response. The compensation used was

$$\frac{1 + 0.0025\ S}{1 + 0.0054\ S}$$

Dynavector actuators generally have higher damping than indicated by analysis, due to friction and eddy currents. Therefore, the compensation may not be required.

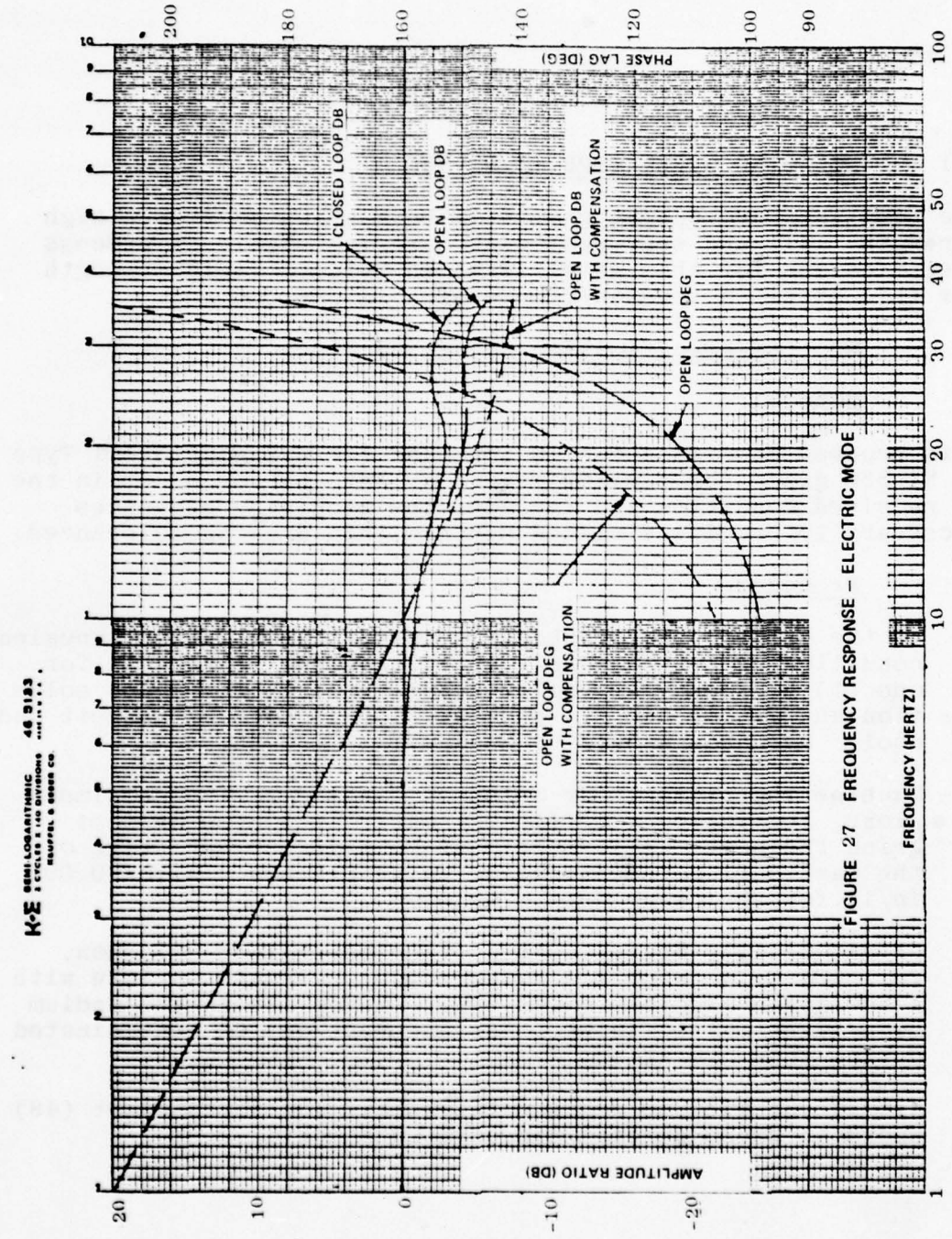

FIGURE 27 FREQUENCY RESPONSE – ELECTRIC MODE

4.0 MATERIALS

4.1 MARAGING STEEL TYPE 18 NI 350

The ring gear and output gear will be fabricated from a high strength, gall-and wear-resistant maraging steel. A process specification for this steel is shown below. Yield strength for this steel in tension/compression is 330,000 psi.

Process Specification, Maraging Steel

General

This process specification is intended for Maraging Steel Type 18 Ni 350 grade (or similar grade) billet, bar or sheet in the as received condition and includes the machining sequences necessary to provide finished parts within drawing tolerances.

Procedure

1) If the billet, bar or sheet is not in the solution annealed condition, solution anneal at 1650 degree Fahrenheit for one (1) hour and air cool to room temperature. Then solution anneal for one (1) hour at 1450 degrees Fahrenheit and cool. Hardness should be Rockwell 'C' 30-35.

2) Machine the billet, bar or sheet forging to finish dimensions, leaving only sufficient material to lap or dust grind the part. Allowance must be made for shrinkage of the part during the nitriding-aging process. Allow 0.001 in/in for shrinkage during aging.

3) Ultrasonically degrease in a trichlorethylene solution, followed by a deionized water rinse. Prepare surface with a 200 grain aluminum oxide blast, using air as the medium to a light matte finish. Surface must not be contaminated during this operation.

4) Nitride at 875-880 degrees Fahrenheit for forty-eight (48) hours in 25-30 percent dissociated ammonia.

5) Harness to be:

Case	Rockwell "C' 66-67
	Superficial Rockwell '15N' 92-93
Core	Rockwell 'C' 55 MIN

6) Dust grind or lap to finish dimensions.

7) A test specimen of ½ inch diameter bar one and one-half (1½) inches long centerless ground and copper plated for half the length to a thickness of 0.001/0.0015 inches shall accompany the parts to determine hardness and case characteristics.

8) Similar grade of steel: Teledyne VASCOMAX 350.

4.2 SILICON STEEL, 2½ SILICON COMPOSITION

The rotor will be fabricated from 2½% silicon steel for optimum magnetic properties, then case-hardened and nickel-plated for wear and corrosion resistance.

Process Specification, Silicon Steel

General

This process specification is intended for an Electrical Steel with a nominal composition of 2.5% Silicon. The material may be received as a billet, bar, or sheet. This specification describes the heat treat and machining sequences necessary to provide finished parts within drawing tolerances.

Procedure

1) Machine the billet, bar or sheet forging to finish dimensions, leaving only sufficient material to lap or dust grind the part. Allowance must be made for .0003 inch nickel plate.

2) Ultrasonically degrease in a trichlorethylene solution, followed by a deionized water rinse. Prepare surface with a grain aluminum oxide blast, using air as the medium to a light matte finish. Surface must not be contaminated during this operation.

3) Carburize part in accordance with 1919225(PS) .018 to .020 inch thick.

4) Hardness, Case: Rockwell C60-64

5) Dust grind or lap to finish dimension allowing for .0003 inch nickel plate and final dust grind or lap.

6) Electroless Nickel Plate all surfaces .0003 to .0005 inch per 1919253(PS).

7) Final dust grind or lap to finish dimensions.

8) A test specimen shall accompany parts to determine hardness and plating characteristics.

9) Suitable grades of steel for this application are:

Allegheny Ludlum "Relay No. 5"
Carpenter "Silicon Core Iron B".

4.3 AISI M-19 TRANSFORMER C STEEL SHEET LAMINATE

The 8-pole stator will be fabricated from stamped 0.014 inch thick M-19 steel sheet stock. This steel is pre-coated with an electrical insulation.

Process Specification, Stator

General

This process specification describes the fabrication and assembly of M-19 Transformer C silicon steel laminates into an 8-pole stator. The material is received as stamped, insulation coated 0.014 inch thick laminates. This specification describes the assembly and machining sequences necessary to provide a finished part within drawing tolerances.

Procedure

1) Eight-pole stator laminations are stamped from C-15 coated M-19 Transformer C silicon steel stock, 0.014 inch thick, then annealed at 1550 to 1650^{o}F for one hour.

2) Stack laminations in assembly jig to drawing dimensions and clamp tightly.

3) Vacuum bond lamination stack using Chrysler Chemical Division Cycleweld 55-9.

4) Grind inside diameter of assembled stator to pre-finish dimensions.

5) Assemble bobbin-wound coils onto stator poles and run hook-up wires in accordance with assembly drawings.

6) Preheat stator assembly for one hour at 110^{o}C.

7) Impregnate coils and pole structure with Dow Corning Sylgard 182, making sure all voids are filled flush. Cure at 110^{o}C for 2 hours.

8) After air cooling to room temperature, finish grind inside diameter to drawing dimension.

9) Suitable grade of steel for this application is:

Allegheny Ludlum "A-L M-19 Transformer C".

5.0 RELIABILITY

A reliability prediction was performed on the Dual Mode Dynavector Actuator in accordance with MIL-STD-756A to provide a computed reliability estimate of the equipment Mean-Time-Between Failures (MTBF). The analysis was performed, utilizing an airborne uninhabited environment and two conditions of altitude:

CONDITION I - Component Ambient Temperature of 71°C (160°F)

(45,000 ft. altitude operation)

CONDITION II - Component Ambient Temperature of 121°C (250°F)

(30,000 ft. altitude operation)

All piece parts were considered to be part of a series configuration. The total equipment failure rate and resultant MTBF were, therefore, computed by adding the individual piece-part failure rates.

Attached as Tables 2 and 3 are tabulations of the individual piece-parts, quantity used, calculated failure rate and the data sources. Failure rates generated for the individual items are based on standard data sources and Bendix experience, and represent a fifty percent (50%) confidence level. A summary of the reliability estimate and design goal is indicated below:

CONDITION	UNIT	PART AMBIENT TEMP.	TOTAL FAILURE RATE	PREDICTED MEAN-TIME BETWEEN FAILURES (MTBF)	DESIGN GOAL MTBF
I (45,000 ft.) Alt.	Dual Mode Electro-Pneumatic Actuator	71°C (160°F)	40.6899 ppmh	24,576 Hours	20,000 Hours
II (30,000 ft.) Alt.		121°C (250°F)	85.0959 ppmh	11,751 Hours	2,500 Hours

TABLE 2.

RELIABILITY FAILURE RATE PREDICTION
FOR THE
DUAL MODE DYNAVECTOR ACTUATOR - CONDITION I

TEMPERATURE - 71°C (160°F) ENVIRONMENT-AIRBORNE UNINHABITED

Part Type	Qty.	Failure Rate λ(ppmh)	Total Failure Rate (λ. Qty)	Failure Rate Data Source
Roller Bearings	4	.284	1.136	1A
Torquer Motor, Brushless, DC	1	10.4575	10.4575	1B
Motor, Stepper, Brushless (pneumatics included)	1	8.68	8.68	2A
Gear Passes, Spur, Epicyclic	3	.0202	.0606	5
LVDT (Solenoid Type)	1	14.22	14.22	2B
RVDT (Synchro Brushless)	1	2.358	2.358	2C
Valve, Spool	1	2.89	2.89	3
Needle Bearings	2	.284	.568	1A
Connector (12 & 16 Pin)	2	.1587	.3174	4
Terminal Board	1	·0012	·0012	2D
Connections, Solder	10	.00012	.0012	2E

Total Failure Rate - 40.6899 ppmh

Mean-Time-Between-Failures (MTBF) - 24,576 Hours

TABLE 3

RELIABILITY FAILURE RATE PREDICTION
FOR THE
DUAL MODE DYNAVECTOR ACTUATOR - CONDITION II

TEMPERATURE - 121°C (250°F) ENVIRONMENT-AIRBORNE UNINHABITED

Part Type	Qty.	Failure Rate λ(ppmh)	Total Failure Rate (λ. Qty)	*Failure Rate Data Source
Roller Bearings	4	.284	1.136	1A
Torquer Motor, Brushless, DC	1	10.4575	10.4575	1B
Motor, Stepper, Brushless (pneumatics included)	1	8.68	8.68	2A
Gear Passes, Spur, Epicyclic	3	.0202	.0606	5
LVDT (Solenoid Type)	1	55.80	55.80	2B
RVDT (Synchro Brushless)	1	5.184	5.184	2C
Valve, Spool	1	2.89	2.89	3
Needle Bearings	2	.284	.568	1A
* Connector (12 & 16 Pin)	2	.1587	.3174	4
Terminal Board	1	.0012	.0012	2D
Connections, Solder	10	.00012	.0012	2E

Total Failure Rate - 85.0959 ppmh

Mean-Time-Between-Failures (MTBF) - 11,751 Hours

* Connectors remain at 71°C.

*FAILURE RATE SOURCES

CODE	FAILURE RATE SOURCE
1	RADC Non-Electrical Reliability Notebook (RADC-TR-75-22), dated Jan. 1975 A) Pg. 2-40 B) Pg. 2-171
2	MIL-HDBK-217B, dated Sept. 7, 1976 A) Pg. 2.8.1-10 B) Pg. 2.9-1 C) Pg. 2.8.3-1 D) Pg. 2.12 E) Pg. 2.13-2 F) Pg. 2.11-1
3	AVCO Reliability Handbook, AVCO Lycoming Corp.
4	MIL-HDBK-2178, dated April 1970 Pg. 3-73 through 3-81
5	Bendix-Operational Reliability Failure Rate Report, RE-6886

6.0 MAINTAINABILITY

A maintainability analysis has been performed on the Dual Mode Dynavector in order to determine a design estimate in terms of Mean-Maintenance Man hours per Flight Hour (MMH/FH) and Mean-Time-To-Repair (MTTR). A description of the analysis performed and a breakdown of the task times to perform organizational level maintenance and item replacement at the Intermediate level are presented in Tables 4 and 5. A summary of the analysis results and design goals is indicated below.

Maintenance Level	Design Goal MTTR	Design Goal MMH/FH	Predicted MTTR	Predicted MMH/FH
Condition I:				
Organizational	-	-	.62 Hrs.	.000075
Intermediate	-	-	1.35 Hrs.	.000165
Total	2.0 Hrs.	.03	1.97 Hrs.	.000240
Condition II:				
Organizational	-	-	.62 Hrs.	.000157
Intermediate	-	-	1.23 Hrs.	.000315
Total	2.0 Hrs.	.03	1.85 Hrs.	.000472

All maintenance on the equipment will be unscheduled. Maintenance can be performed by one man so MTTR equals MMTR. Calculations for MMH/FH are based on a maintenance rate of 2.0, the failure rates determined by the Reliability predictions (Condition I and Condition II), and an operating hour per flight hour ratio (OH/FH) of 1.5.

QUANTITATIVE DATA SHEET DESCRIPTION

The following Quantitative Data Sheets are used to present the times that would be required to perform each task required for maintenance. These task times then combined and used in further calculations of the mean-time-to-repair.

An explanation of the columnar headings follows:

1) Item/Part Number - Used to identify the replaceable unit.

2) Qty. - This shows the number of items of this type in the system, so located, physically and functionally, as to have the same task times.

3) Task Time, Hrs. - This shows the amount of time in hours estimated to perform a task. These tasks are:

TP	Test Preparation
TS	Trouble Shooting
DA	Disassembly
RR	Remove and Replace
RA	Reassemble
AC	Adjust/Calibrate
FT	Functional Test
SS	Secure Setup

4) Total Time (T) - This is the summation of the task times in hours for each item.

5) Failure Rate - This appears in two columns. The first is the reliability failure rate of maintenance rate in parts per million hours for one item. The second column indicatest the quantity of items associated with that failure rate.

6) T x λ x Q - This column is the mean elapsed time in hours per million operating hours to perform the task. This column is summarized and used in the calculation of MTTR and MMH/OH.

TABLE 4
MAINTAINABILITY PREDICTION
DUAL MODE ELECTRO-PNEUMATIC ACTUATOR - CONDITION I

MAINTENANCE LEVEL / ITEM/PART NO.	Q	TASK TIME - HOURS								T	FAILURE RATE		$T_T \times \lambda \times Q$
		TP	TS	DA	ER	R_R	AC	FT	SS		λ	$\lambda \times Q$	
ORGANIZATIONAL													
DME-PA 3854020-1	1		.250	-	.181	-	-	.184		.615	40.6899	40.6899	25.0243

TABLE 5
MAINTAINABILITY PREDICTION
DUAL MODE ELECTRO-PNEUMATIC ACTUATOR- CONDITION I

MAINTENANCE LEVEL ITEM/PART NO.	Q	TASK TIME - HOURS								T	FAILURE RATE		$T_r \times \lambda \times Q$
		TP	TS	DA	RR	RA	AC	FT	SS		λ	$\lambda \times Q$	
INTERMEDIATE													
Servo Valve Assy.	1	.088	.333	-	.061	-	-	.500	.083	1.065	27.5675	27.5675	29.3594
Angular Sensor	1	.088	.250	-	.259	-	.167	.500	.083	1.347	2.3580	2.3580	3.1762
Connector, 16 Pin	1	.088	.167	-	.257	-	-	.500	.083	1.095	.1587	.1587	.1738
Connector, 12 Pin	1	.088	.250	-	.192	-	-	.500	.083	1.113	.1587	.1587	.1766
Output End Fixed Gear	1	.088	.500	.019	.184	.008	.167	.500	.083	1.549	.0151	.0151	.0234
Sensor End Fixed Gear	1	.088	.500	.022	.184	.028	.167	.500	.083	1.572	.0151	.0151	.0237
Roller Bearings	2	.088	.500	.088	.008	.135	.167	.500	.083	1.569	.2840	.5680	.8912
Roller Bearings	2	.088	.500	.212	.008	.340	.167	.500	.083	1.898	.2840	.5680	1.0781
Thrust Bearings	2	.088	.500	.181	.008	.274	.167	.500	.083	1.801	.2840	.5680	1.0230
Output Gear	1	.088	.500	.176	.010	.269	.167	.500	.083	1.793	.0151	.0151	.0271
Ring Gear	1	.088	.500	.203	.018	.330	.167	.500	.083	1.889	.0151	.0151	.0285
Stator Assy.	1	.088	.250	.402	.301	.628	.167	.500	.083	2.419	8.6812	8.6812	20.9998

TABLE 5
MAINTAINABILITY PREDICTION
DUAL MODE ELECTRO-PNEUMATIC ACTUATOR-CONDITION II

MAINTENANCE LEVEL / ITEM/PART NO.	Q	TASK TIME - HOURS								T	FAILURE RATE		$T_r \times \lambda \times Q$
		TP	TS	D_t	TR	Ra	AC	FT	SS		λ	$\lambda \times \Omega$	
ORGANIZATIONAL													
DME-PA	1		.250	-	.181	-	-	.184		.615	(85.0959)	(85.0959)	52.3340
3854020-1													

TABLE 5
MAINTAINABILITY PREDICTION
DUAL MODE ELECTRO-PNEUMATIC ACTUATOR - CONDITION II

MAINTENANCE LEVEL ITEM/PART NO.	Q	TASK TIME - HOURS								T	FAILURE RATE		$T_T \times \lambda \times Q$
		TP	TS	DA	RR	RA	AC	FT	SS		λ	$\lambda \times Q$	
INTERMEDIATE													
Servo Valve Assy.	1	.088	.333	-	.061	-	-	.500	.083	1.065	69.1475	69.1475	73.6421
Angular Sensor	1	.088	.250	-	.259	-	.167	.500	.083	1.347	5.1840	5.1840	6.9828
Connector, 16 Pin	1	.088	.167	-	.257	-	-	.500	.083	1.095	.1587	.1587	.1738
Connector, 12 Pin	1	.088	.250	-	.192	-	-	.500	.083	1.113	.1587	.1587	.1766
Output End Fixed Gear	1	.088	.500	.019	.184	.008	.167	.500	.083	1.549	.0151	.0151	.0234
Sensor End Fixed Gear	1	.088	.500	.022	.184	.028	.167	.500	.083	1.572	.0151	.0151	.0237
Roller Bearings	2	.088	.500	.088	.008	.135	.167	.500	.083	1.569	.2840	.5680	.8912
Roller Bearings	2	.088	.500	.212	.008	.340	.167	.500	.083	1.898	.2840	.5680	1.0781
Thrust Bearings	2	.088	.500	.181	.008	.274	.167	.500	.083	1.801	.2840	.5680	1.0230
Output Gear	1	.088	.500	.176	.010	.269	.167	.500	.083	1.793	.0151	.0151	.0271
Ring Gear	1	.088	.500	.203	.018	.330	.167	.500	.083	1.889	.0151	.0151	.0285
Stator Assy.	1	.088	.250	.402	.301	.628	.167	.500	.083	2.419	8.6812	8.6812	20.9998

Sample calculations and applicable formulas used in the analysis are as follows for Condition I:

Organizational Level

Maintenance Data read directly from table

$$\Sigma\ T \times \lambda \times Q = 25.0243 \times 10^{-6}$$

$$= .0000250 \text{ MMH/OH}$$

$$MTTR = .615$$

Intermediate Level

Summations from Data Summary Table

System Repair

$$\Sigma \left(\lambda \times Q\right) = 40.6885 \times 10^{-6}$$

$$\Sigma \left(T \times \lambda \times Q\right) = 54.9808 \times 10^{-6}$$

Mean Time to Repair (MTTR)

$$\Sigma \frac{(T \times \lambda \times Q)}{\lambda \times Q}$$

$$= \frac{54.9808 \times 10^{-6}}{40.6885 \times 10^{-6}}$$

$$= 1.35 \text{ Hrs.}$$

Mean Maintenance Man Hours per Operating Hour

$$\Sigma\ (T \times \lambda + Q) \times 10^{-6}$$

$$= .000055 \text{ MMH/OH}$$

Convert to Flight Hours and at a frequency based on Mean Time Between Maintenance actions.

OH/FH = 1.5

MR = 2.0

MMH/FH = $\Sigma(T \times \lambda \times Q) \times OH/FH \times MR$

Organizational Level = .000075

Intermediate Level = .000165

The values for Condition II MTTR, and MMH/FH were calculated as above but using the figures from Table 5.

APPENDIX A

COMPUTER MODEL OF DYNAVECTOR ACTUATOR

A flow model was constructed for the servovalve-Dynavector motor combination and was programmed on a digital computer. By means of this routine, the pressure and flow characteristics of the valve and motor were determined for any specified operating condition. The approach was sufficiently general to allow a broad range of servovalve-motor designs to be investigated.

The pneumatic Dynavector actuator flow model determines the pressure drops, motor and leakage flows, and output torque for a given supply pressure and motor displacement and an assumed speed and valve opening. The model is depicted in Figure A-1. Leakage from the motor commutation ports is represented by orifices $A_{\ell 1}$ and A_{cpm} in the figure. The leakage area from the high-pressure ports to ambient is essentially one-half the motor circumference multiplied by the total axial clearance between the ring gear and the manifold plates. The area of the leakage path from the low pressure side of the motor to ambient is determined likewise. The cross-port leakage area of the Dynavector actuator is the product of the total periphery of the exhaust slots and the total axial clearance between the ring gear and manifolds. The motor commutation area, A_c, is determined directly by the commutation slot dimensions and the number of chambers. The motor is represented in terms of its displacement, D_m, and the working flow is denoted W_m. Cross-port leakage in a well-designed servovalve is very small and consequently is ignored in the flow model. Also tending to justify this assumption is the fact that the servovalve lands are generally underlapped to achieve linearity and high gain about the on-center spool position.

The equations for describing the operation of the servovalve-Dynavector motor combination are written directly, using the pneumatic orifice flow equations and node equations for the flows. The symbols are defined in Table A-1 and the equations are:

$$W_r = \frac{C_d\, C_2\, P_{v2}\, A_v\, f_1\left(\frac{P_a}{P_{v2}}\right)}{\sqrt{T}} \qquad \text{(A-1)}$$

$$W_{c2} = W_r \qquad \text{(A-2)}$$

$$P_{m2} = \frac{W_{c2}\sqrt{T}}{C_d\, C_2\, A_c\, f_1\left(\frac{P_{v2}}{P_{m2}}\right)} \qquad \text{(A-3)}$$

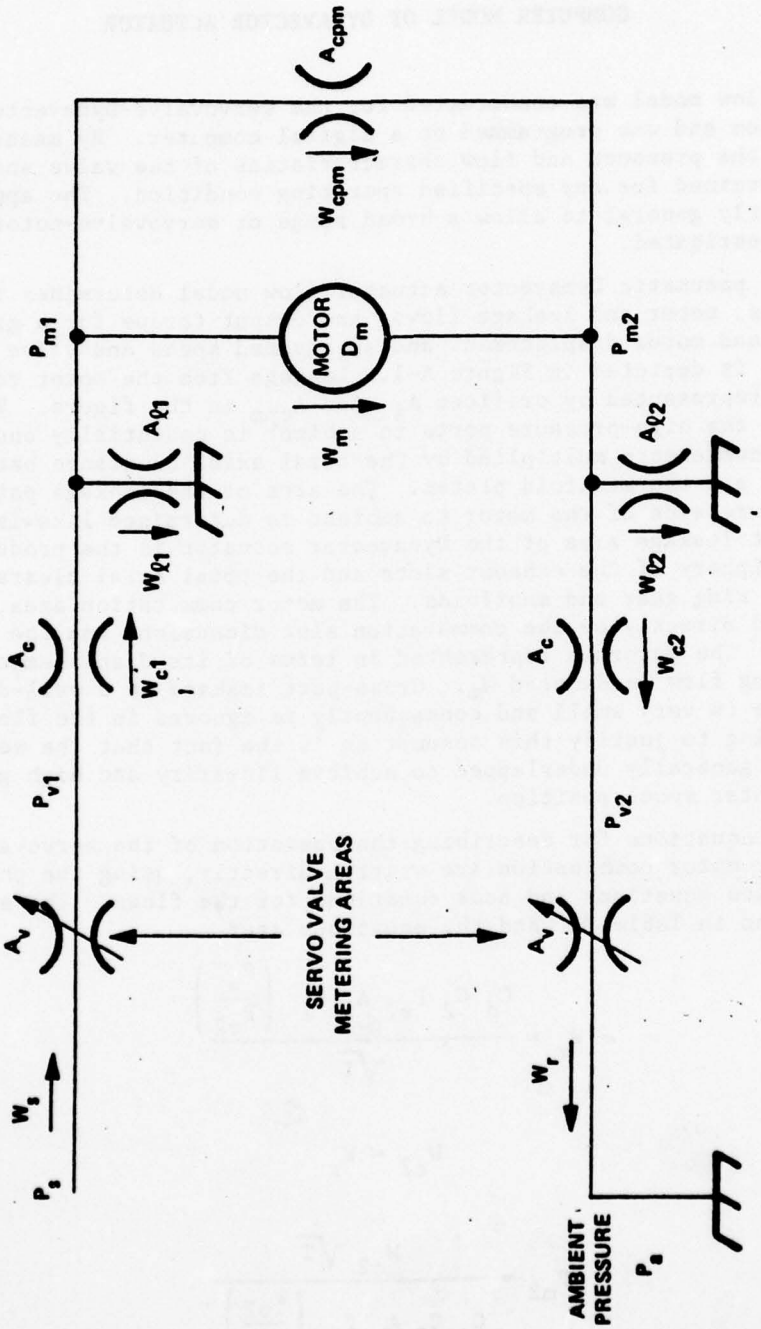

Figure A-1 - Flow Model of Servo-Valve - Dynavector Motor Combination

Table A-1 - Servovalve-Dynavector Motor Torque-Speed Curve Parameters

Parameter	Definition
A_c	Dynavector motor commutation area - in^2
A_v	Servovalve metering area - in^2
A_{cpm}	Dynavector motor cross-port leakage area - in^2
$A_{\ell 1}$	High pressure motor leakage to ambient area - in^2
$A_{\ell 2}$	Low pressure motor leakage to ambient area - in^2
C_d	Orifice discharge coefficient
C_2	Thermodynamic constant for the working fluid - $°R^{1/2}/sec$
D_m	Dynavector motor displacement relative to output shaft - in^3/rev
f_1	Compressibility function for flow of working fluid through an orifice dependent on ratio of pressures across orifice
η	Dynavector motor torque efficiency for pressures measured directly across chambers
$\dot{\theta}_o$	Output shaft speed - rad/sec
P_{m1} (P_{m2})	High (low) motor pressure - lb/in^2
P_{v1} (P_{v2})	High (low) servovalve pressure - $lb\text{-}in^2$
P_a	Ambient pressure - lb/in^2
P_s	Supply pressure - lb/in^2
R	Gas constant for the working fluid - in-lb/lb - °R
T	Temperature of the working fluid - °R
T_o	Dynavector motor output torque - in-lb

$$W_{\ell 2} = \frac{D_d\, C_2\, P_{m2}\, A_{\ell 2}\, f_1 \left(\frac{P_a}{P_{m2}}\right)}{\sqrt{T}} \qquad \text{(A-4)}$$

$$W_m + W_{cpm} = W_{\ell 2} + W_{c2} \qquad \text{(A-5)}$$

$$W_m = 2\pi\, D_m\, \dot{\theta}_o\, \frac{P_{m1}}{RT} \qquad \text{(A-6)}$$

$$W_{cpm} = \frac{D_d\, C_2\, P_{m1}\, A_{cpm}\, f_1 \left(\frac{P_{m2}}{P_{m1}}\right)}{\sqrt{T}} \qquad \text{(A-7)}$$

$$W_{\ell 1} = \frac{C_d\, C_2\, P_{m1}\, A_{\ell 1}\, f_1 \left(\frac{P_a}{P_{m1}}\right)}{\sqrt{T}} \qquad \text{(A-8)}$$

$$W_{c1} = W_m + W_{cpm} + W_{\ell 1} \qquad \text{(A-9)}$$

$$P_{v1} = \frac{W_{c1}\sqrt{T}}{C_d\, C_2\, A_c\, f_1 \left(\frac{P_{m1}}{P_{v1}}\right)} \qquad \text{(A-10)}$$

$$W_s = \frac{C_d\, C_2\, P_s\, A_v\, f_1 \left(\frac{P_{v1}}{P_s}\right)}{\sqrt{T}} \qquad \text{(A-11)}$$

These equations are solved iteratively until the flows and pressures balance and then the output torque is computed from

$$T_o = 2\pi\, D_m\, \eta\, (P_{m1} - P_{m2}) \qquad \text{(A-12)}$$

The algorithm for solution of the flow model equations is shown in the flow diagram of Figure A-2.

The algorithm was programmed in a very general manner to maximize its usefulness as a design tool. In addition to the input parameters given in Figure A-2 the temperature and other thermodynamic properties of the working fluid may readily be changed. A four-way servovalve was assumed and provisions were made for individually selecting supply and return land areas and their degree of underlap. For convenience, normalizing values for speed and torque are computed from the input supply pressure, motor displacement, and valve area. The normalizing values are theoretical maximum values; for computing normalizing speed, $\dot{\theta}_n$, it is assumed that there is no leakage and that the entire pressure drop from supply to ambient occurs across the motor, or:

$$\dot{\theta}_n = \frac{R\sqrt{T}\, C_d\, C_2\, A_v\, f_1 \left(\frac{P_v}{P_v + P_s}\right)}{2\pi\, D_m} \qquad \text{(A-13)}$$

The normalizing torque value is based upon 100 percent torque efficiency and the assumption that the full pressure drop occurs across the motor, or:

$$T_m = 2\pi\, D_m\, (P_s - P_v) \qquad \text{(A-14)}$$

The program requires, in addition to the input parameters already mentioned, percentage values of normalizing speed and valve opening. A sample printout with legends added is shown below; the data are for valve areas of 0.1 in^2, 0 percent land underlap, 155 psia supply pressure, 14.7 psia ambient pressure, and a motor displacement of 180.0 in^3/rev. The commutation, leakage to ambient, and cross-port leakage areas are: 0.100, 0.00275, 0.00267 in^2, respectively.

```
NORMALIZING VALUES ARE
SPEED RAD/SEC=,        .2571E+02  TORQUE LB-INCH=        .4019E+04 =TN
PERCENT MAX AREA=       .1000E+03
A1              A2              A3              A4
     .1000E+00       .0000E+00       .1000E+00       .0000E+00
PERCENT SPEED=        .2500E+02
  PV1 .1513E+03   PM1 .1474E+03   PM2 .5380E+02   PV2 .4341E+02
  WS  .1088E+00   WC1 .1089E+00   WCPM .8755E-02  WL1 .9018E-02
  WR  .9655E-01   WC2 .9655E-01   WM  .9109E-01   WL2 .3290E-02
  TO  .2682E+04   %TN .6674E+02
```

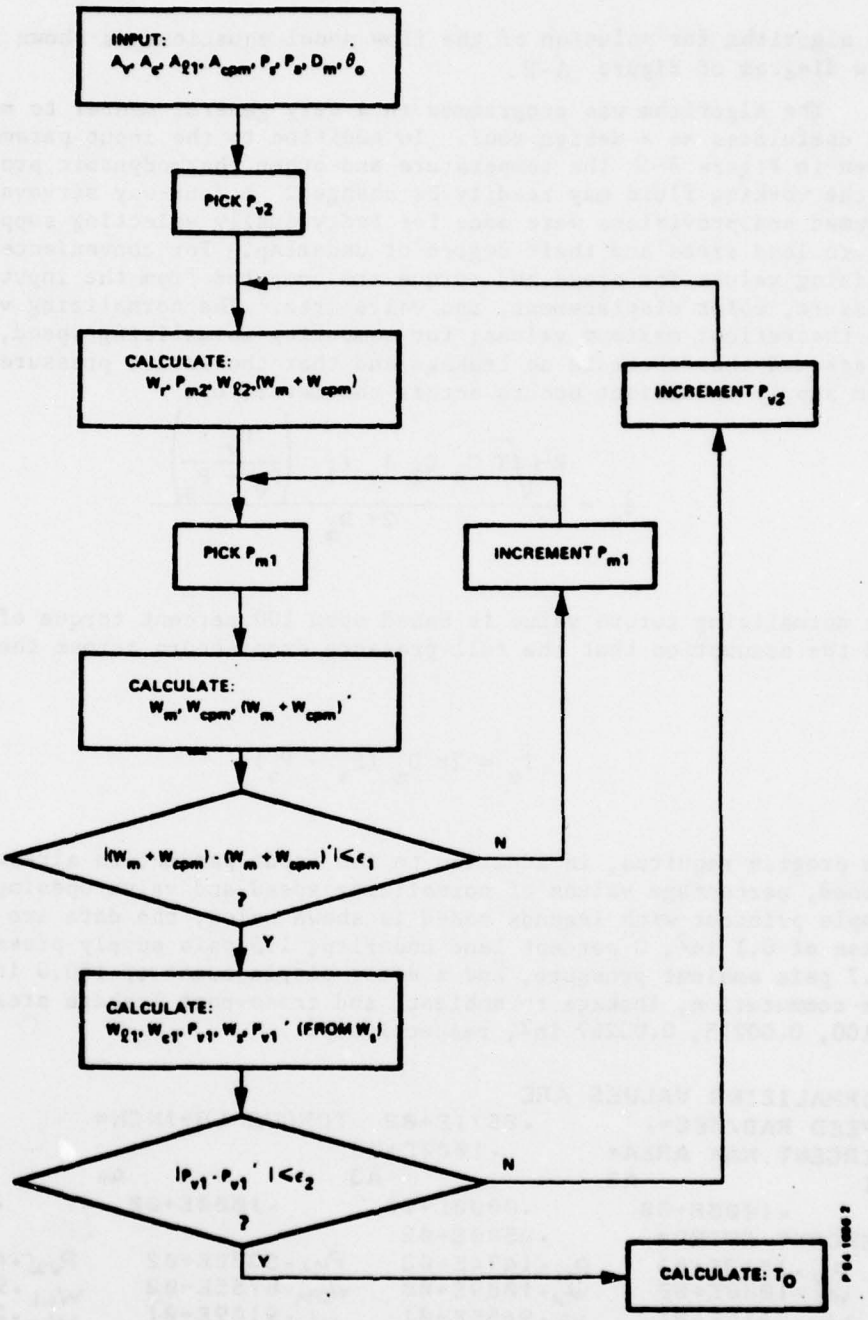

Figure A-2- **Algorithm for Solution of Flow-Model Equations**

High accuracy is achieved in the routine by using a half-interval search in the iterations.

SEL EXTENDED FORTRAN IV (REV K/77FEB15)

MAIN

```
1                       C *** PNEUMATIC MOTOR WITH 4-WAY VALVE AND SERIES COMMUTATION ORIFICES
2                       C *** PS=PSIA SUPPLY, PV=PSIA VENT
3                       C *** R=GAS CONSTANT IN-LB/LB-DEG
4                       C *** C3=CONSTANT DEPENDING ON SPECIFIC HEAT RATIO OF GAS
5                       C *** (INCH)(1/2)/SEC
6                       C *** NEG H=UNDERLAP(OPEN CENTER, PERCENT OF ZERO LAP MAX AREA)
7                       C *** D=DISPLACEMENT/REV (INCH**3/REV)
8                       C *** CONVERTED FROM 12/18/73 TIME SHARE TAPE BY L. ERWIN
9                       C *** ON 7/29/77, BY L ERWIN
10                            DATA PI, G/3.1415927, 386.264/
11                      C *** NORMALIZING VALUES BASED ON ZERO TORQUE, ZERO LEAK, ZERO LAP
12                      C *** CD=1. FOR NORMALIZING CALCULATION
13                      C *** AV1 THRU AV4=VALVE MAX PORT AREAS, ZERO LAP.
14                            NAMELIST/CONS/R, T, CD, XK
15                            NAMELIST/LST1/AV1, AV2, AV3, AV4, H1, H2, H3, H4, PS, PV, D, AC, AL, ACPM,
16                           1XJ1N, XDJ1, M1, XJ2N, XDJ2, M2
17                            READ(5, CONS)
18                            C3=C33(XK, G)
19                            RRT=SQRT(R*T)
20                      C *** THIS IS RETURN POINT FOR EXTRA LST1 SETS
21                        102 READ(5, LST1, END=99)
22                            WRITE(6, 150)
23                        150 FORMAT(1H1, 'PNEUMATIC MOTOR WITH 4-WAY VALVE, INPUT DATA')
24                            WRITE(6, 151)R, T, CD, XK
25                        151 FORMAT(1H , 'GAS CONSTANTS', 2X, 'R=', F10.3, 2X, 'T=', F10.3, 2X,
26                           1'CD=', F10.3, 2X, 'XK=', F10.3)
27                            WRITE(6, 152)AV1, AV2, AV3, AV4, H1, H2, H3, H4
28                        152 FORMAT(1H , 'VALVE CONSTANTS', /, ' AV1=', E15.4, 2X, 'AV2=', E15.4, 2X,
29                           1'AV3=', E15.4, 2X, 'AV4=', E15.4, /, ' H1 =', F15.4, 2X, 'H2 =', F15.4, 2X,
30                           2'H3 =', F15.4, 2X, 'H4 =', F15.4)
31                            WRITE(6, 153)PS, PV
32                        153 FORMAT(1H , 'EXTERNAL PRESSURES, PSIA', /, ' PS=', E15.4, 2X, 'PV=',
33                           1E15.4)
34                            WRITE(6, 154)D, AC, AL, ACPM
35                        154 FORMAT(1H , 'MOTOR PARAMETERS, D INCH**3/REV, AREAS IN**2', /, 1X,
36                           1'D=', E15.4, 2X, 'AC=', E15.4, 2X, 'AL=', E15.4, 2X, 'ACPM=', E15.4)
37                            WRITE(6, 155)XJ1N, XDJ1, M1
38                        155 FORMAT(1H , 'VALUE AREA RANGE IN PERCENT', /, ' INITIAL PERCENT AREA',
39                           1F11.3, 2X, 'INCREMENT IN PERCENT', F10.3, 2X, 'NUMBER OF VALUES', I4)
40                            WRITE(6, 156)XJ2N, XDJ2, M2
41                        156 FORMAT(1H , 'SPEED RANGE IN PERCENT', /, ' INITIAL PERCENT SPEED',
42                           1F10.3, 2X, 'INCREMENT IN PERCENT', F10.3, 2X, 'NUMBER OF VALUES', I4)
43                            DM=D/(2.*PI)
44                            CDN=1.
45                      C *** NORMALIZING VALUES
46                            DELP=1.E-5*PS
47                            WPSM=W(PV, PS, XK, CDN, AV1, C3, RRT)
48                            DELT=1.E-5*WPSM
49                            PM1H=PS
50                            PM1L=0.
51                            PM1=.5*(PS+PV)
52                            DO 10 J=1, 30
53                            WPS=W(PM1, PS, XK, CDN, AV1, C3, RRT)
```

SEL EXTENDED FORTRAN IV (REV K/77FEB15)

MAIN

```
                        WPV=W(PV,PM1,XK,CDN,AV3,C3,RRT)
                        ERR=WPS-WPV
                        IF(ERR.GT.DELT*.5)GOTO 5
                        IF(ERR.LT.-DELT*.5)GOTO 3
                        GOTO 20
                      3 PM1H=PM1
                        PM1=.5*(PM1L+PM1)
                        GOTO 10
                      5 PM1L=PM1
                        PM1=.5*(PM1H+PM1)
                     10 CONTINUE
                        WRITE(6,11)
                     11 FORMAT(1H ,'OVERRUN DO 10 PM1 LOOP')
                     20 CONTINUE
                   C* * LOOP EXIT
                        SPN=(WPS*T*R/PM1)/DM
                        TN=DM*(PS-PV)
                   C* * SPN=NORMALIZING SPEED, TN=NORMALIZING TORQUE
                        WRITE(6,21)
                     21 FORMAT(1H ,'NORMALIZING VALUES ARE')
                        WRITE(6,22)SPN,TN
                     22 FORMAT(1H ,'SPEED RAD/SEC=',E15.4,2X,'TORQUE LB-INCH=',E15.4)
                   C* * AREA LOOP
                        WRITE(6,180)
                    180 FORMAT(1H1)
                        DO 100 J1=1,M1
                        IF(J1.EQ.1)GOTO 105
                    101 FORMAT(1H1,'NEXT VALVE AREA')
                        WRITE(6,101)
                    105 CONTINUE
                        XJ1=XJ1N+(J1-1)*XDJ1
                        A1=AV1*.01*(XJ1-H1)
                        IF(A1.LT.0.)A1=0.
                        A2=AV2*.01*(XJ1+H2)*(-1.)
                        IF(A2.LT.0.)A2=0.
                        A3=AV3*.01*(XJ1-H3)
                        IF(A3.LT.0.)A3=0.
                        A4=AV4*.01*(XJ1+H4)*(-1.)
                        IF(A4.LT.0.)A4=0.
                        WRITE(6,380)XJ1
                    380 FORMAT(1H ,'PERCENT MAX AREA=',F10.3)
                        WRITE(6,382)
                    382 FORMAT(1H ,4X,'A1',13X,'A2',13X,'A3',13X,'A4')
                        WRITE(6,360)A1,A2,A3,A4
                    360 FORMAT(1H ,4E15.4)
                        WRITE(6,383)
                    383 FORMAT(1H0,'PV1',12X,'PM1',12X,'PM2',12X,'PV2')
                        WRITE(6,384)
                    384 FORMAT(1H ,'WS',13X,'WC1',12X,'WCPM',11X,'WAL1')
                        WRITE(6,385)
                    385 FORMAT(1H ,'WR',13X,'WC2',12X,'WM',13X,'WAL2')
                        WRITE(6,386)
                    386 FORMAT(1H ,'TORQUE',9X,'PCT TORQUE')
```

SEL EXTENDED FORTRAN IV (REV K/77FEB15)

MAIN

```
107                     C* *  SPEED LOOP
108                           DO 200 J2=1,M2
109                           XJ2=XJ2N+(J2-1)*XDJ2
110                           WRITE(6,390) XJ2
111                       390 FORMAT(1H ,'PERCENT SPEED=',F10.3)
112                           PV2H=2.*PS
113                           PV2L=0.
114                           PV2=.5*(PS-PV)
115                     C* *  PRESSURE LOOP
116                           DO 300 J3=1,30
117                           WA3=W(PV,PV2,XK,CD,A3,C3,RRT)
118                           WA4=W(PS,PV2,XK,CD,A4,C3,RRT)
119                           PM2H=2.*PS
120                           PM2L=0.
121                           IF(J3-2.GE.0)GOTO 402
122                           PM2=PV2
123                       402 DO 400 J4=1,30
124                     C* *  PM2 LOOP
125                           WC2=W(PV2,PM2,XK,CD.AC,C3,RRT)
126                           ERR4=WC2-(WA3+WA4)
127                           IF(ABS(ERR4).LT.DELT)GOTO 403
128                           IF(PM2H-PM2L.LT.DELP)GOTO 403
129                           IF(ERR4)405,403,406
130                       405 PM2L=PM2
131                           PM2=.5*(PM2+PM2H)
132                           GOTO 400
133                       406 PM2H=PM2
134                           PM2=.5*(PM2+PM2L)
135                       400 CONTINUE
136                           WRITE(6,401)
137                       401 FORMAT(1H ,'OVERRUN DO 400 PM2 LOOP')
138                       403 CONTINUE
139                     C* *  403 IS NORMAL EXIT OF DO 400
140                           QM=XJ2*.01*SPN*DM
141                           WAL2=W(PV,PM2,XK,CD,AL,C3,RRT)
142                           PM1H=2.*PS
143                           PM1L=0.
144                           IF(J3-2.GE.0)GOTO 502
145                           PM1=PM2
146                       502 DO 500 J5=1,30
147                     C* *  PM1 LOOP
148                           WCPM=W(PM2,PM1,XK,CD,ACPM,C3,RRT)
149                           WM=(QM+PM1)/(R*T)
150                           ERR5=WCPM+WM-WAL2-WC2
151                           IF(ABS(ERR5).LT.DELT)GOTO 504
152                           IF(PM1H-PM1L.LT.DELP)GOTO 504
153                           IF(ERR5)506,504,507
154                       506 PM1L=PM1
155                           PM1=.5*(PM1+PM1H)
156                           GOTO 500
157                       507 PM1H=PM1
158                           PM1=.5*(PM1+PM1L)
159                       500 CONTINUE
```

SEL EXTENDED FORTRAN IV (REV K/77FEB15)

MAIN

```
160                          WRITE(6,508)
161                      508 FORMAT(1H ,'OVERRUN DO 500 PM1 LOOP')
162                      504 CONTINUE
163                    C* *  504 IS NORMAL EXIT OF DO 500
164                          WAL1=W(PV,PM1,XK,CD,AL,C3,RRT)
165                          PV1H=2.*PS
166                          PV1L=0.
167                          IF(J3-2.GE.0)GOTO 602
168                          PV1=PM1
169                      602 DO 600 J6=1,30
170                    C* *  PV1 LOOP
171                          WC1=W(PM1,PV1,XK,CD,AC,C3,RRT)
172                          ERR6=WC1-(WAL1+WCPM+WM)
173                          IF(ABS(ERR6).LT.DELT)GOTO 604
174                          IF(PV1H-PV1L.LT.DELP)GOTO 604
175                          IF(ERR6)606,604,607
176                      606 PV1L=PV1
177                          PV1=.5*(PV1+PV1H)
178                          GOTO 600
179                      607 PV1H=PV1
180                          PV1=.5*(PV1+PV1L)
181                      600 CONTINUE
182                          WRITE(6,608)
183                      608 FORMAT(1H ,'OVERRUN DO 600 PV1 LOOP')
184                      604 CONTINUE
185                    C* *  604 IS NORMAL DO 600 EXIT
186                          WA1=W(PV1,PS,XK,CD,A1,C3,RRT)
187                          WA2=W(PV1,PV,XK,CD,A2,C3,RRT)
188                          DW=WA1+WA2-WC1
189                          IF(ABS(DW).LT.DELT)GOTO 350
190                          IF(PV2H-PV2L-DELP.LE.0.)GOTO 375
191                          IF(DW)365,350,353
192                      365 PV2H=PV2
193                          PV2=.5*(PV2+PV2L)
194                          GOTO 300
195                      353 PV2L=PV2
196                          PV2=.5*(PV2+PV2H)
197                      300 CONTINUE
198                          WRITE(6,301)
199                      301 FORMAT(1H ,'OVERRUN DO 300 PRESSURE LOOP')
200                      375 WRITE(6,376)
201                      376 FORMAT(1H ,'P EXIT FROM DO 300 PRESSURE LOOP')
202                          GOTO 359
203                      350 WRITE(6,351)
204                      351 FORMAT(1H ,'W EXIT FROM DO 300 PRESSURE LOOP')
205                      359 CONTINUE
206                    C****  EXIT PRESSURE LOOP
207                          WR=WA3+WA4
208                          WS=WA1+WA2
209                          WRITE(6,360)PV1,PM1,PM2,PV2
210                          WRITE(6,360)WS,WC1,WCPM,WAL1
211                          WRITE(6,360)WR,WC2,WM,WAL2
212                          TR=DM*(PM1-PM2)
```

SEL EXTENDED FORTRAN IV (REV K/77FEB15)

MAIN

```
213                         PTR=100.*TR/TN
214                         WRITE(6,360)TR,PTR
215                   200 CONTINUE
216                 C**** END OF SPEED LOOP
217                   100 CONTINUE
218                 C**** END AREA LOOP
219                         GOTO 102
220                 C**** AT 102,READ NEW LST1,IF PRESENT
221                    99 STOP
222                         END
```

SEL EXTENDED FORTRAN IV (REV K/77FEB15)

C33

```
1                               FUNCTION C33(XK,G)
2                               A=XK*G
3                               B=((XK+1.)/2.)**((XK+1.)/(XK-1.))
4                               C33=SQRT(A/B)
5                               RETURN
6                               END
```

AD-A063 992 BENDIX CORP TETERBORO N J FLIGHT SYSTEMS DIV F/G 1/3
ADVANCED FLIGHT CONTROL ACTUATION SYSTEM (AFCAS-E/P). FEASIBILI--ETC(U)
JUN 78 R E FEUCHT, R W PRESLEY, P FORMAN N62269-77-C-0171
UNCLASSIFIED FSD-7411-78-05 NADC-77001-60 NL

2 OF 2
ADA
063992

END
DATE
FILMED
4-79
DDC

SEL EXTENDED FORTRAN IV (REV K/77FEB15)

F1

```
1                                FUNCTION F1(PD,PU,XK)
2                                IF(PD-PU)1,2,3
3                              3 PD1=PU
4                                PU1=PD
5                                GOTO 4
6                              1 PD1=PD
7                                PU1=PU
8                              4 PR=PD1/PU1
9                                PCRIT=(2./(XK+1.))**(XK/(XK-1.))
10                               IF(PR-PCRIT)6,6,7
11                             6 F1=1.
12                               GOTO 12
13                             7 XNUM=(PR**(1./XK))*SQRT(1.-PR**((XK-1.)/XK))
14                               XDEN=PCRIT**(1./XK)*SQRT(1.-PCRIT**((XK-1.)/XK))
15                               F1=XNUM/XDEN
16                            12 IF(PD-PU)9,2,11
17                            11 F1=-F1
18                             9 RETURN
19                             2 F1=0.
20                               RETURN
21                               END
```

SEL EXTENDED FORTRAN IV (REV K/77FEB15)

W

```
      FUNCTION W(PD,PU,XK,CD,A,C3,RRT)
      IF(PD-PU)1,2,3
    1 P=PU
      GOTO 4
    3 P=PD
    4 W=CD*A*P*C3*F1(PD,PU,XK)/RRT
      RETURN
    2 W=0.
      RETURN
      END
```

APPENDIX B

COMPUTER MODEL FOR ELECTRIC MODE TORQUE-SPEED CURVES

The voltage applied to a motor coil equals the sum of the voltage drop in the coil resistance and the back emf.

$$V = R\,i + E_b \tag{1}$$

The back emf is proportional to the product of the number of turns and the rate of change of magnetic flux.

$$E_b = 10^{-8}\,N\,\frac{d\phi}{dt} \tag{2}$$

The flux crossing a pole face equals the pole face area times the flux density. Thus

$$\phi = 6.452\,A_p B \tag{3}$$

$$E_b = 10^{-8}\,N \times 6.452\,A_p\,\frac{dB}{dt} \tag{4}$$

$$V = R\,i + 6.452 \times 10^{-8}\,NA_p\,\frac{dB}{dt} \tag{5}$$

The flux density is proportional to the number of ampere turns divided by the air gap length.

$$B = \frac{0.4\pi\,N\,i}{2.54g} = 0.496\,\frac{N\,i}{g} \tag{6}$$

Differentiating equation 6 gives

$$\frac{dB}{dt} = 0.496\,\frac{N}{g}\,\frac{di}{dt} - 0.496\,\frac{Ni}{g^2}\,\frac{dg}{dt} \tag{7}$$

The air gap length is given by

$$g = C + (1+\cos\theta)e \tag{8}$$

Differentiating gives

$$\frac{dg}{dt} = e\,\omega\sin\theta \tag{9}$$

Combining equations 5, 7, and 9 and rearranging terms gives

$$\frac{di}{dt} = 3.125 \times 10^{7}\,\frac{g}{A_p N^2}\,(V-Ri) - \frac{e\,\omega i}{g}\sin\theta \tag{10}$$

The instantaneous current is

$$i = \int_0^t \frac{di}{dt}\,dt$$

The torque is computed by determining the torque for an incremental pole face area dA, and integrating this torque over the complete area. The incremental pole face area is

$$dA = \text{radius} \times \text{length} \times d\theta$$

The torque developed by area dA is

$$dT = 3.75 \times 10^{-7} \, eB^2 \, dA \sin\theta \times \text{ratio} \times \text{eff}$$

The efficiency term eff accounts for mechanical losses. The constant 3.75×10^{-7} includes an empirical factor to account for the difference between the theoretical force developed by a pole and the actual force.

The portion of the circumference occupied by the pole face is

$$T_m = 8 \times \frac{\text{pole face area}}{\text{stator length}} \times \frac{1}{\text{circumference}}$$

$$T_m = \frac{A_p}{\text{length}} \times \frac{8}{2\pi \times \text{radius}}$$

The motor torque is

$$T = T_m \int_0^{\pi} dt$$

Eddy current power loss is given by

$$P_e = Kt^2B^2f^2W_i$$

where

f = frequency

t = iron thickness

W_i = weight of iron

The power loss for magnetic sheet steel is given by a curve of watts per pound at 60 hertz versus flux density.

For analysis, the eddy current power loss is generally accounted for by an equivalent resistor R_e. Thus

$$I^2R_e = P_e = Kt^2B^2f^2$$

$$R_e = K\left(\frac{tBf}{I}\right)^2$$

R_e is added to the coil resistance.

Due to flux leakage, all of the flux generated does not cross the working air gap. A flux leakage factor of 0.65 was established for Dynavectors. Using this leakage factor, the flux density is given by

$$B = \frac{NI}{3.113\ g}$$

Fringing reduces the effective flux density in the air gap. The effective flux density with fringing is given by

$$B_g = \frac{L \times W}{(L + 2G)(W + 2G)} B$$

where

B = Flux density without fringing

B_g = Flux density with fringing

G = Air gap length

L = Length of pole face

W = Width of pole face

Iron reluctance reduces the effective number of ampere turns. The effective ampere turns are given by

$$NI_e = NI - 0.029\left(\frac{B}{1000}\right)^2 L_i$$

where L_i is the length of the flux path through iron.

CORRELATION OF COMPUTER PROGRAM WITH TEST DATA FOR SOLID ROTOR

The model EH-441-U1 Electric Dynavector, which was correlated with the computer model, has a solid rotor. According to theory the power loss will increase as the square of the thickness. Thus the theoretical increase in power loss due to the solid rotor, compared with 0.025 sheet stock, is

$$C_e = \left(\frac{0.375}{0.025}\right)^2 \times \frac{\text{rotor weight}}{\text{total iron weight}} = 60$$

The actual power loss of the solid rotor will be less than indicated by theory, because the magnetic flux travels near the surface of the rotor, and the flux density at the center of the rotor iron is low. C_e equal to 1/3 the calculated value (20) was therefore used for the solid rotor model. C_e equals 1.0 for the laminated rotor. The equivalent resistor R_e in the computer program was multiplied by this factor.

```
10 *       DELM04-ELECTRIC DYNAVECTOR TORQUE-SPEED CURVES
20 *       DIMENSIONS IN INCHES,POUNDS,GAUSS(VOLTAGE WAVE FORM)
30 *       PROGRAM GIVES TORQUE FOR EACH SPEED OMEGA(K)
50         DIMENSION OMEGA(6),DES(6)
60         REAL LENGTH,I,N
62         DATA ACAP/1.000/,BS/15000./,C/.005/,CAP/.0000/,EFF/.64/
64         DATA PI/3.14159/,AMAX/10./,RATIO/360./
70         DATA DES/10.,20.,30.,40.,50.,60./
71         DATA DIAMO/8./,DIA/4.875/,ECC/.048/,VO/265./
72         DATA HCOIL/.750/,WCOIL/.500/,WIDTH/.8/,TCOIL/144./
73         DATA V1/90.0/
130    600 WRITE(9,99):99 FORMAT('LENGTH,RATIO,N,V1')
140        READ(9,99)LENGTH,RATIO,N,V1
141        DO 19 K=1,6
142        OMEGA(K)=DES(K)*PI*RATIO/180.
143     19 CONTINUE
150     99 FORMAT(7F10.3)
154        ACOIL=WCOIL*HCOIL
155        TSI=N/ACOIL
156        COEFR=8.046+.0135*(TSI-688.)
157        WIRLEN=N*2.*(LENGTH+WIDTH+2.*WCOIL)
158        R=COEFR*WIRLEN/12000.
159        R=10.
160        AC=LENGTH*WIDTH
161        DI=DIA-WIDTH
162        WI=.29*.785*(DIAMO**2.-DI**2.)*LENGTH
163        WIC=.00155*WI
164        XLI=2.8*DIAMO-1.5*DIA
170        AP=AC/ACAP
180        PERI=2.*(LENGTH+WIDTH)
190        RADIUS=.5*DIA
200        DA=RADIUS*LENGTH*.01
210 *      CALCULATE TM TO CORRECT FOR SPACE BETWEEN POLES
220        TM=.9*(AP/LENGTH)**8./(2.*PI*RADIUS)
230        WRITE(9,101)
240 101 FORMAT(3X,7HDEG/SEC,4X,6HIN-LBS,6X,4HHMPS,5X,5HWATTS,7X,3HEFF)
250        DO 720 K=1,6
260        V=VO:THETA=0.0:T=0.0:SDT=0.0:SIDT=0.0:B=0.0:I=0.0
261        XHI=0.0:J=0:POW=0.0:POUT=0.0
270        DT=.01/OMEGA(K)
271        ST1=.010*(1.-.00122*OMEGA(K))
272        STMAX=PI/OMEGA(K)
274        ST2=.33*STMAX
275        IF(ST2.GT.ST1)GO TO 666
276        ST2=ST1
277    666 CONTINUE
280    615 G=C+(1.+COS(THETA))*ECC
281        IF(SDT.LT.ST1)GO TO 634
283        IF(SDT.LT.ST2)GO TO 635
284        V=V1*(1.-(SDT-ST2)/(STMAX-ST2))
285        GO TO 634
288     635 V=V1
289     634 CONTINUE
290        AG=AP+G*PERI+1.57*G**2.
291        Y=AP/AG
292        BG=B*Y
```

```
294         RE=RED*OMEGA(K)
295         IF(V-5.)638,639,639
296    638  V=5.
297    639  CONTINUE
298         B5=B/100000.
299         RE=WIC*B5**2*(OMEGA(K)/(I+.1))**2
300         D11=3.125E07*G*(V-I*(R+RE))/(AP*N*N)
310         D12=I*ECC*OMEGA(K)*SIN(THETA)/G
320         DIDT=D11-D12
330         I=I+DIDT*DT
332         IF(I-AMAX)616,616,617
333    616  GO TO 618
334    617  I=AMAX
335    618  CONTINUE
340         B=(N*I-XMI*XL1)/(3.113*G)
350         BI=B/ACAP
360         IF(BI-BS)619,620,620
370    619  GO TO 621
380    620  B=BS*ACAP
382         XMI=.039*(B/1000.)**2.
383  621  CONTINUE
390         DPOW=V*I
400         POW=POW+DPOW*DT
420         GO TO 626
440    623  CONTINUE
443         BG=B*AP/AG
450    626  DELT=0.375E-06*DR*ECC*RATIO*BG*BG*SIN(THETA)*EFF
460         T=T+DELT
470         THETA=THETA+OMEGA(K)*DT
480         SIDT=SIDT+I*DT
490         SDT=SDT+DT
491         J=J+1
492         IF(J-10)511,512,512
493    511  GO TO 513
494    512  CONTINUE
495         J=0
496    513  CONTINUE
497    514  FORMAT(F10.2,F10.4,3F10.2)
500         IF(THETA-PI)615,700,700
510    700  AVGI=SIDT/SDT
511         WATTS=4.*POW/SDT
520         T1=TM*T-TCOL
523         POUT=T1*OMEGA(K)*.113/RATIO
524         XMEFF=POUT/WATTS
530         AMPS=4.*AVGI
540         SPS=(OMEGA(K)*4.)/PI
550         WRITE(9,710)DES(K),T1,AMPS,WATTS,XMEFF,SPS
560    720  CONTINUE
570    710  FORMAT(4F10.2,F10.4,F10.2)
572         WRITE(9,222)222 FORMAT('KY')
574         READ(9,223)KY223 FORMAT(1I2)
580         GO TO (500,800),KY
590    800  STOP
600         END
```

APPENDIX C

DUAL MODE DYNAVECTOR WITH COMMUTATED PNEUMATIC/COMMUTATED ELECTRIC DRIVE

C.1 FOREWORD

This report has been written to describe preliminary studies investigating the feasibility of operating a Bendix Combination Electric-Pneumatic Dynavector Rudder Actuator in both electric and pneumatic modes simultaneously, each acting as an implicit standby for the other to improve the probability of aircraft rudder control survival when this device is installed.

It will be noted that the basic dynavector design can be implemented as *either* "commutated-proportional" or "pure-stepper" in both the pneumatic and electrical modes. However, the arrangement choice is subtly restricted by the fact that electric designs are more cost-effective as steppers whereas pneumatic versions work better with the commutated proportional approach. And as a further complication, the successful marriage of dissimilar types would appear to impose complex dynamic problems on the common control system which, in addition to its normal duties, must also deal with load sharing (a problem which resolves itself naturally when similar devices are used).

Because of its apparent simpler load-sharing control problem, the combination of commutated-proportional pneumatic with commutated-proportional electrical has been chosen as the first target of this investigation. Stepper modes and dissimilar combinations will be presented later.

C.2 OBJECTIVES

It is the objective of this phase of the Bendix Dynavector Development Program to create a CSMP dynamic model of paired proportional electric and pneumatic actuators integrated into the T-2C airplane rudder channel. The model is exercised in a manner that will demonstrate performance capability, dynamic response, load-sharing characteristics and the impact of simulated battle-damage on the pilot's ability to safely control the aircraft rudder channel.

C.3 CONCLUSIONS

Operation of the Bendix Dynavector Dual-Mode T-2C Rudder Channel Model demonstrated satisfactory compliance with the aircraft dynamic requirements while exhibiting acceptable load-sharing throughout. Simple failures such as the loss of an electrical (or pneumatic) power source or an electrical controller (or pneumatic amplifier) were so easily absorbed by the system's redundancy that such problems might readily pass unnoticed by the pilot. On the other hand, off-center malfunctions such as a sticking displaced pneumatic valve or an amplifier hard-over failure yield more severe problems to the extent that the pilot must exert considerable effort just to maintain a center position and can only achieve full rudder displacement by applying maximum physical effort.

To prevent any hardovers caused by a malfunction in electrical signal paths it is necessary to make the signal paths redundant and employ in-line monitoring and voting schemes.

To take care of situations where the pneumatic valve is stuck open, a provision must be made to cut off the pneumatic air supply.

C.4 RECOMMENDATIONS

C.4.1 Flight Safety

Based on these findings, it is recommended that the system arrangement of the Dual-Mode Dynavector Actuator ultimately selected for flight test be configured in such a manner that either (or both) channel(s) will be automatically decoupled in case of emergency.

C.4.2 Further Investigation

This study should be continued by creating a CSMP Electrical Dynavector Stepper Model operating in dual-mode with a Commutated Pneumatic partner. The program would resolve load-sharing problems and simulate critical battle damage to determine the related impact on flight-safety.

C.4.3 Flight Test Configuration

It will be necessary to compare relative merits of paired Commutated-Pneumatic/Commutated -Electric with paired Commutated-Pneumatic/Stepper-Electric Dynavector Actuators to identify the best combination for eventual flight test on the T-2C airplane.

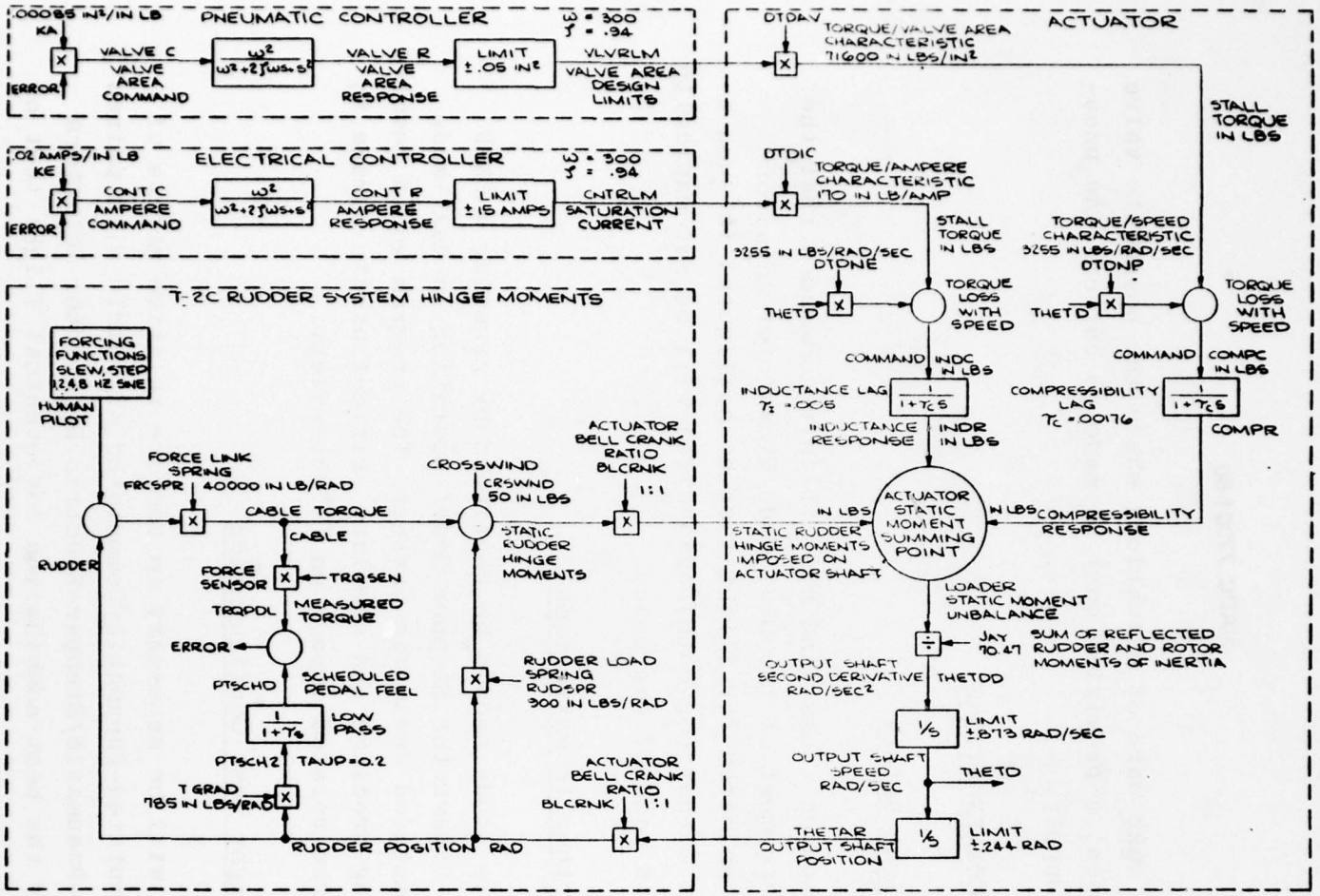

BLOCK DIAGRAM
T2-C RUDDER CONTROL SYSTEM SIMULATION
ACTUATOR: DUAL MODE DYNAVECTOR
CONTROLLERS: PROPORTIONAL ELECTRIC AND
PROPORTIONAL PNEUMATIC

FIGURE C-1

C.5.1 Dual-Mode Commutated-Pneumatic/Commutated-Electric Dynavector Model Configuration

Please refer to Figure C-1 describing the T-2C Rudder Channel CSMP Model used for this study. The overall approach is a classic application of angular dynamic equilibrium theory. The instantaneous rudder hinge-pin torques applied by the pilot via pedals and cable, cross-wind from the rudder, centering spring, pneumatic actuator and electric actuator are all added arithmetically and the unbalanced sum applied to impart angular acceleration to the combined rudder and actuator moments of inertia. The resultant angular acceleration is iteratively integrated first to obtain shaft angular speed and again to obtain output shaft position. Pilot effort is measured by a torque sensor, compared with a displacement schedule of pedal 'feel', and residual errors directed to simultaneously drive the electrical controller and the amplifier-positioned pneumatic transfer valve. Because it is technically difficult to measure rotor orbit-speed on a dynavector-type mechanism, the natural damping provided by pumping losses, back EMF and friction is used to the fullest extent and open-loop gains are adjusted accordingly. The short-term lags associated with the transfer-valve, compressibility, and winding inductance are rigorously simulated and, in fact, were the cause of considerable load-sharing difficulties before compensating networks were devised to correct the problem.

C.5.2 Test Methods

To obtain sufficient test data on the above Dynavector-Assisted Rudder Channel Configuration to properly evaluate its true performance capability, the simulated human pilot was programmed to impose a series of critical forcing-functions into the cockpit pedal mechanism, including small step-changes, sinusoidal motion at 1, 2, 4 and 8 Hz, and finally a rated-speed full-left, full-right rudder position traverse to demonstrate slew-speed capability. Baseline visibility into the system functions was provided by means of sets of time-based parametric data plots describing exactly how each parameter responds during the programmed disturbances.

Next, destructive logic was implemented to simulate the occurrence of certain failures during the early stages of each forcing function. By this method, it was possible not only to determine how much the channel performance would be degraded but also the absolute capability of the pilot to cope with the problem and maintain acceptable standards of flight safety. In addition to a baseline-run, the following failures were simulated during the testing.

- Pneumatic pressure loss
- Transfer valve hang-up at point of peak test-mode excursion.
- Pneumatic amplifier gain loss of 75%.
- Electrical power loss.
- Electrical controller hard-over type failure.

C.5.3 Test Results

C.5.3.1 Commentary

In general, the Dual Mode Dynavector System was found to be highly tolerant of catastrophic failures such as the loss of basic electrical or pneumatic power, the occurrence of a completely "dead" controller or the gross deterioration of pneumatic amplifier gain. On the other hand, unusual failures such as a stuck transfer valve or the loss of one side of a push/pull electrical driver creates the condition of the actuators opposing each other, backing up not only the full rudder load but also the force-sensor thrust on the overburdened pilot. An automatic disconnect system has been proposed to enable the pilot to free such a failure should one be encountered during flight test.

C.5.3.2 Specific Findings

Base-line system performance and the impact of the various failure modes discussed above are presented numerically in Figure C-2.

FAILURE MODES	DAMPING RATIO	PHASE LAG AT 4 Hz (DEGREES)	PEDAL FORCE AT 1 Hz (POUNDS)	PEDAL FORCE TO ACHIEVE HARD OVER SLEW(POUNDS)	FLIGHT SAFETY IMPACT
No-Failure Baseline	0.7	32.2	± 2.6	+41.6	Baseline
75% Loss of Pneumatic Amplifier Gain	1.0	47.1 (45% Incr)	+ 4.3 (50% Incr)	+56.6 (36% Incr)	This type failure is an acceptable risk
Complete Loss of Pneumatic Supply Pressure	1.0	57.2 (77% Incr)	+ 5.3 (103% Incr)	68.4 (64% Incr)	This type failure is an acceptable risk
Hung Up Pneumatic Transfer Valve at Maximum Excursion	1.0	54.4 (69% Incr)	+ 7.0 - 1.9 (150% Incr)	+179.1 (330% Incr)	This type failure requires an automatic disconnect for complete safety.
Complete Loss of Electrical Power Supply	0.5	31.1 (3% Decr)	+ 3.1 (21% Incr)	+40.0 (3.8% Decr)	This type failure is an acceptable risk
Electrical Controller Hard-Over Failure	1.0	34.6 (7% Incr)	+48. +40. (1746%Incr)	+103.3 (340% Incr)	This type failure requires an automatic disconnect for complete safety.

Figure C-2

APPENDIX D

DUAL MODE DYNAVECTOR WITH COMMUTATED PNEUMATIC/STEPPER ELECTRIC DRIVE

D.1 FOREWORD

This report has been written to describe follow-on studies investigating the feasibility of operating a Bendix Combination Electric-Pneumatic Dynavector Rudder Actuator simultaneously in both electric and pneumatic modes, each acting as an implicit standby for the other to improve the probability of aircraft rudder control survival when this device is installed.

It will be noted that the basic dynavector design can be implemented as either 'commutated-proportional' or 'pure-stepper' in both the Pneumatic and Electric Modes. However, the arrangement choice is subtly restricted by the fact that electric designs are more cost-effective as steppers whereas pneumatic versions work better with the commutated proportional approach. And as a further complication, the successful marriage of dissimilar types would appear to impose complex dynamic problems on the common control system which, in addition to its normal duties must also deal with load-sharing (a problem which resolves itself naturally when similar devices are used).

Because of its apparently simplistic load sharing problems, the combination of Commutated Proportional Pneumatic with Commutated Proportional Electrical was studied first and the results presented in Appendix C. This document addresses the dynamic problems of the more cost-effective combination of stepper-electric with proportional pneumatic, and compares its technical risk with the all proportional alternate.

D.2 OBJECTIVES

It is the objective of this phase of the Bendix Dynavector Development Program to create a CSMP Dynamic Model of paired stepper-electric and proportional-pneumatic actuators integrated into the T-2C Airplane Rudder Channel. The model is exercised in a manner that will demonstrate performance capability, dynamic response, load sharing characteristics and the impact of simulated battle-damage on the pilot's ability to safely control the aircraft rudder channel.

D.3 CONCLUSIONS

Operation of the Bendix Dynavector Dual-Mode T-2C Rudder Channel Model demonstrated satisfactory compliance with the aircraft dynamic requirements. Simple failures such as the loss of an electrical (or pneumatic) power source or an electrical controller (or pneumatic amplifier) were so easily absorbed by the system's redundancy that such problems might readily pass unnoticed by the pilot. Even the occurrence of a pneumatic valve sticking at maximum displacement caused no trouble to the pilot who could readily overide the unwanted pneumatic torque making use of the abundant electrical stepper torque to continue operations. Only one failure-type produced a true flight-safety problem when it was shown that the maximum effort of the pilot reinforced by full pneumatic torque could not restrain the hard-over slew of the powerful stepper, inadvertently responding to the drive of a malfunctioning controller (which was assumed to have failed outputing an undesired train of pulses at maximum frequency).

It is probably necessary to make the electrical signal paths redundant with in-line monitoring and voting circuits to prevent any hardovers caused by a malfunctioning electrical controller.

D.4 RECOMMENDATIONS

D.4.1 Flight Safety

In view of these findings, it is recommended that the system arrangement of the Dual-Mode Dynavector Actuator ultimately selected for flight test be configured in such a manner that either (or both) channel(s) will be automatically decoupled in case of emergency.

D.4.2 Best Configuration Selection

Because paired Stepper-Electric and Proportional-Pnaumatic Dynavectors not only easily meet T-2C Rudder Channel Performance requirements but are beyond doubt the most cost-effective candidates proposed, it is recommended that this combination be chosen as the best possible configuration for the detail design phase scheduled to begin during the up-coming period.

D.4.3

D.5 RESULTS

D.5.1 Dual Mode Commutated-Pneumatic/Stepper-Electric Dynavector Model Configuration

Please refer to Figure D-1 describing the T-2C Rudder Channel CSMP Simulation used for this study. The overall approach is a classic application of angular dynamic equilibrium theory. The instantaneous rudder hinge-pin torques applied by the pilot via pedals and cable, cross-wind from the rudder, centering spring, pneumatic actuator and electric stepper actuator are all added arithmetically and the unbalanced sum applied to impart angular acceleration to the combined rudder and actuator moments of inertia. The resultant angular acceleration is iteratively integrated first to obtain shaft angular speed and again to obtain angular shaft position. Pilot effort is measured by a torque sensor, compared with a displacement schedule of pedal 'feel' and residual errors directed to simultaneously drive the electrical controller and the amplifier-positioned pneumatic transfer valve. As might be expected, the basic stepper design requirement of having the abundent momentary torque peaks required to start(and stop) the entire inertial load at frequencies up to 500 pulses/second tended to produce a motor with a stiffness factor capable of easily overpowering its relatively soft pneumatic partner. Under these circumstances, the original concept of using natural load-sharing tendency as a system figure-of-merit had to be completely abandoned.

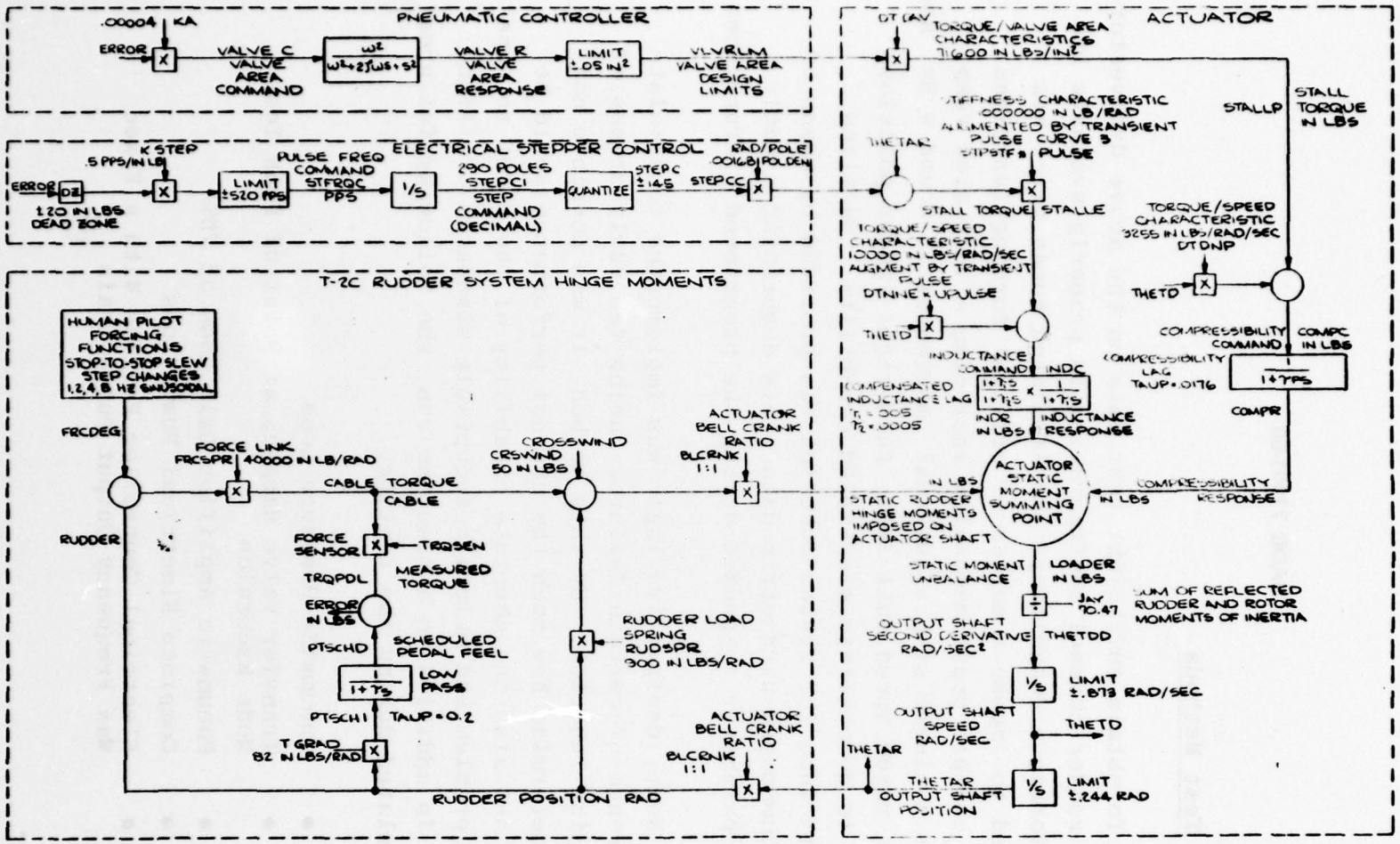

BLOCK DIAGRAM
T2-C RUDDER CONTROL SYSTEM SIMULATION
ACTUATOR: DUAL MODE DYNAVECTOR
CONTROLLERS: STEPPER ELECTRIC AND
PROPORTIONAL PNEUMATIC

FIGURE D-1

D.5.2 Test Methods

To obtain sufficient test data on the above dynavector-assisted rudder channel configuration to properly evaluate its true performance capability, the simulated human pilot was programmed to impose a series of critical forcing-functions into the cockpit pedal mechanism including a very slow ramp to expose a single step, sinusoidal motion at 1, 2 and 4 Hz, and finally a rated speed full-left, full-right rudder position traverse to demonstrate slew-speed capability. Baseline visibility into the system function was provided by means of sets of time based parametric data plots describing exactly how each parameter responded during the programmed disturbances.

Next, destructive logic was implemented to simulate the occurence of certain failures during the early stages of each forcing function. By this method, it was possible not only to determine how much the channel performance would be degraded but also the absolute capability of the pilot to cope with the problem and maintain acceptable standards of flight safety. In addition to a baseline run, the following failures were simulated during the testing.

- Pneumatic Pressure Loss
- Transfer Valve Hang-up at Point of Peak Test Mode Excursion
- Pneumatic Amplifier Gain Loss of 75%
- Complete Electrical Power Loss
- Electrical Controller Failing With a Fixed Max Frequency Output Pulse Train

D.5.3 Test Results

D.5.3.1 Commentary

In general, the Electric Stepper varient of the Dual Mode Dynavector System was found to be even more tolerant of catastrophic failures than the proportional electric varient tested previously. The pilot would normally be completely unaware of the loss of basic electrical or pneumatic power, the occurrence of a completly 'dead' controller or gross deterioration of pneumatic amplifier gain. Even the conflicting output of a hung-up pneumatic transfer valve could be easily overpowered by the exceptionally stiff stepper. As might be expected, the one unacceptable malfunction proved to be the electrical controller failing hard-over with an unwanted pulse-train output. Under these conditions, the pilot would be physically incapable of restraining the actuator from migrating against one of its maximum displacement stops unless the system was provided with automatic disconnect hardware.

D.5.3.2 Specific Findings

Baseline System performance and the impact of the various failure modes discussed above are presented numerically in Figure D-2

FAILURE MODES	DAMPING RATIO	PHASE LAG AT 4 Hz (DEGREES)	PEDAL FORCE AT 1 Hz (POUNDS)	PEDAL FORCE TO ACHIEVE HARD OVER SLEW(POUNDS)	FLIGHT SAFETY IMPACT
No-Failure Baseline	1.0(Approx) Hidden By Step Coarseness	43.2	6.8	51.6	Baseline
75% Loss of Pneumatic Amplifier Gain	1.0(Approx) Hidden By Step Coarseness	43.2	6.9	51.6	This type of failure is an acceptable risk
Complete Loss of Pneumatic Supply Pressure	1.0(Approx) Hidden By Step Coarseness	43.2	6.9	51.0	This type of failure is an acceptable risk
Hung Up Pneumatic Transfer valve at max excursion	1.0(Approx) Hidden by Step Coarseness	43.2	6.9	51.6	This type of failure is an acceptable risk
Complete Loss of Electrical Power Supply	1.0	43.2	3.8	34.5	This type of failure is an acceptable risk
Electrical Controller Fails with Unwanted Pulse Train Output	Non Responsive to Forcing Function	Non Responsive to Forcing Function	Stepper Failure Induces A 795 Pound Cable Force	Stepper Failure Induces a 708 Pound Cable Force	This type of failure requires an automatic disconnect for complete safety.

FIGURE D-2

DISTRIBUTION LIST

REPORT NADC 77001-60

	NO. OF COPIES
NAVAIR SYSCOM AIR 50174 WASHINGTON, D. C. 20361	17
6 FOR RETENTION 1 FOR AIR 03 1 FOR AIR 04 1 FOR AIR 05 1 FOR AIR 340 2 FOR AIR 340D 1 FOR AIR 530 1 FOR AIR 5303 2 FOR AIR 530311 1 FOR AIR 52040	
NAVAIR DEVCEN WARMINSTER, PA. 18974	29
3 FOR 813 1 FOR 10 1 FOR 20 1 FOR 30 1 FOR 40 1 FOR 50 1 FOR 60 1 FOR 70 1 FOR 80 1 FOR 601 1 FOR 607 1 FOR 609 15 FOR 6013 (T. JANSEN)	
AIR FORCE FLIGHT DYNAMICS LAB WRIGHT-PATTERSON AFB, OHIO 45433	2
1 FOR FGL (PAUL BLATT) 1 FOR FGL (DANIEL BIRD)	
DDC CAMERON STATION VIRGINIA 22314	12